RESEARCH DEPARTMENT
TECHNICAL REPORT No. 53

THE PERFORMANCE AND SYSTEMATIC ERRORS OF THE ECMWF TROPICAL FORECASTS (1982 - 1984)

by

William A. Heckley

November 1985

Abstract

The performance of the ECMWF forecasting system in tropical prediction is discussed in terms of objective scores and systematic errors for the period 1982-1984. The temperature, humidity and wind errors appear to be mutually consistent. The forecasts exhibit a cooling in the tropical stratosphere, warming at and immediately below the tropical tropopause and a cooling in the mid and lower tropical troposphere. The analyses appear too humid in the lower troposphere while the forecasts show a drying. Precipitation and evaporation are both too weak; a new energy balance within the model is slowly established through cooling, this new balance having a reduced total energy ($Lq + C_p T$). The associated wind errors are seen to have a highly baroclinic structure and a meridional extent such as to significantly affect the baroclinicity of the mid latitude flow, particularly over the north and south Atlantic. Systematic errors are large compared to the variability of the fields themselves and show a remarkable temporal consistency from month to month.

C O N T E N T S

1. INTRODUCTION

An increasing number of operational centres are using sophisticated, global, general circulation models as aids to their routine weather forecasting. An understanding of the behaviour of individual models is very important for the forecaster, who has to interpret these products. This understanding is just as important in the research work of these centres, enabling them to concentrate effort on areas most likely to lead to significant improvement. It is apparent from earlier GCM intercomparisons (ICSU/WMO(1978); Gilchrist (1977); Gilchrist et al. (1982); Rowntree (1978)), that different models may share some systematic errors and yet differ widely in others. This information can be valuable in isolating the causes of errors, which is the first step towards eliminating them.

Documentation and diagnosis of the errors of the European Centre for Medium Range Weather Forecasts (ECMWF) forecasting and analysis system has received considerable attention in recent years. This paper concentrates on documenting the systematic, time-mean errors in the tropical prediction; however no attempt is made to provide a complete explanation for these errors. The emphasis of the research has been on the systematic errors quite simply because they are so large: the whole tropical climatology is changed within a few days. Also, it is becoming of increasing concern that these tropical errors may be the source of many of the mid-latitude errors (Klinker and Capaldo, 1984).

The ECMWF operational forecast model is described by Hollingsworth et al. (1980), the physical parameterisations are described by Tiedtke et al.(1979) and the analysis scheme by Bengtsson, et al.(1982). The analysis/forecasting system at ECMWF is subject to a process of continual development. Some of the more recent changes of significance are:

27 July 1982	Analysed sea surface temperatures from NMC introduced
21 September 1982	Diabatic initialisation introduced
21 April 1983	Introduction of spectral model (T63)
21 April 1983	Introduction of envelope orography
1 May 1984	Introduction of diurnal cycle in forecast and assimilation models
21 May 1984	Extensive revision of the analysis scheme

A description of the diabatic initialisation may be found in Wergen, (1985); the spectral model in Simmons and Jarraud, (1984); the envelope orography in Wallace et al. (1983); and the revision of the analysis scheme in Shaw et al. (1984).

The diurnal cycle is introduced through a variation in the local solar zenith angle, in association with this an extra soil layer is added with reduced heat capacity so as to allow a realistic diurnal variation of soil temperature. Radiative fluxes are calculated at each timestep (about 20 minutes), but the optical transmission properties are only recalculated every three hours.

Results and conclusions presented in this paper were obtained largely from the operational spectral model prior to the introduction of the diurnal cycle and revision of the analysis system in May 1984. With very little reservation, these results are equally applicable to the grid point model, operational prior to the introduction of the spectral model in April 1983.

The first section describes the performance of the forecasts in terms of objective scores and is intended to give an overall indication of the quality of the forecasts and to provide a perspective for the discussion of the systematic errors that follows.

As a brief overview, before examining the errors in detail, a list of specific errors discussed in this study are summarised below.

(a) cooling in the tropical stratosphere

(b) warming on and immediately below the tropical tropopause

(c) cooling in the mid and lower tropical troposphere

(d) analyses too moist in the lower troposphere

(e) slow 'spin up' of the model convection

(f) hydrological cycle too slow - insufficient evaporation and precipitation - insufficient latent heat release

(g) inability to maintain subsidence inversions in a realistic manner

(h) tendency to smooth out vertical structure in divergence fields

(i) weakening of the upper branch of the Hadley circulation, which becomes spread over a greater depth

(j) upper level tropical easterlies too strong

(k) highly-baroclinic wind errors which have a large meridional scale, extending well into the mid latitudes.

Since this study was completed significant progress has been made in reducing many of these errors, and a new evaluation should be carried out in the light of these changes. In the meantime it is worthwhile briefly mentioning some of the recent changes to the forecasting system and their effect upon the tropical forecasts.

Recent changes of significance include:

4 December 1984	Revision of the treatment of longwave radiation
1 May 1985	Increased horizontal resolution (T106) Revision of the parameterisation of deep cumulus convection Parametermisation of shallow convection New cloud scheme

Other changes include modifications to horizontal diffusion and analysis of the large scale wind field.

The revised long wave radiation scheme now incorporates the absorber gases directly throughly the technique of exponential sum fitting (Wiscombe and Evans, 1977). It has reduced the stratospheric cooling, particularly at the top model level (a); there is also a modest reduction in the warming on and immediately below the equatorial tropopause (b) (Ritter, 1985).

The most dramatic improvement in the tropical forecasts has occurred following the introduction in May 1985 of a parameterization of shallow cumulus convection, modification of the (Kuo) deep cumulus convection, and increase of horizontal resolution. The decrease in the time mean systematic errors in the tropics comes largely from the revised physics. Evidence from individual forecasts, however, shows a benefit from the increased resolution on transient features, such as tropical cyclones. The effects of shallow convection are incorporated in the model through turbulent fluxes of sensible heat and moisture, which have been parameterized by means of a mixing length theory (Tiedtke, 1984). Shallow convection ensures that water vapour is accumulated in the cloud layer at the top of a well mixed boundary layer; the effect in the model is to deepen and dry the boundary layer (it was too moist and too

shallow (d,g), enhance the moisture supply from the sub-tropical oceans, and increase the moisture transport into the deep tropics through the trade wind circulation. The resulting increased moisture supply to the deep cumulus convection in the tropics drives a faster hydrological cycle (f), and produces larger diabatic heating through latent heat release, which improves the energy balance of the model and reduces the model's tendency to cool the troposphere (c).

The deep cumulus convection (Kuo) has been modified in two ways (Tiedtke, 1986): the cloud base is redefined at the condensation level for low level air, rather than for air with the mean characteristics of the well mixed layer. This increased the occurrence of cumulus convection and gives a more realistic response by convection to the diurnal surface heating over the continents. The second change involves the moistening parameter, which determines the partitioning between convective heating and moistening; this has been modified to give less moistening and more heating.

The modifications to the deep cumulus convection and the addition of the parameterization of shallow cumulus convection combine to enhance considerably the hydrological cycle in the model (f). Global values of precipitation are now much nearer climatological values (though a little high), and the geographical distribution is generally good, with a good description of the ITCZ's (previously too weak). The enhanced latent heating has eliminated the previous tendency to cool the tropical troposphere (c); there is now however a slight warming.

A new cloud scheme has been developed based on a diagnostic approach, which allows for four cloud types: convective cloud and three layer clouds - high, medium and low level (Slingo, 1986). The scheme gives realistic cloud distributions, however the impact of the scheme on medium range forecasts is not very large, but gives a modest improvement. The representation of the diurnal cycle in cloudiness is however much improved with the new scheme (Slingo, pers.comm).

The improvements to the forecasts are not confined to the model's hydrological cycle and thermal state; the improvements in diabatic heating also lead to significant improvements in the simulation of the tropical flow, in particular a much more realistic trade wind circulation (k).

Despite these improvements many problems remain to be solved; the tropical upper troposphere is still too stable; the upper branch of the Hadley circulation is still too weak and spread over too deep a layer (i), and the upper level tropical easterlies are too strong (j). The deep convection over Indonesia appears to be too intense, and it may well be the cause of significant wind errors in the region of the South China Sea (k).

Another problem which still remains is that of 'spin-up' of the model divergence field (e).

2. OBJECTIVE ASSESSMENT OF THE FORECASTS

The forecast quality is assessed in terms of root mean square (rms) errors of model and persistence forecasts, for the vector wind and temperature. The results are presented for a number of relatively (except for the tropical belt) data rich areas:

1.	India/East Asia	33N-06N, 72E-102E	110 points
2.	Indonesia	18N-12S, 102E-132E	121 points
3.	Central Africa	12N-12S, 06W-42E	117 points
4.	Tropical Belt	18N-18S, 00E-354E	420 points

Fig. 1 shows the location of these areas.

The horizontal grid resolution used in the verification procedure is 3 x 3 degrees, except for the whole tropical belt where a resolution of 6 x 6 degrees is used. A latitudinal cosine weighting is used to compensate for the decreasing grid interval along latitudes in the meridional direction. The forecasts are verified against initialised analyses, and the results are presented as area mean, monthly mean scores, together with the corresponding twelve month running mean.

The scores described in this section were obtained from the ECMWF operational field verification system (Nieminen, 1983).

Daily operational forecasts have been produced at ECMWF since 1 August 1980; before that, from 1 August 1979, they were produced five days a week (i.e. excluding weekends). Therefore the sample number in the monthly means varies from 20 to 23 in the first part of 1980, and 28 to 31 after July 1980. One exception to this occurred in May 1980 when the number of cases was reduced to 14, due to archiving problems.

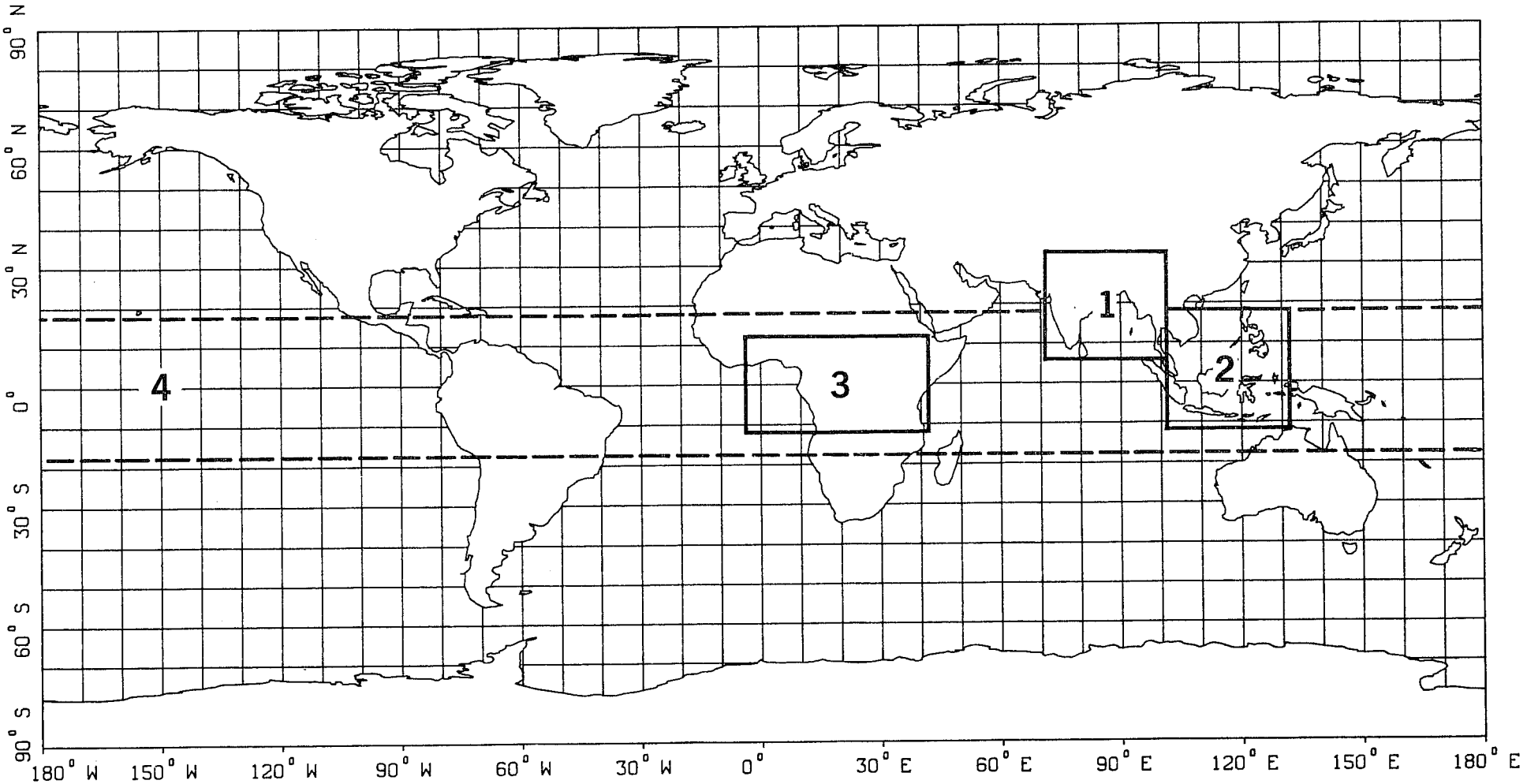

Fig. 1 Areas used for the objective field verification of the operational forecasts, the boundary of the latitude belt is denoted by a dashed line.

2.1 24 hour forecasts for the tropical belt

The rms error of the 24 hour model forecast of the 850 mb vector wind for the tropical belt, Fig. 2a, shows a fairly steady improvement from about 4 m s^{-1} in January 1980 to below 3 m s^{-1} during 1984. The corresponding rms error of the persistence forecast, Fig. 2b, has remained fairly constant at under 4 m s^{-1}. At 200 mb the rms error of the 24 hour model forecast of vector wind, Fig. 2d, shows an improvement from about 8 m s^{-1} in the summer of 1981 to just over 6 m s^{-1} in spring 1984; the persistence forecast error, Fig. 2e, is typically 9 m s^{-1} and varies between 8 and 10 m s^{-1}. In absolute terms the errors at 200 mb are larger than those at 850 mb by about a factor of two.

The normalised rms vector wind errors at 850 mb and 200 mb are shown in Figs. 2c and 2f. These show that, relative to persistence, the 200 mb forecast is better than that at 850 mb. Also they reveal that there has been a steady improvement in the forecasts from early 1980, though this trend has levelled at 200 mb since the latter part of 1983.

Over the tropical belt as a whole the rms temperature error at 850 mb in the 24 hour model forecast decreased from about 1.8°C in January 1980 to about 1.1°C in December 1980. Thereafter it remained fairly steady at this level. The persistence forecast error over this period followed a similar trend, although dropping slightly earlier in 1984 than the model forecast error. Normalising the forecast error with the persistence error (Fig. 3a) one sees that the forecast quality has remained fairly constant since about December 1980 at a level slightly better than that of persistence. The improvement in the November and December 1980 model scores is probably associated with a more consistent use of virtual temperature in the analysis cycle and with interpolation changes in the analysis that took place on 11 November 1980.

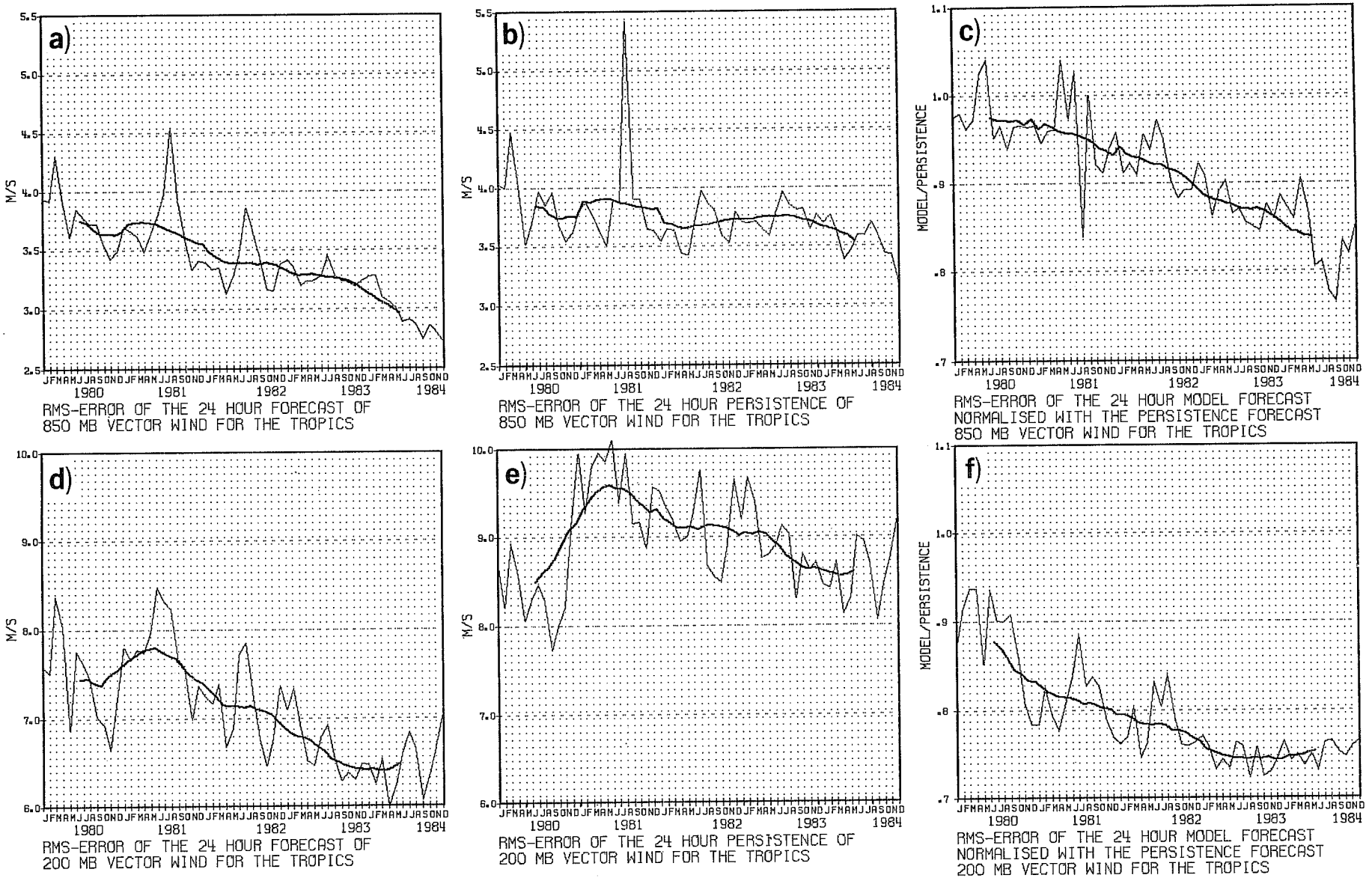

Fig. 2 RMS error of the 24 hour forecast of vector wind for the tropical belt 18N - 18S. Units: m s^{-1}. Area 4 in Fig. a) Model forecast at 850 mb b) Persistence forecast at 850 mb c) Model forecast normalised by persistence forecast at 850 mb d) Model forecast at 200 mb e) Persistence forecast at 200 mb f) Model forecast normalised by persistence forecast at 200 mb The thin solid line indicates area mean, monthly mean, scores; the thick solid line is a twelve-month running mean of the latter.

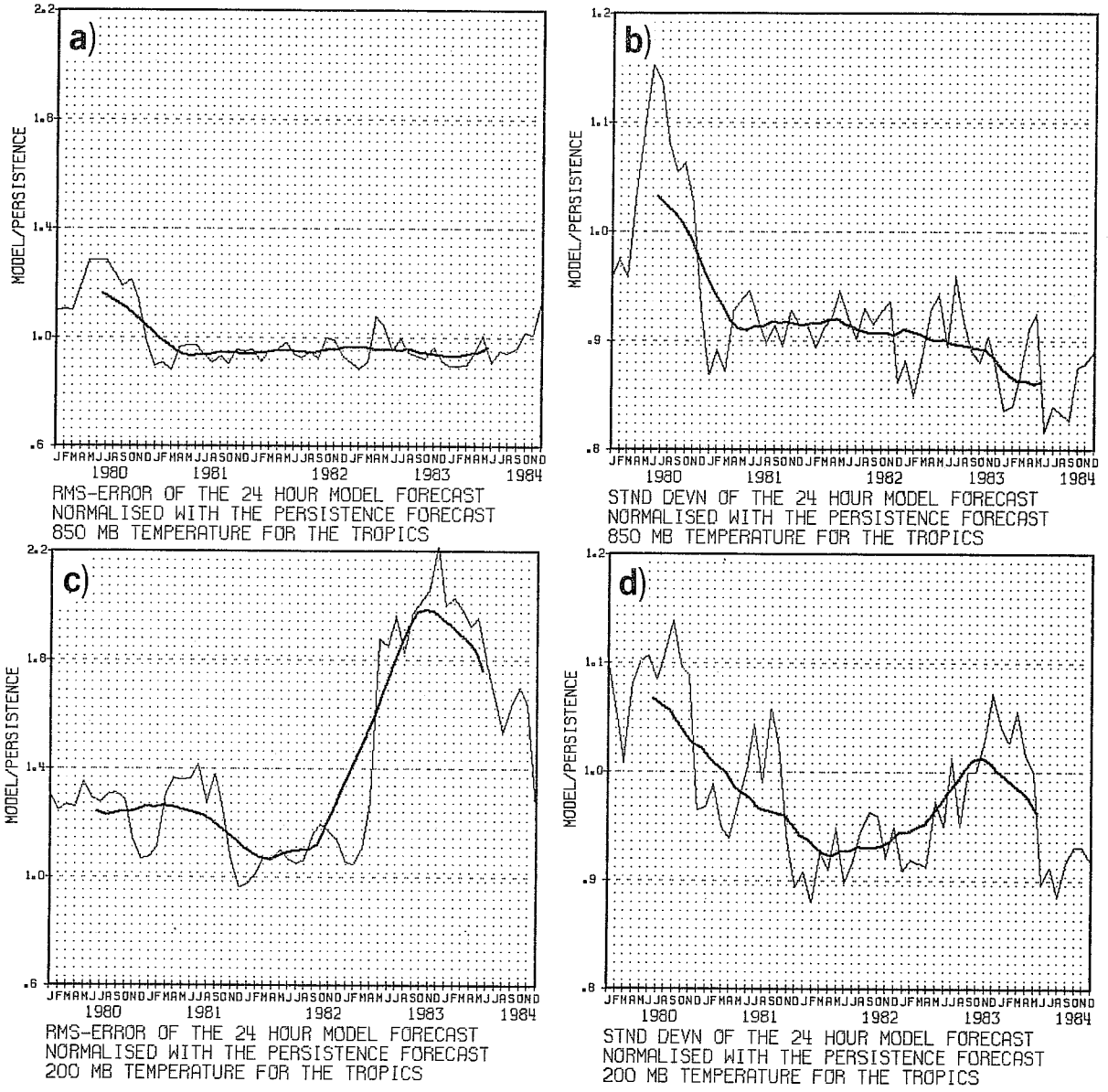

Fig. 3 24-hour forecast error of temperature for the tropical belt 18N-18S.
a) RMS error of the model forecast normalised by the persistence forecast error. 850 mb
b) Standard deviation of the model forecast normalised by the persistence forecast error. 850 mb
c) As a) but for 200 mb
d) As b) but for 200 mb
The thin solid line indicates area mean, monthly mean scores; the thick solid line is a twelve month running mean of the latter.
Units: °C.

The smaller increases in errors in April 1983 corresponded with the introduction of the spectral model, the decrease in June 1983 to the modified physics (radiation code changed to eliminate excessive cooling at low levels) and the increase in December 1984 to the introduction of the ESFT radiation scheme. A decrease in errors follows the introduction of the diurnal cycle and the changes to the analysis system in May 1984. The improvement is largest at low levels over the continental regions, and is particularly dramatic over central Africa. Both the model and persistence forecasts are improved, resulting in little change in the forecast errors relative to those of persistence, at least for the tropical belt as a whole (Fig. 3a).

The rms temperature errors of the model forecast at 200 mb for the tropical belt vary from about .8°C in November 1980 to about 1.5°C in July 1983 with a typical value over the period being about 1.1°C; these errors are larger than those of the corresponding persistence forecasts as is demonstrated by the normalised forecast error shown in Fig. 3c, this being typically about 1.2 and reaching a maximum of 2.2 in December 1983. The clearest signal coincides with the introduction of the spectral model in April 1983. An improvement in the forecasts follows the introduction of the diurnal cycle and revised analysis scheme in May 1984 and again following the introduction of the ESFT radiation scheme in December, 1984.

The standard deviation may be defined as

$$\sigma = \left\{\left(\frac{1}{n}\right)\sum\left[(F\text{-}Av) - \overline{(F\text{-}Av)}\right]^2\right\}^{\frac{1}{2}} ,$$

where F = forecast; Av = verifying analysis; the overbar denotes the area mean and n is the number of grid points in the verifying area. The monthly mean σ is then the monthly mean of the daily values.

Fig. 3b shows the standard deviation of the forecast temperature error compared to the standard deviation of the persistence temperature error; it is similar in character to the rms error at 850 mb but is less in magnitude. For the tropical belt the normalised rms error is ~1.0 whereas the normalised standard deviation is ~.9. Thus for the 24 hour forecast at 850 mb the fact that the rms error is greater than the standard deviation suggests that there is a significant temperature bias. At 200 mb (Fig. 3d) the normalised standard deviation is different in character to the normalised rms errors, but once again the difference in magnitude indicates a significant temperature bias. It is interesting to note that the signal in the rms that coincides with the introduction of the spectral model is much less obvious in the standard deviation suggesting that the error is largely one of a temperature bias. A significant reduction in the standard deviation follows the introduction of the diurnal cycle and new analysis system in May 1984.

The forecast skill shows some distinct regional variability particularly in terms of seasonal variations and it is interesting to examine some of these individually.

2.2 24 hour regional forecasts

(a) India/East Asia

Over India/East India (Fig. 4,5) a strong annual cycle occurs in the skill of the 24 hour persistence forecasts, at 200 mb, for both temperature (Fig. 5e) and wind (Fig. 4e). The rms errors are least in summer (~7 ms^{-1}; 9°C) and greatest in winter (~12 ms^{-1}; 1.8°C). This behaviour is presumably linked to the seasonal migration of the sub tropical jet. During the northern hemisphere summer the region is under the influence of the Indian summer monsoon, at which time the wind and temperature fluctuations are relatively small.

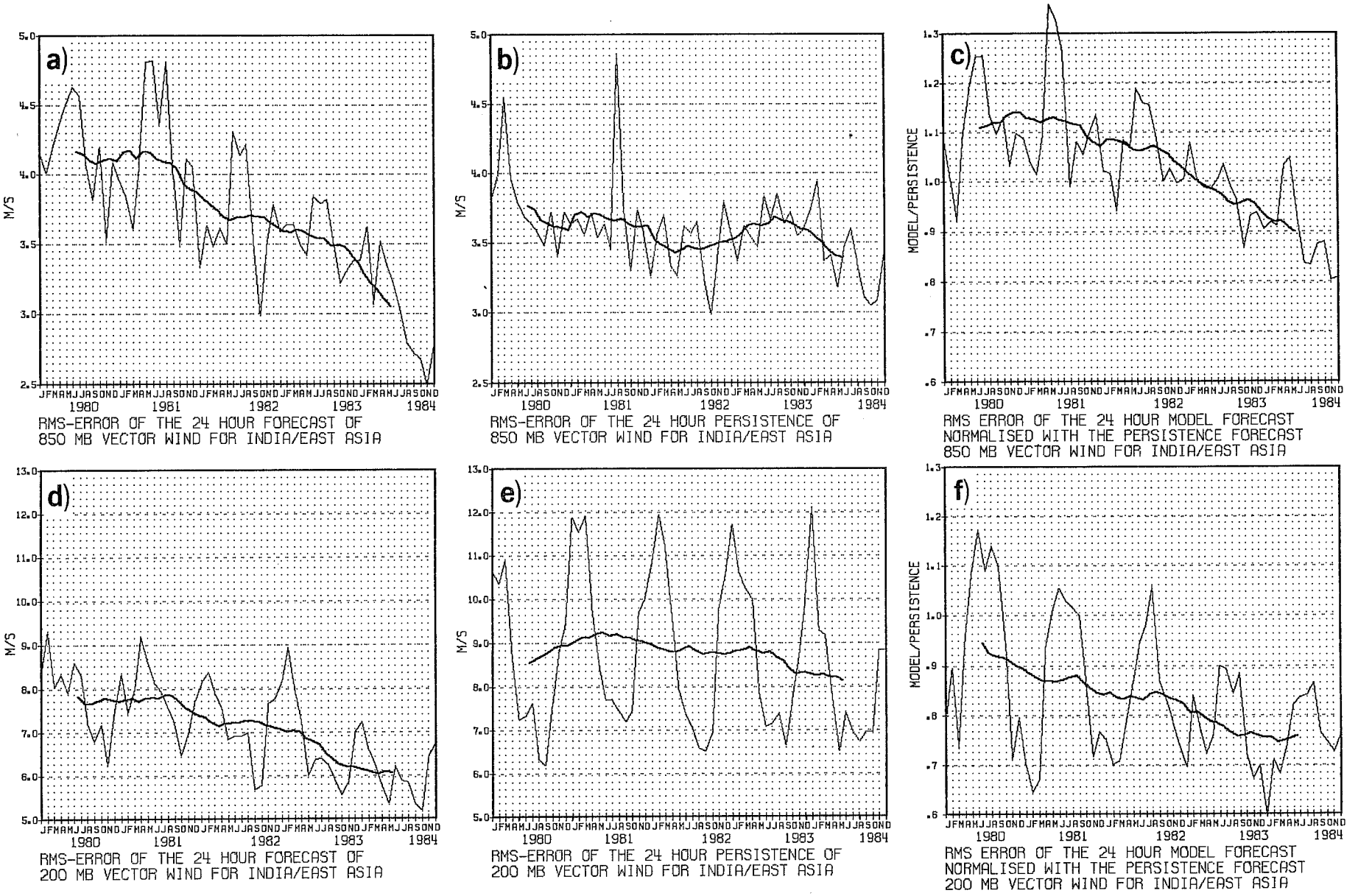

Fig. 4 As Fig. 2 but for India/East Asia. Area 1 in Fig. 1

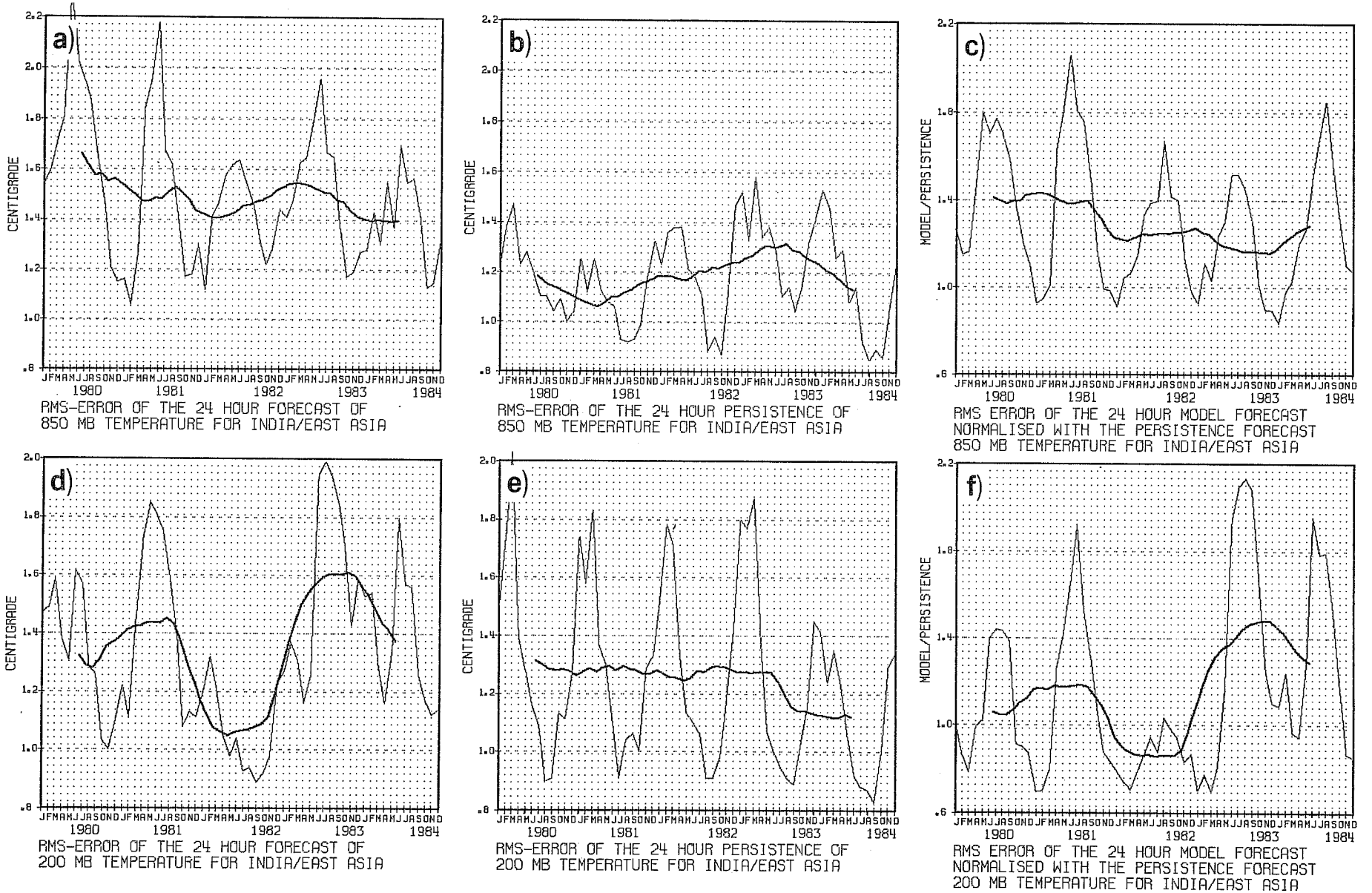

Fig. 5 As Fig. 4 but for temperature

However during the northern hemisphere winter the sub tropical jet moves southwards bringing the region under the influence of mid-latitude 'weather'; this is a period of relatively large temperature and wind fluctuations. The 24 hour model forecasts at 200 mb for temperature (Fig. 5d) and wind (Fig. 4d) show more random, and, at least for the wind, weaker fluctuations in skill for the India/East Asia region than the persistence forecasts. The model wind forecasts for this region (Fig. 4a,d) show greatest skill in late summer/early autumn and least in winter. It is difficult to distinguish any clear annual cycle in the model temperature scores at 200 mb but at 850 mb the model forecasts show a stronger annual cycle than for the persistence forecasts with the model forecasts having largest errors in winter and smallest in summer. Although both model and persistence forecasts are better in summer than in winter in this region, because the seasonal variability in the skill of the model forecast is relatively small, the model forecasts are more useful, relative to persistence, in winter than in summer. This can be clearly seen from Figs. 4c,f and Figs. 5c,f which show the 24 hour normalised rms model forecast error at 850 and 200 mb in the India/East Asia region for the vector wind and temperature.

(b) Central Africa

The wind scores for central Africa (Fig. 6) also exhibit an annual cycle, but in contrast to the scores for India (Fig. 4) the cycle is more prominent in the model errors than in the persistence errors. Also, the cycle is 180° out of phase with that over India; the better model forecasts occurring in winter. The persistence forecasts at 200 mb exhibit more of a semi-annual cycle with the best forecasts being during the equinones; at 850 mb it is difficult to distinguish any period behaviour. The normalised scores (Figs. 6c,f) indicate big improvements over the last few years particularly at 850 mb.

(c) Indonesia

The wind scores for the Indonesian region, Fig. 7, show a clear semi-annual cycle at both 850 and 200 mb, the scores at these two levels being in phase. Greatest skill occurs during the equinoxes; this is a time of least transient activity in these regions.

2.3 Forecasts beyond 24 hours

At 850 mb the model and persistence forecast scores for 48 hours are similar in character to those at 24 hours both for the tropical belt as a whole and regionally. The 48 hour rms errors at 850 mb are typically 1 m s^{-1} larger than those at 24 hours, corresponding to an increase of about 20%. The scores at 48 hours have a larger temporal variability than those at 24 hours; the annual and semi-annual signals apparent in the 24 hour scores being enhanced in the 48 hour scores. Fig. 8 is a good example of this (c.f. Fig. 4). These remarks for the 850 mb scores apply equally well to those at 200 mb although at this level the errors typically increase by about 2 m s^{-1} which is again ~20%.

As the errors of both the model and persistence forecasts increase between 24 and 48 hours by similar amounts, the normalised error (i.e. the model error relative to persistence error) changes very little. Compared to persistence the 48 hour model forecast at 200 mb is almost as good as the 24 hour model forecast, both of which are better than persistence.

Both the model forecast and the persistence forecast rms errors increase with forecast length. Fig. 9 shows the rms vector wind error as a function of forecast length for model and persistence forecasts at 850 and 200 mb for

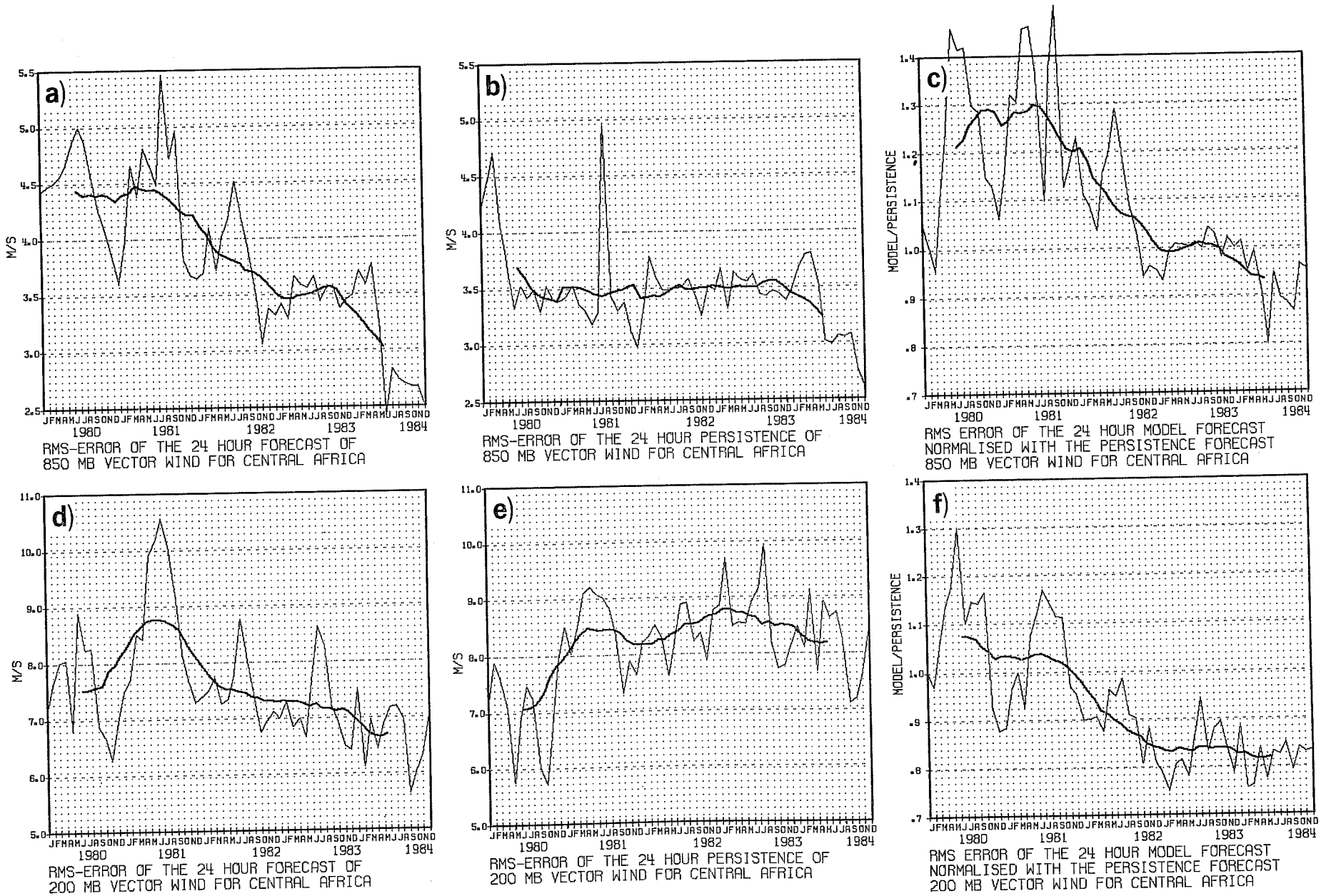

Fig. 6 As Fig. 2 but for central Africa. Area 3 in Fig. 1

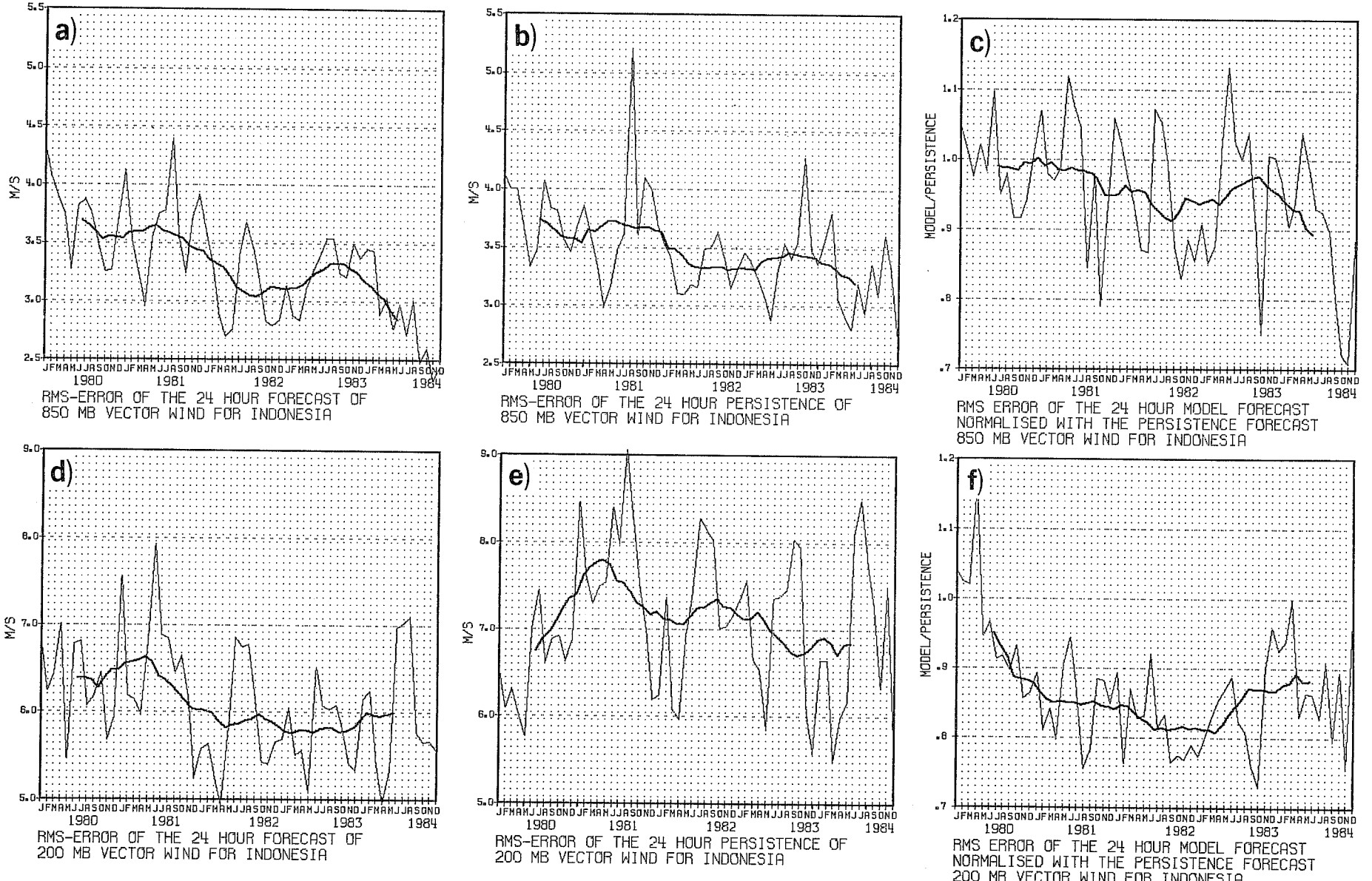

Fig. 7 As Fig. 2 but for Indonesia. Area 2 in Fig. 1

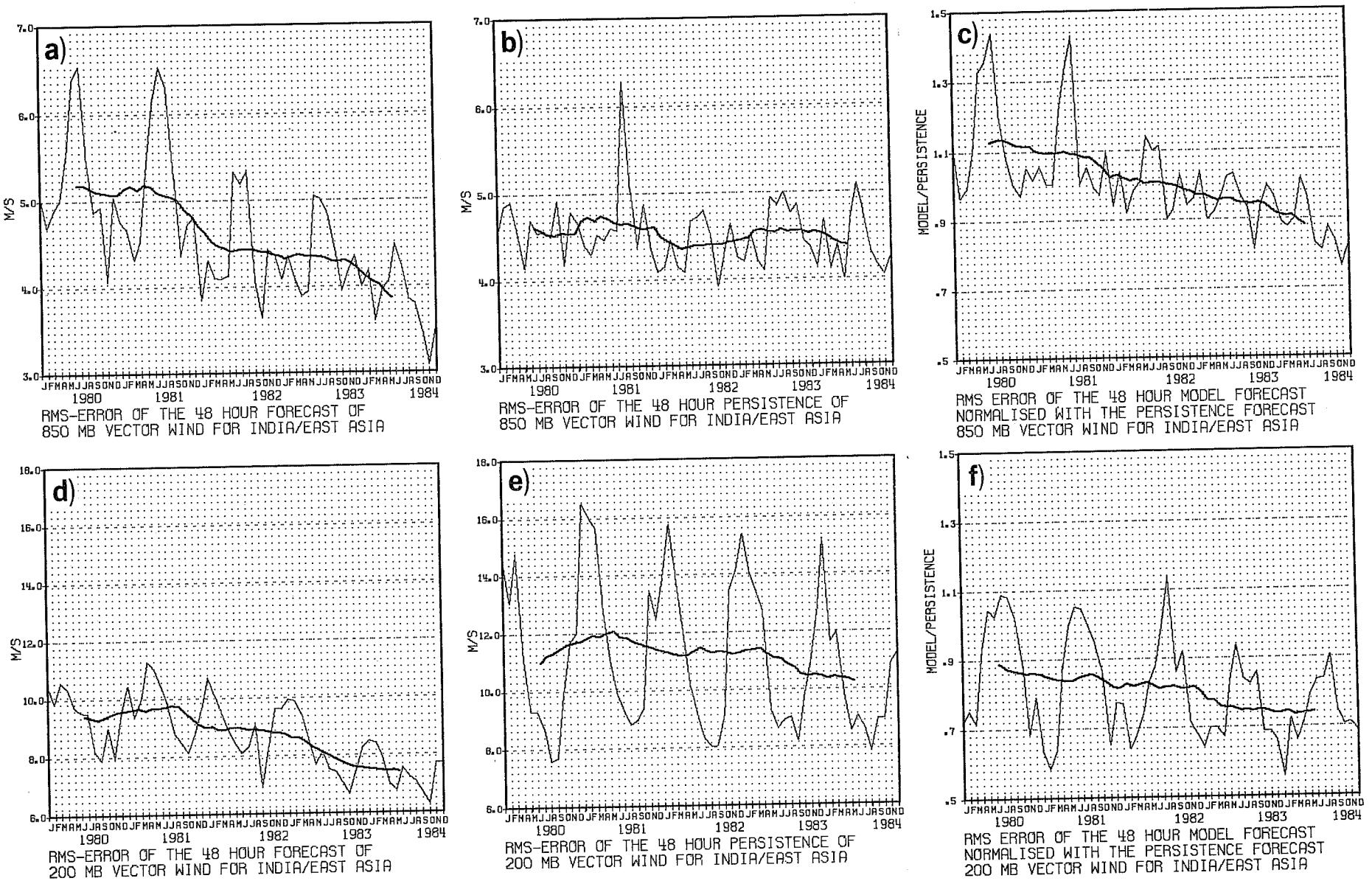

Fig. 8 As Fig. 2 but for India/East Asia, Area 1 in Fig. 1, for the 48-hour forecasts.

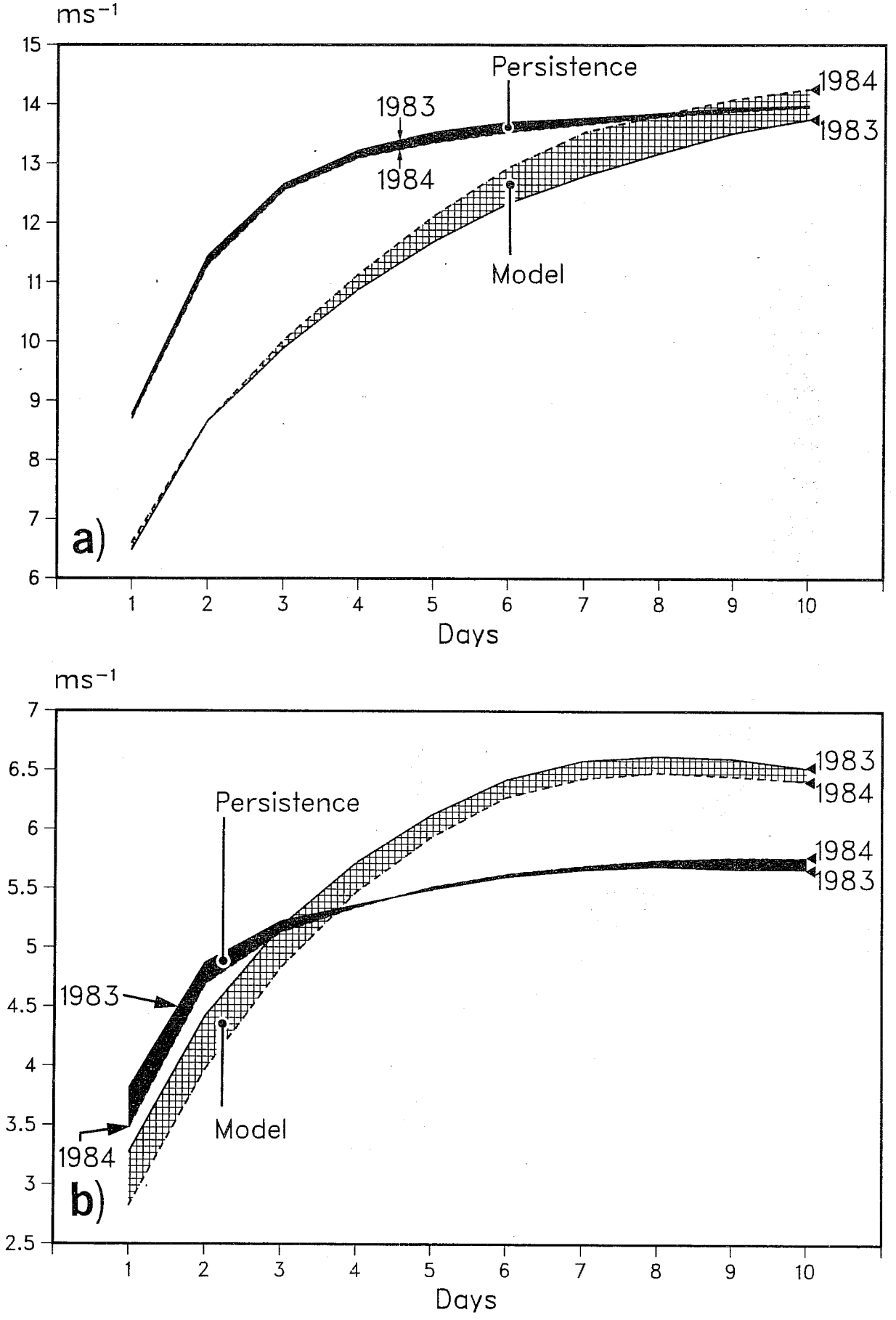

Fig. 9 RMS vector wind forecast error as a function of forecast length, for the tropical belt, 18N-18S, as a mean over the periods i) June-Dec 1983 and ii) June-Dec 1984.
a) 200 mb b) 850 mb

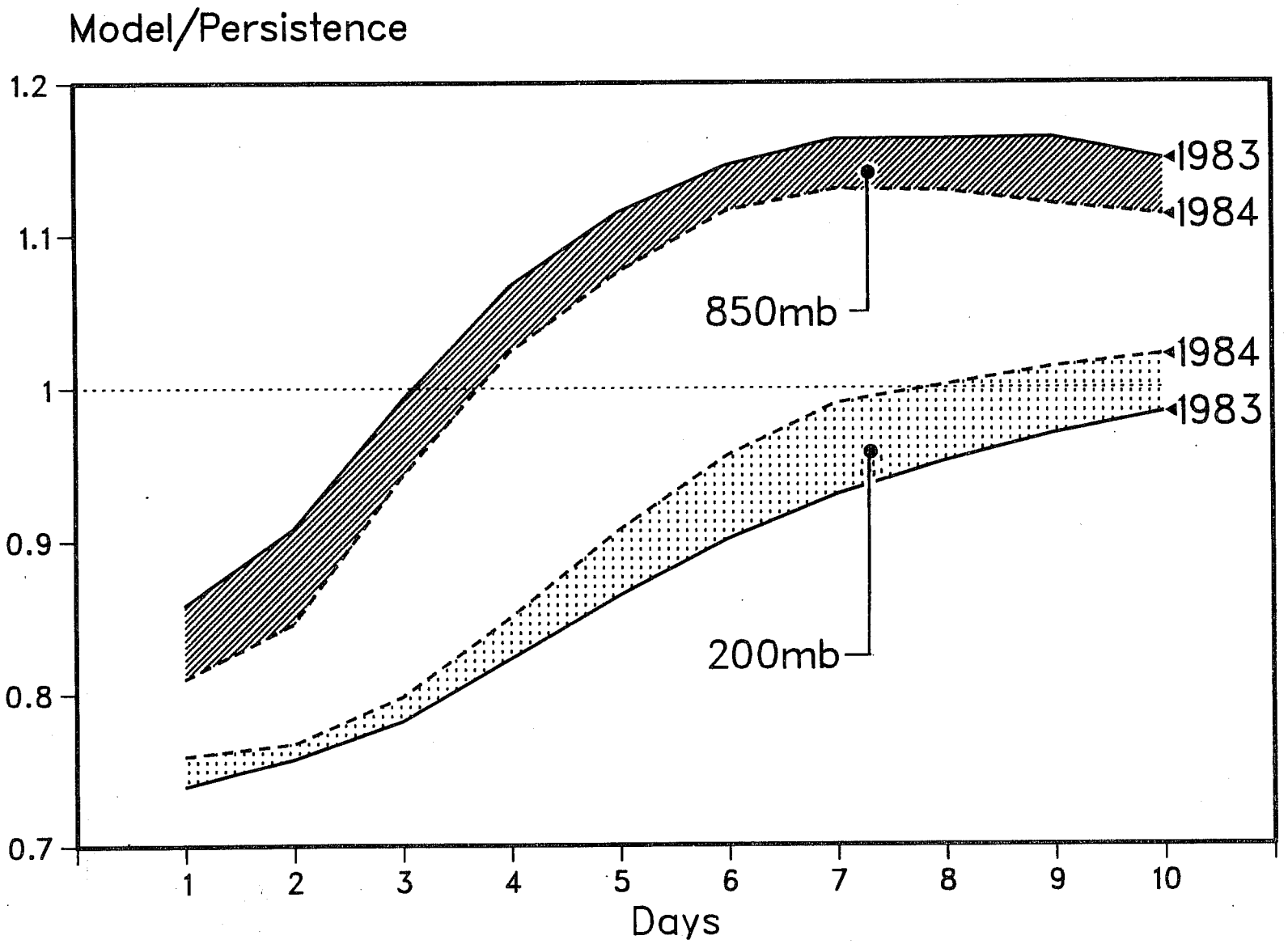

Fig. 10 RMS vector wind model forecast error normalised by the persistence error, as a function of forecast length, for the tropical belt. 18N-18S as a mean over two periods (i) June-Dec 1983 and (ii) June-Dec 1984

June-Dec 1983 and June-Dec 1984 for the tropical belt. These six month periods were chosen because the main change in the forecasting system between these two periods was the introduction of the new analysis system and the diurnal cycle in May 1984. At 200 mb there appears to be a clear deterioration in the forecast quality between 1983 and 1984; this is true throughout the ten days of the forecasts, but particularly clear after about three days. In contrast the persistence forecast at 200 mb shows a clear reduction in rms error throughout the ten days of the forecasts.

At 850 mb there is an equally clear reduction in rms forecast error between 1983 and 1984, and again this is evident throughout the ten days of the forecasts. Unlike the changes in quality of the 200 mb forecasts, those at 850 mb are largest during the first few days of the forecasts. The persistence forecasts show a reduced rms error at 850 mb up to about day four and thereafter a slight deterioration.

When the rms errors are normalised with the persistence errors (Fig. 10) the differences between 1983 and 1984 are even more apparent, showing a clear improvement at 850 mb and deterioration at 200 mb. The 200 mb forecasts are still very much better than those at 850 mb when compared with a persistence forecast; being better than persistence to about day eight, even in 1984. At 850 mb the model forecasts now beat persistence out to about $3\frac{1}{2}$ days.

2.4 Summary of objective scores

Underlying the annual and semi-annual cycles in forecast skill, one can see a steady improvement in forecast predictability over the last few years. Availability of conventional data in the tropics has declined since the FGGE during 1979, this factor could influence the scores through the effect of the

first guess field (in the absence of observational data the model will, in effect, be verified against itself). However, the scores over relatively data rich regions e.g. India, show the same general trend. Also, the use of satellite data has improved in recent years. There is some confidence that this trend is real. The wind scores show few sharp jumps in the underlying trend and except in a few cases it is difficult to assign credit to particular model or analysis changes for this very definite reduction in the errors. The 200 mb flow is more predictable (relative to persistence) than that of 850 mb, and at both these levels the forecasts are now useful (i.e. better than persistence) at least to three days. This is, however, a poor performance when compared to the quality of mid-latitude forecasts (Bengtsson and Simmons, 1983).

3. SYSTEMATIC ERRORS OF THE FORECASTS AND ANALYSES

The rest of this report will discuss systematic errors of the time mean flow. As far as possible the uninitialised analyses have been used for verifying all fields; the one exception is the vertical velocity which was only available from the archives in initialised form during the periods studied.

The diurnal cycle was introduced into the forecasting system in May 1984. For periods prior to this the analysis and first guess fields, as presented here, include both the 00Z and the 12Z fields (in order to mitigate the influence of the diurnal cycle, which is introduced into the analysis through the data); after May 1984 they include only the 12Z fields. In this way the most appropriate 'analysis' is used for verification.

All the fields shown are means over monthly or seasonal periods and the forecast ensembles are means over verifying dates, e.g. for any given period the mean of the one day forecasts will contain a different ensemble to the mean of the ten day forecasts.

For convenience the terms 'summer' and 'winter' are used to denote the northern hemisphere summer and winter. Their use is merely to denote the time of year and not used to imply any specific seasonal characteristics.

Much of the discussion will concentrate on comparing summer 1983 with summer 1984.

3.1 Zonal mean errors

Before describing the errors themselves it is worthwhile looking at the analyses. Fig. 11 shows the zonal mean analyses of temperature and zonal wind for JJA 1984. Summer 1984 is fairly similar to summer 1983 though the tropical stratosphere is slightly cooler in 1984 (this may be a result of the El Chicon erruption in 1983) and the tropical stratospheric easterlies are stronger. The southern hemisphere subtropical jet is slightly weaker in 1984 and the northern hemisphere subtropical jet is slightly stronger.

Fig. 12 shows the forecast zonal mean temperature errors at day five for a) DJF 1982/83; b) JJA 1983; c) DJF 1983/84; and d) JJA 1984. In each case the forecast errors indicate a strong warming in the region on and immediately below the equatorial tropopause. The warming shows little seasonal variation (compare 12b and 12c), but a slight latitudinal migration occurs.

Above this warming, in the equatorial stratosphere, the forecast errors show a strong cooling; this cooling extends from pole to pole but has a maximum extending over about the same latitude range as the warming at and immediately below the equatorial tropopause. The cooling starts at about 100 mb and increases in magnitude with height.

In the lower and mid-equatorial troposphere, the forecast errors show a cooling. Although the overall cooling shifts slightly meridionally with the seasons, the area of maximum cooling appears quite stationary, being located between the equator and 15°N, and at about 700-900 mb.

Fig. 13 shows the zonal mean vertical temperature profile for the belt 30°N to 30°S for a)DJF 1982/83; b) JJA 1983; c) DJF 1983/84; d) JJA 1984. In

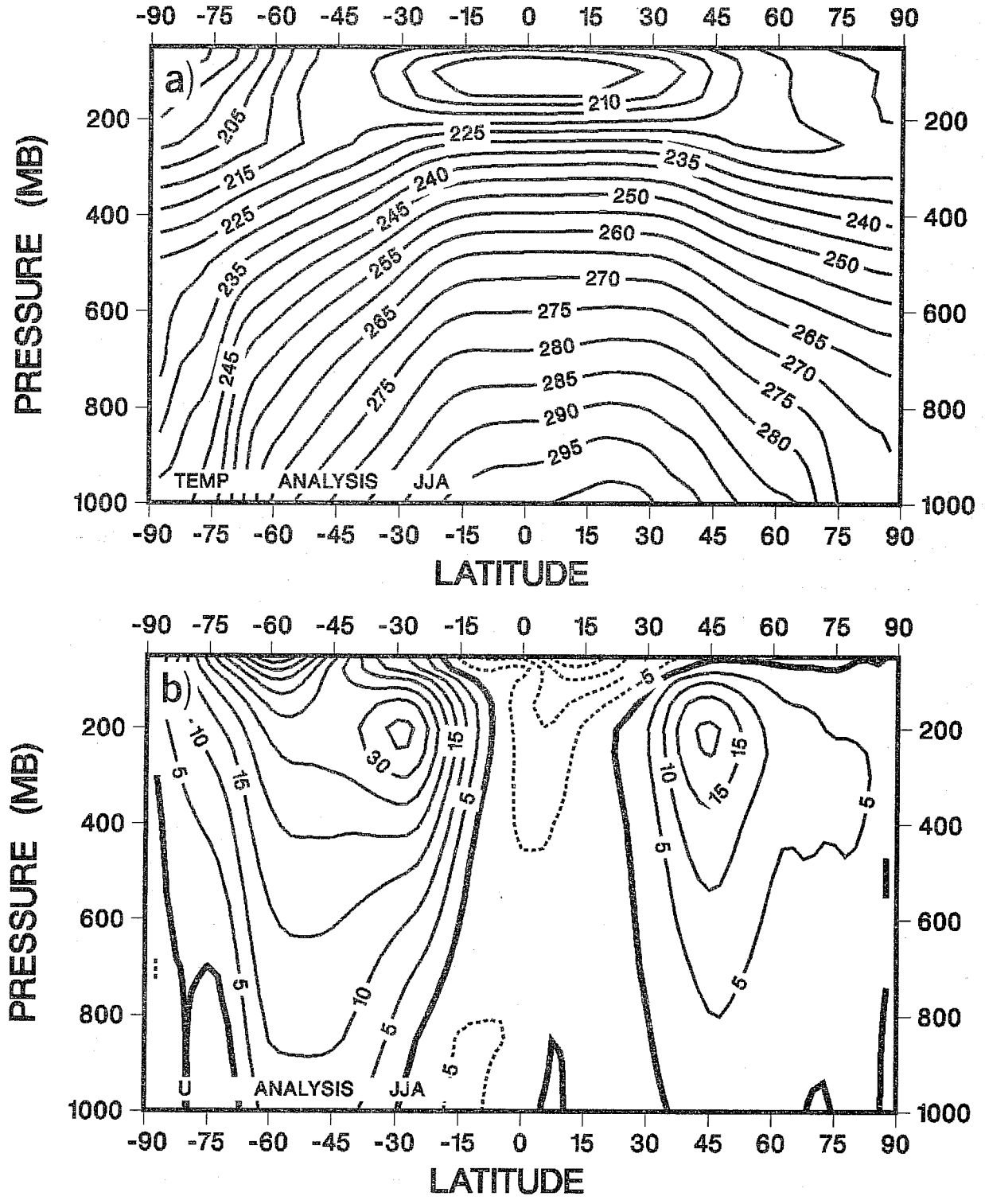

Fig. 11 Zonal mean cross sections of the uninitialised analyses for JJA 1984.
a) Temperature Units: K
b) Zonal wind Units: ms^{-1}

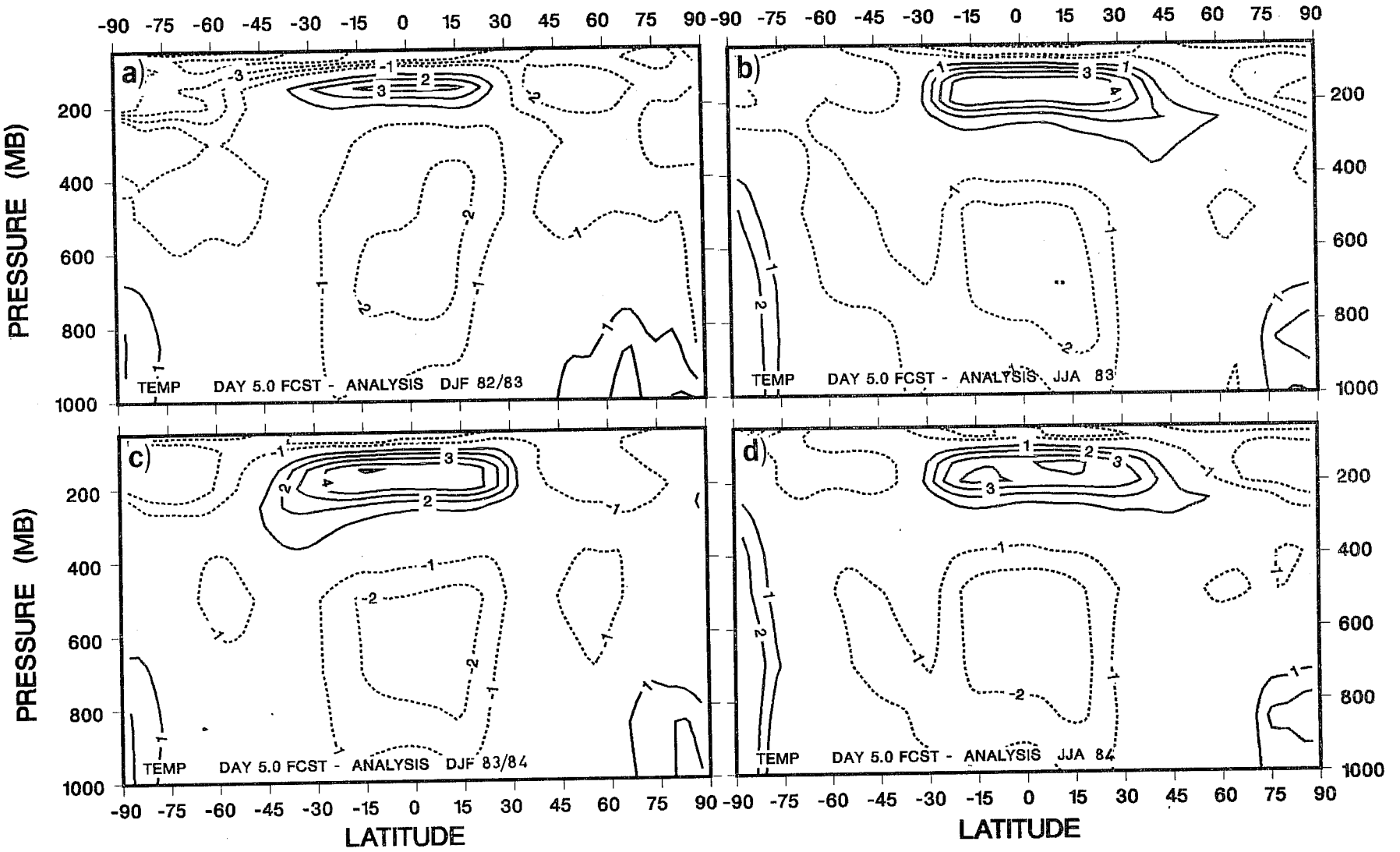

Fig. 12 Zonal mean cross sections of the 120 hour forecast errors of temperature. Units °C.
a) DJF 1982/83 b) JJA 1983 c) DJF 1983/84 d) JJA 1984

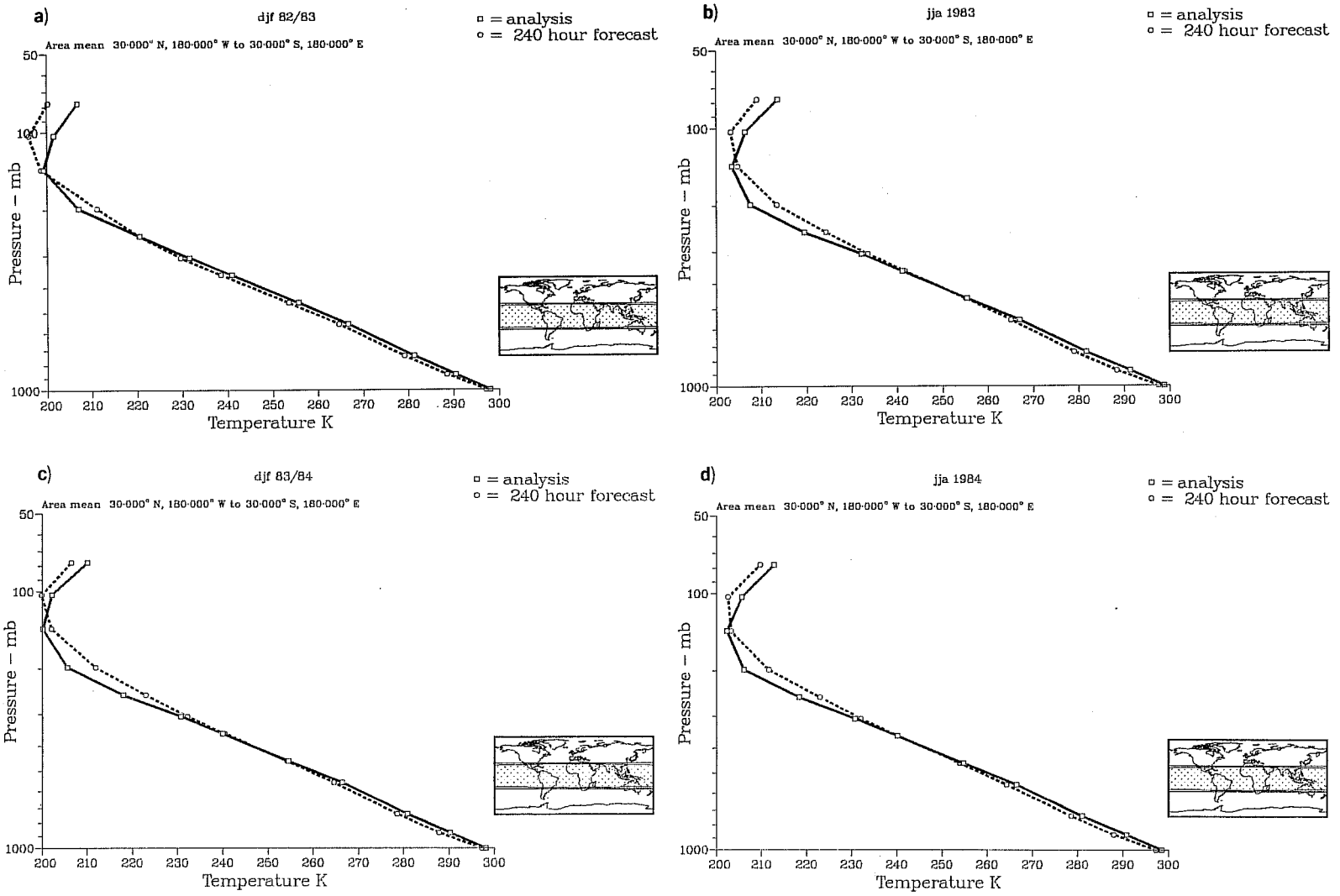

Fig. 13 Zonal mean vertical temperature profiles for the tropical belt 30°N-30°S of (i) the uninitialised analysis and (ii) the 240 hour forecast. Units: K a) DJF 1982/83 b) JJA 1983 c) DJF 1983/84 d) JJA 1984

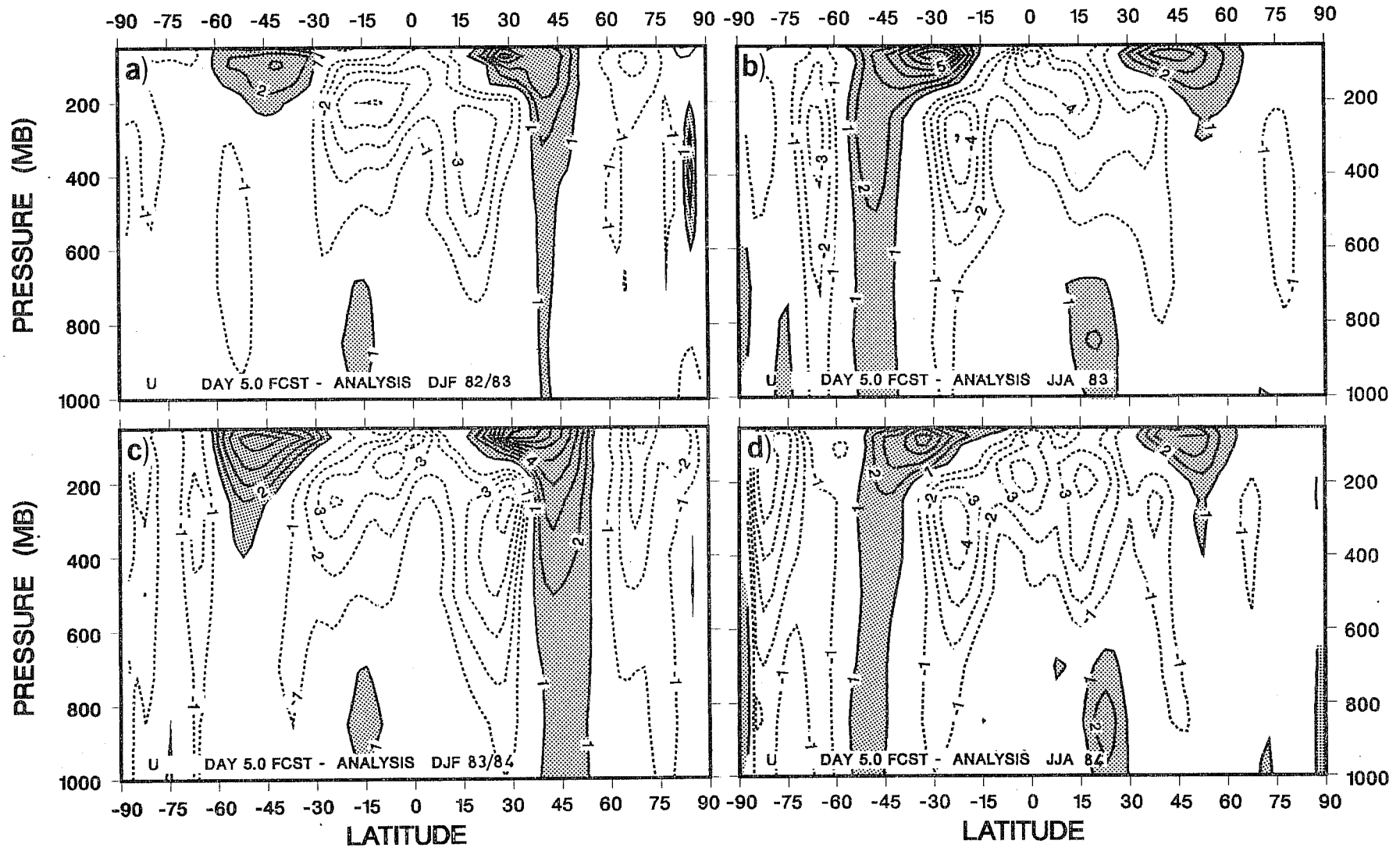

Fig. 14 Zonal mean cross sections of the 120 hour forecast errors of zonal wind. Units m s^{-1}.
a) DJF 1982/83 b) JJA 1983 c) DJF 1983/84 d) JJA 1984

individual analyses and forecasts the tropopause is sharper than the profiles shown here, (these profiles are means over three month periods); the seasonal change in height of the tropopause manifests itself as a broadening of the tropopause in the mean. In each of the seasons shown there is a vertical displacement of the mean tropopause height from about 150 mb to about 100 mb. The warming immediately below the equatorial tropopause together with the cooling in the mid and lower tropical troposphere increases the stability of the tropical mid and upper troposphere. As the cooling has a maximum at around 700 to 900 mb there is a slight reduction in the stability below this level.

Comparing Figs. 13a and 13c or Figs. 12a and 12c, it is apparent that the grid point model suffered less from the warming below the equatorial tropopause but more from cooling in the mid-troposphere and equatorial stratosphere. It is difficult to ascribe these differences in the errors between the two winters to inter-annual variability in view of their size relative to inter-seasonal variability, and therefore they are most likely due to model changes.

Fig. 14 shows the forecast zonal mean zonal wind field errors at day five for a) DJF 1982/83; b) JJA 1983, c) DJF 1983/84; JJA 1984. As mentioned earlier the temperature errors for the two winters 1982/83, 1983/84 (Figs. 12, 13) have some distinct differences, although similar in their general nature. The wind errors in the sub tropical upper troposphere also have differences; the increased horizontal temperature gradients in 83/84 compared to 82/83 are accompanied by increased vertical wind shear as one would expect from thermal wind balance considerations. In the deep tropical stratosphere the wind errors are similar in both winters despite considerable changes to the temperatures. These errors may be dynamically induced.

There is clearly a relation between the wind and temperature errors in the sub-tropical regions referred to above, but this in itself is no indication as to cause and effect. The temperature errors are consistent with known deficiencies in the radiation scheme. In the formulism used to which the results in this paper relate (Geleyn and Hollingsworth, (1977)), gaseous absorption is considered as a perturbation term against other effects (i.e. Rayleigh scattering and scattering and absorption by clouds and aerosols - the so-called 'grey' gaseous transfer problem). Radiative fluxes are first calculated without any gaseous absorption for each spectral interval. Effective gaseous absorber amounts are then derived from the computed 'grey' fluxes, assuming an isothermal atmosphere; these are then used to compute the broad band transmission functions. Finally, the required fluxes result from applying these transmission functions, using a cooling to space approximation, to the fluxes determined without gaseous absorption.

However, assuming an isothermal atmosphere in the computation of the 'grey fluxes' implies only one source of radiation and leads to difficulties both with emitters within the atmosphere and at the surface, particular difficulties occur in the vicinity of clouds, sharp inversions (e.g. the tropopause) and large gradients in humidity.

The technique also produces an exaggerated masking effect in the presence of partial cloud cover due to the neglect of the absorber gases in the initial calculation of the fluxes; this results in a relative warming near cloud base and an enhanced cooling near cloud top. This relative warming, however, partially offsets a general tropospheric cooling and may be responsible for the minima in cooling seen near the equator at about 900 mb in Fig. 3b. The exaggerated cooling near the cloud top (about 500 mb in the ECMWF model) over stabilises, particularly the tropical, upper troposphere.

Apart from the general difficulties of the radiation scheme in the vicinity of sharp inversions, the warming on, and immediately below, the tropical tropopause may also be partly due to a reduced adiabatic cooling associated with a weakened Hadley circulation in the presence of the increased stability.

The stratospheric cooling is partly a product of the cooling to space approximation used in the calculation of the final fluxes, but it may also be partly due to reduced thermal radiation at high altitudes, caused by the exaggerated masking effect of the scheme, implying a lower effective atmospheric temperature.

Recently a revised long wave radiation scheme has been in use at the ECMWF; the absorber gases are incorporated directly through the technique of exponential sum fitting, Wiscombe and Evans (1977), in which the gaseous transmission function is approximated by a series of decaying exponentials, allowing the determination of 'pseudo-grey' gaseous absorption coefficients. Forecasts using this new scheme show a modest reduction in the warming on and immediately below the equatorial tropopause, and reduced stratospheric cooling particularly at the top model level (Ritter, 1985); the errors, although reduced, are still significant.

The warming and cooling changes the horizontal gradients of temperature in the sub-tropics and, through the thermal wind relation, the vertical wind shear. Comparing Figs. 14d and 11b it is clear that the change in the vertical wind shear will effectively modify the sub-tropical jets by shifting them slightly upward and poleward. The changed baroclinicity can be expected to influence

the mid-latitude forecasts of transient phenomena. It is possible that the wind errors are dynamically induced and that the temperature field adjusts to the wind field. Possible mechanisms include the absence of orographic forcing through form drag and gravity wave breaking, and vertical momentum transports through cumulonimbus convection (Miller and Moncrieff, 1984).

In the sub-tropics, apart from the wind errors at or near the tropopause discussed above, the wind errors show a dependence on the magnitude of the zonal mean flow; the errors being larger in the winter hemisphere than in summer hemisphere (where the flow is weaker).

The changes in the zonal wind errors between summer 1983 and summer 1984 are smaller than those between the two winters. During this period a slight improvement can be seen in the upper stratosphere and a slight deterioration in the tropical upper troposphere and lower stratosphere. This is in agreement with a slight reduction in the temperature errors in the upper stratosphere.

It is interesting to note that the temperature errors in the NCAR community climate model, Fig. 15a, show a cooling throughout the depth of the tropical atmosphere with no evidence of any particular problems at the tropopause. The wind errors, Fig. 15b, in agreement with this are almost barotropic. (Baumhefner, personal communication).

The zonal mean temperature error for the tropical belt, 30°S to 30°N, for a number of forecast lengths is shown in Fig. 16, for JJA 1984. The error growth is very similar to that of JJA 1983 (not shown) but the error at 200 mb and above is slightly reduced in summer 1984. The error growth is consistent

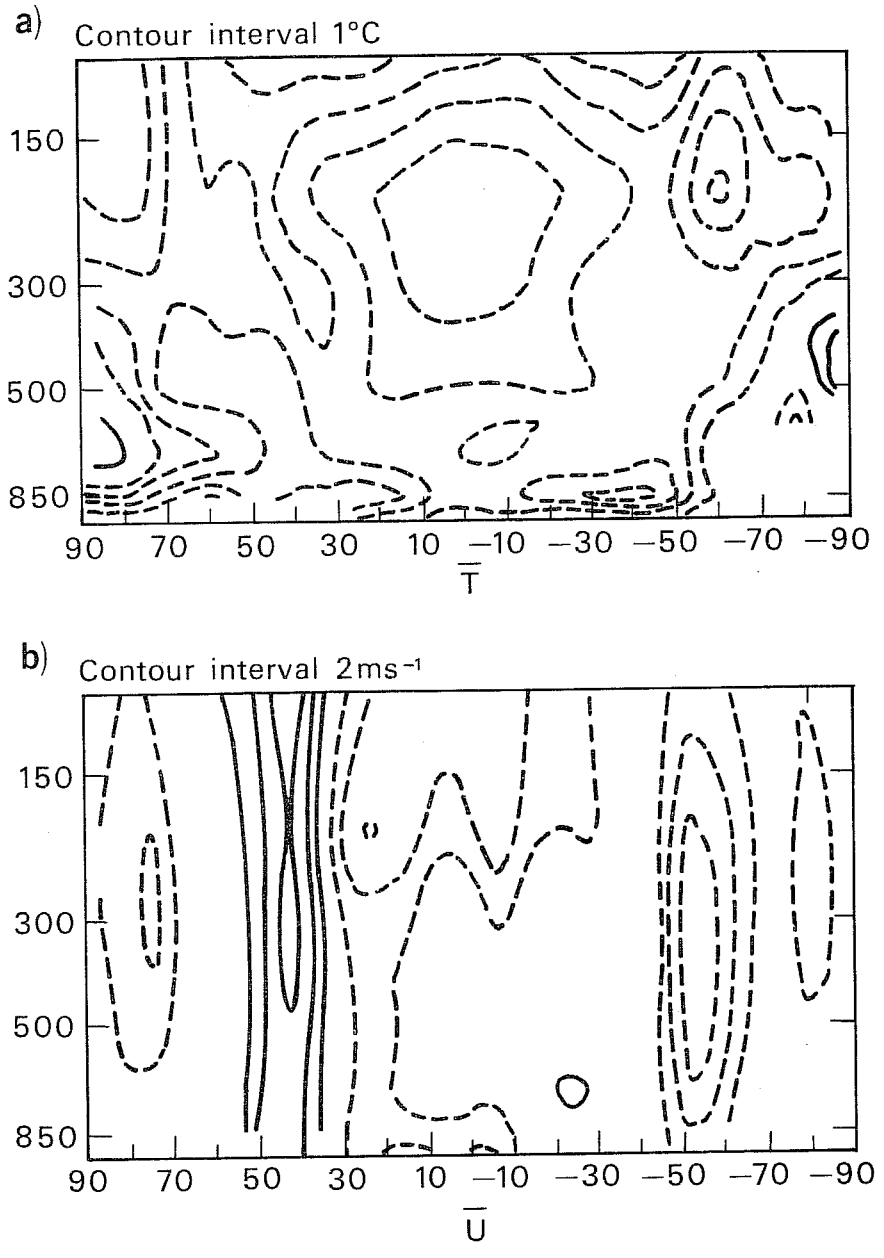

Fig. 15 Zonal mean cross sections of the systematic errors in the NCAR community climate model.
a) Temperature Contour interval 1°C
b) Zonal wind Contour interval 2 m s^{-1}
Solid lines positive, dashed lines negative
(Baumhefner, personal communication)

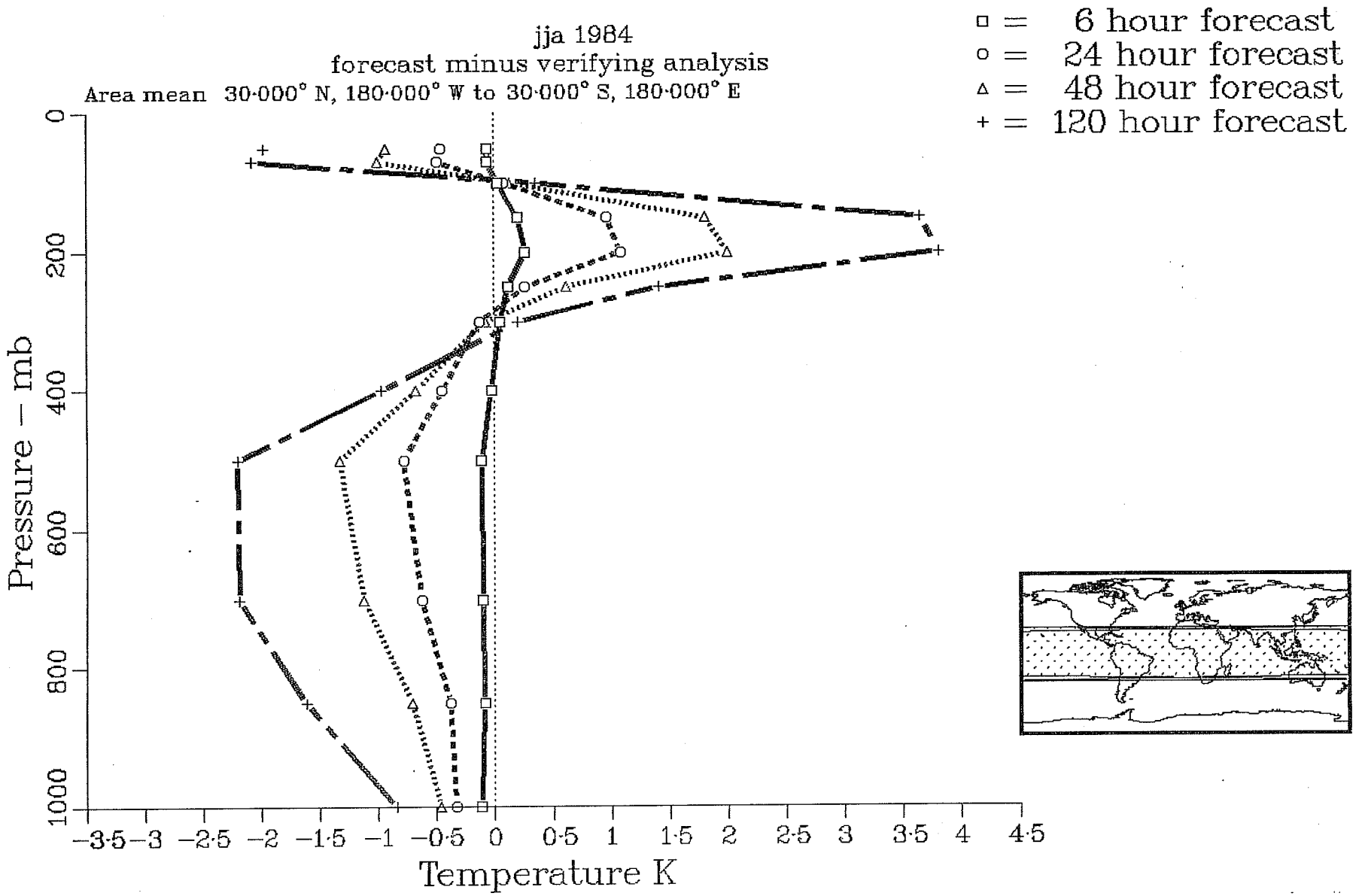

Fig. 16 Zonal mean temperature error for JJA 1984, for the tropical belt 30°N-30°S

from the 6-hour forecast onwards, showing a general cooling below about 300 mb, a warming between 300 and 100 mb, and a cooling above. The growth rate of the error is rapid at first and then slows down; it is not linear, although it is not far from it, particularly during the first few days. The figure indicates rapid and large changes in stability.

The mean meridional circulation for JJA, 1983 is illustrated in Fig. 17 and for JJA 1984 in Fig. 18; these show a) the initialised analysis of the omega field (dp/dt), and c) the corresponding uninitialised analysis of the meridional velocity. The Hadley, Ferrel and high-latitude direct cells are all clearly evident.

Corresponding fields for the 5-day forecasts are also shown in Figs. 17 and 18. The meridional velocity at 10°S and 150 mb in 1983 has been reduced from 2.5 m s^{-1} to 1.5 m s^{-1} in the forecasts. Vertical velocities show a single maximum in the mid troposphere rather than separate maxima in the upper and lower troposphere, although there is some doubt as to the validity of the analyses in this respect (Arpe, 1985). Loss of the maxima in the upper troposphere is consistent with the increased static stability associated with the warming below the tropical tropopause. The decreased static stability close to the surface, associated with the maximum cooling being in the mid troposphere, may act to enhance the vertical circulation in the lower troposphere.

Summer 1984 shows a weaker Hadley circulation in the analyses than that of summer 1983, this is also reflected in the 5-day forecasts. The weakening of the upper level circulation in the forecasts that was so apparent in 1983 is less so in 1984; this may be because it is already weak in the analyses.

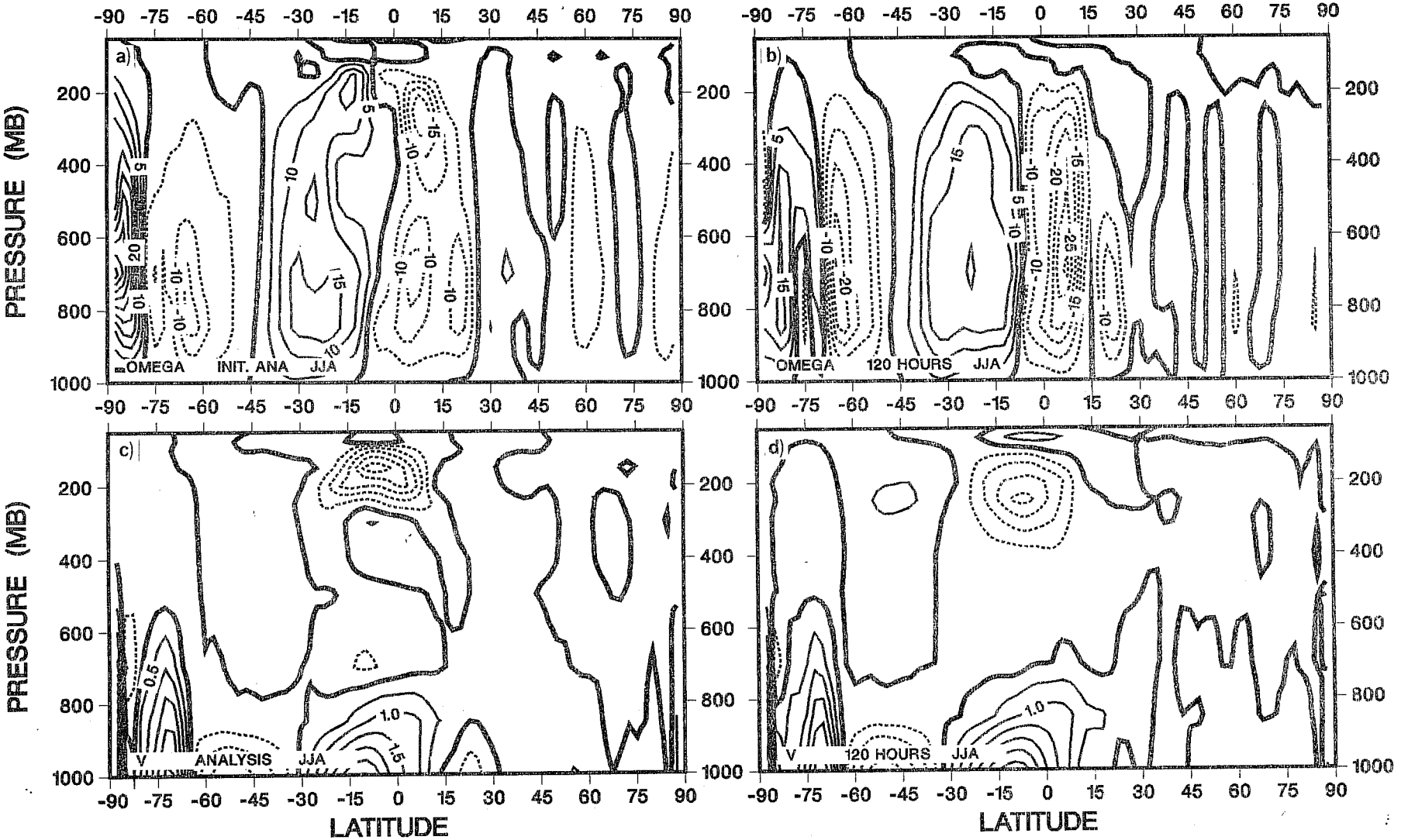

Fig. 17 Zonal mean cross sections for JJA 1983 a) The (initialised) analysis of ω b) The 120 hour forecast of ω c) The analysis of meridional wind d) The 120 hour forecast of meridional wind Contour intervals 0.5 m s^{-1} for v and 5 mPa s^{-1} for ω

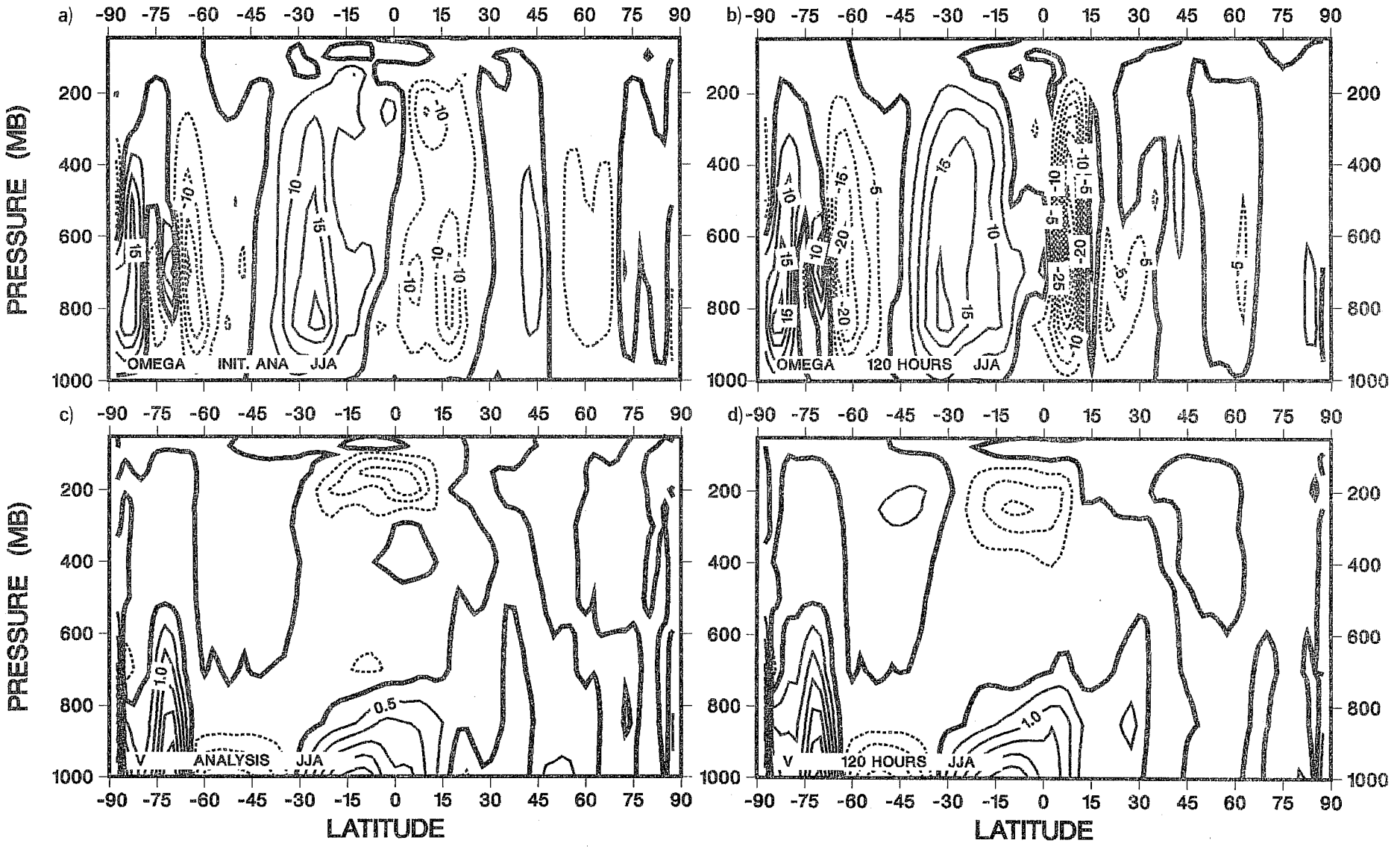

Fig. 18 As Fig. 17 but for JJA 1984

3.2 The temperature errors

Fig. 19 shows the 48 hour forecast temperature errors for summer 1984. In the mid and lower tropical troposphere the forecasts show a tendency to cool the atmosphere. At 1000 and 850 mb this cooling is largely associated with the tropical continents (Fig. 19c), and the western coasts of Mexico and South America. However, at very low levels (1000 mb) a warming occurs over the sub-tropical oceanic highs. At 700 mb the cooling becomes less associated with the tropical continents and more associated with the tropical oceans (Fig. 19b). The errors at 300 mb are quite small, whereas at 200 mb there is a fairly uniform warming over much of the tropical belt. At 150 mb there is again a general warming over the whole tropical belt but distinct, seasonal, local maxima occur located in the vicinity of the Arabian Sea in summer (Fig. 19a) and, to a lesser extent, southern Indonesia in winter (not shown). The stratosphere exhibits a cooling that increases with height.

Another distinct seasonal variation in the temperature errors is a low level cooling over India, Burma and southern China that occurs in summer, and a warming over southern China that occurs in the winter; again this is most likely linked to the seasonal excursion of the monsoons.

The errors are quite similar in character to those of summer 1983, especially at lower levels; at 150 mb the errors in summer 1984 are slightly smaller and appear to be less uniform along the tropical belt.

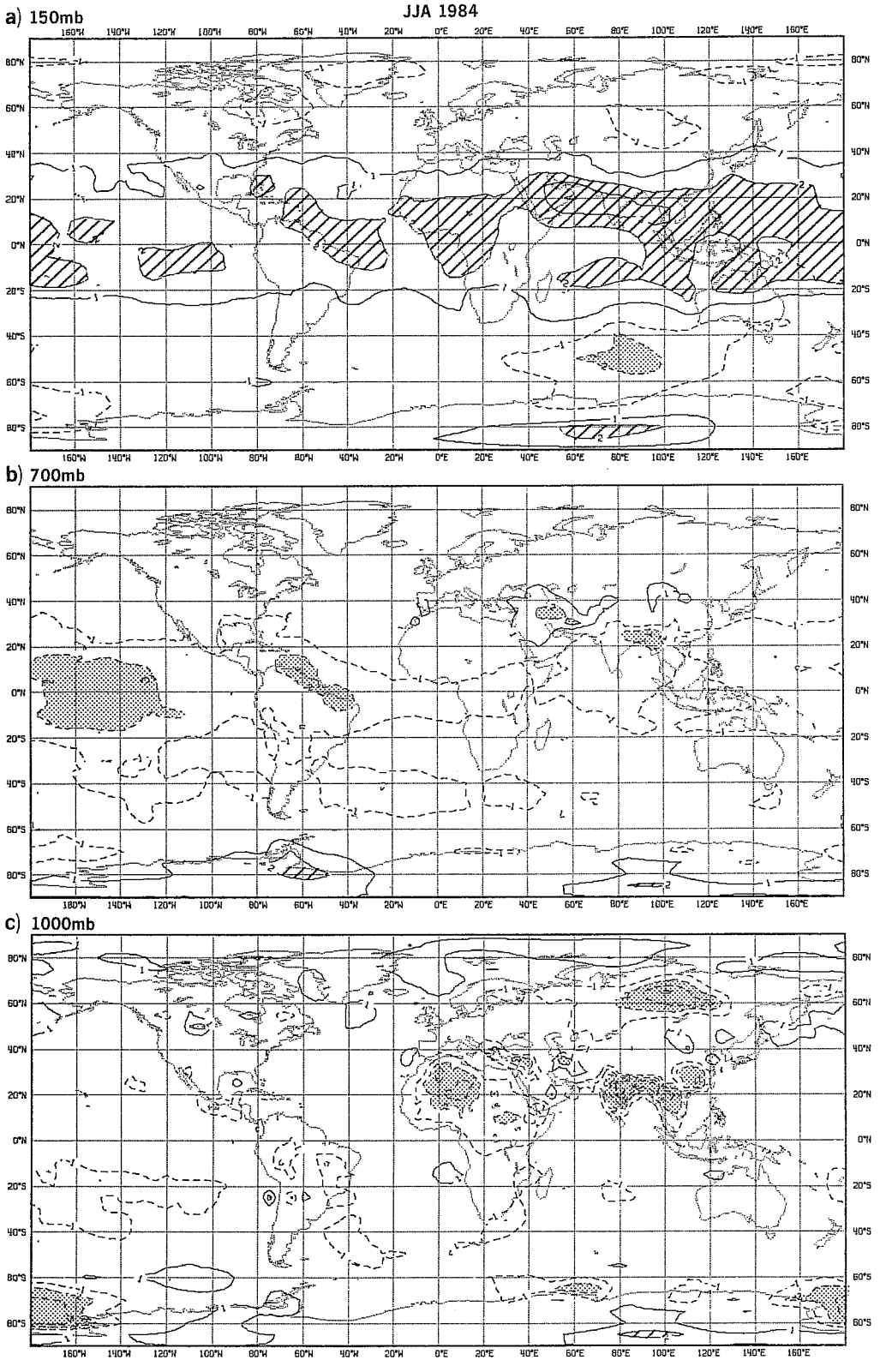

Fig. 19 The errors in the 48-hour forecast of temperature for JJA 1984
a) 150 mb
b) 700 mb
c) 1000 mb
The resolution is 5° lat/long and the contour interval is 1°C. Positive errors are drawn solid and negative dashed. Errors greater than $|\pm 2°C|$ are shaded.

3.3 The humidity field

Specific humidity has been calculated from monthly means of temperature and relative humidity. Since it is a non-linear function of these variables (due to the temperature dependence) the field shown here is only an approximation to the monthly mean of the specific humidity as calculated from daily values of temperature and humidity. As the temperature variability is much less in the tropics than in the extratropics the approximation will be better for the tropics than for the extratropics. This report will only concern itself with gross features of the humidity field in the tropics and these agree reasonably well with daily values. The above remarks also apply to the calculation of equivalent potential temperature (θ_e).

Fig. 20a shows Oort's (1983) climatological estimate of the 850 mb specific humidity for June, July and August. The corresponding ECMWF analysis field for JJA 1983 is shown in Fig. 20b.

In comparing the ECMWF analyses of specific humidity with the climatological values given by Oort (1983) one finds that, in general, the analyses are too moist in the lower troposphere, about right at 300 mb and too dry above this level. Differences are largest near the surface and are consistent both spatially and temporally. Both Oort's climatology and the analyses should be most reliable over areas with a dense radiosonde network. Elsewhere (e.g. the oceans and deserts), Oort's climatology is presumably less reliable, and the analyses will be based primarily on the first guess forecast humidity field. The analyses show low humidity over deserts which may be more reasonable than Oort's values. The largest discrepancies, however, occur over the non-desert

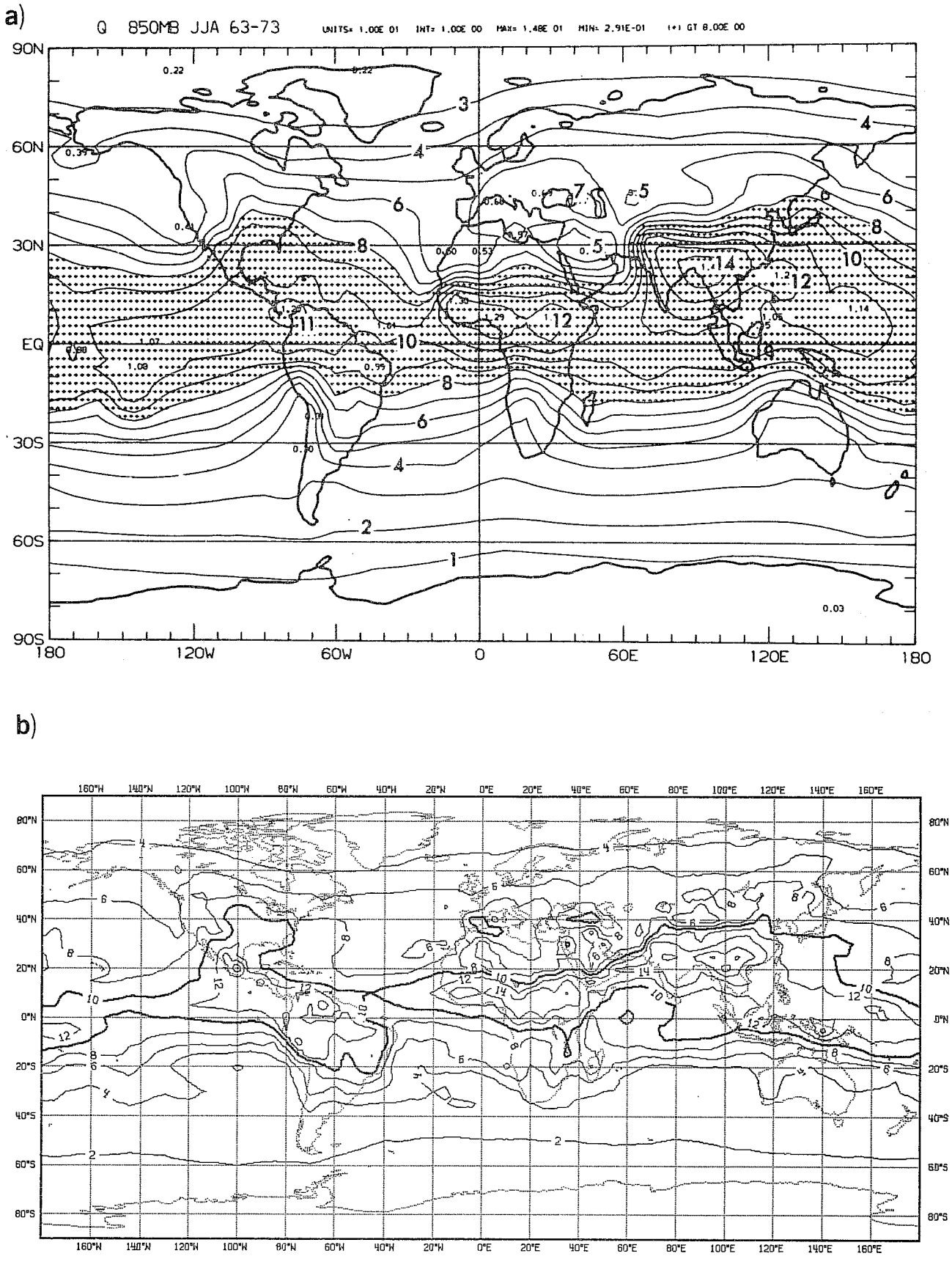

Fig. 20 Specific humidity at 850 mb for JJA
a) Climatology (from Oort (1983)) Units g kg^{-1}
b) ECMWF analysis 1983 (resolution 5° lat/long)

areas of the tropical continents where one should have a greater confidence in both Oort's climatology and in the analyses. If one believes Oort's climatology, then it must be concluded that the analyses are too moist in the lower troposphere.

This is in general agreement with some recent findings of Illari (personal communication) who has verified the model first guess fields directly against radiosonde observations. Illari found that for the tropics (20°N-20°S) the first guess field tended to be too moist between the surface and about 700 mb and too dry above 700 mb.

The reason for this error in the humidity analyses is at least partly understood. Both the initialisation and the analysis itself act as filters on small scale features in the divergence field. Initialisation has a damping effect because the physical tendencies used in the initialisation are explicitly filtered both temporally and spatially in order to avoid projection of the divergence field onto unrealistic structure in the diabatic heating. The analysis has a damping effect because the analysed increments (deviations of observations from the first guess) are effectively constrained to be non-divergent on all but the very largest scales (see e.g. Daley, 1983). These factors together lead to a tropical divergence field that is erroneously weak at small scales. The forecast model takes some time to recreate divergence on these scales. This process is often referred to as 'spin up'. Model convection is partly driven by intense small scale convergence (due to the dependence of the convection parameterisation on moisture convergence) and this may be one reason why it is initially too weak.

During the first few hours of the forecasts there is a net increase in the specific humidity at all levels. This does not imply that the model atmosphere is too dry; it is a consequence of the spin up time of the model divergence. Fig. 21 shows the mean precipitation and evaporation rates for a) 1983, and b) 1984, as a function of forecast length, averaged over the tropical and sub tropical belt (30°N to 30°S), for the months of June, July and August. The evaporation starts almost immediately; the precipitation, however, is delayed.

Thus in the first few hours of the forecast there is an excess of evaporation over precipitation and consequent moistening of the model atmosphere. These remarks are particularly relevant to the 6-hour forecast used in the data assimilation cycle. In the absence of data the analysis/assimilation moistens the low levels to an extent that the evaporation is sufficiently reduced to balance the weak precipitation in the first guess forecast. In this way a 'wet' analysis is seen to be a direct consequence of a slow spin up of the model convection. The fact that evaporation exceeds precipitation in the assimilation forecasts implies that the humidity data are acting to dry out the analyses, at least in some regions. The spin up problem will not be removed by improving the analysis alone; the drier the analysed moisture field, the greater the excess of evaporation over precipitation that will occur during the spin up. It is necessary to both analyse the humidity field more accurately and to eliminate the spin-up of the model convection.

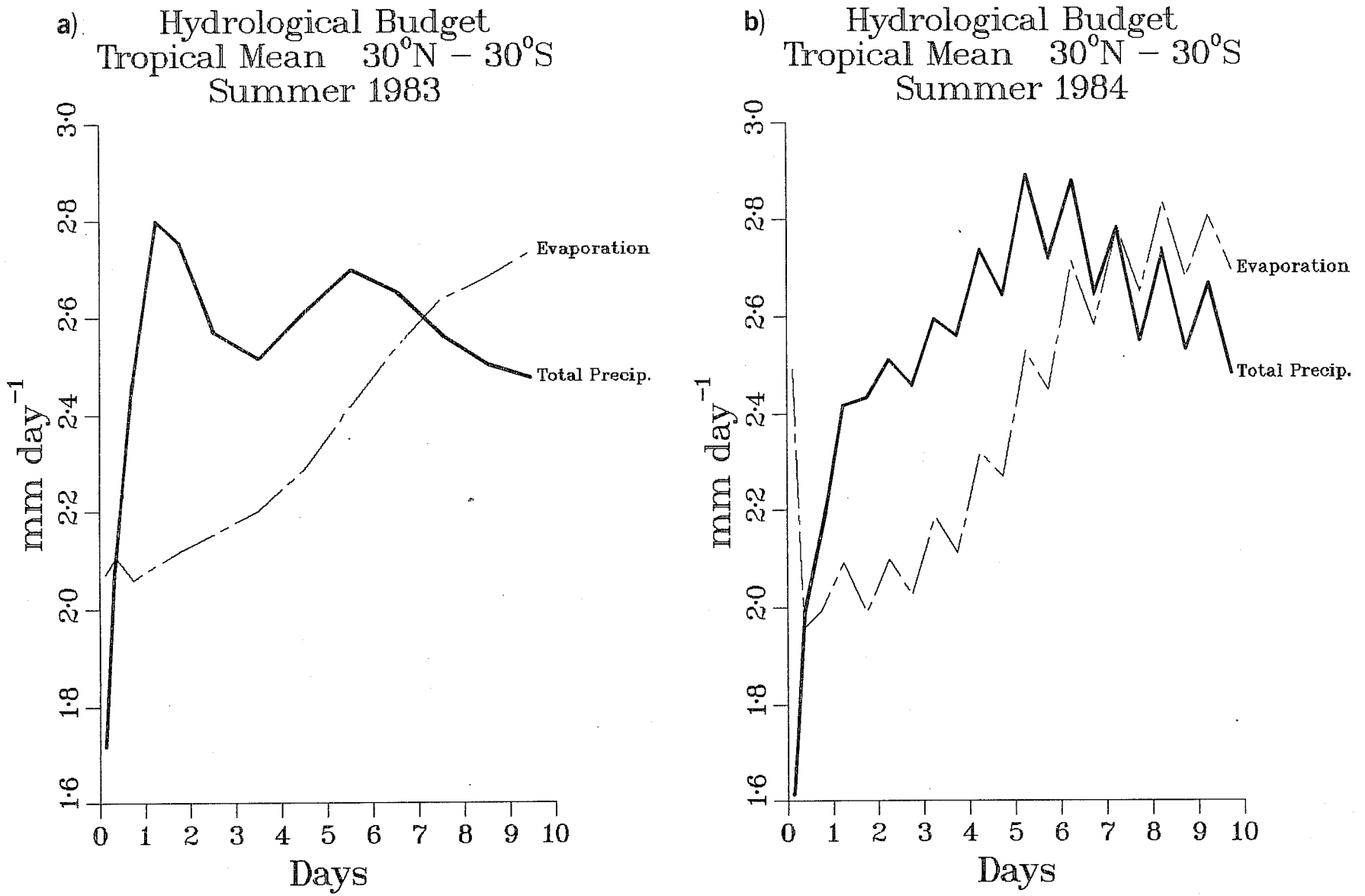

Fig. 21 Mean precipitation and evaporation rates for the tropical belt 30°N-30°S. Units mm day^{-1} a) JJA 1983 b) JJA 1984

After the first few hours of the forecasts, and certainly by 24 hours, the forecasts show a tendency to dry out the mid and lower troposphere: there is an excess of precipitation over evaporation (Fig. 21). This excess is largest at about 36 hours, and in a global mean, decreases to almost zero at day ten: as the relative humidity decreases, evaporation is able to increase. By about ten days the model is beginning to reach some sort of hydrological balance. The excess of precipitation over evaporation between about day 1 and day 6 is not surprising in view of the excessively moist analyses and the further moistening that occurs during the first few hours of the forecasts. The fact that evaporation exceeds precipitation in the tropical regions, in Fig. 21, after about day 7 is reasonable as the area mean contains both the deep tropics and nearly all of the sub tropics; this area as a whole, is a net source of water vapour for the extratropics (see e.g. Sellers, 1966).

These general remarks apply equally well to the summer 1983 and the summer 1984 forecasts. However, comparing Figs. 21a and b it is clear that there are also a number of striking differences.

- In 1984 the evaporation in the six hour forecast is much larger than that in 1983. This is a manifestation of the diurnal cycle. The evaporation has a very strong diurnal cycle over the continents, in the first guess forecasts, evaporating strongly when the sun is overhead and hardly at all at night. The period 06Z to 12Z represents a maximum in the global mean as the sun crosses the Asian, African and European continents. Thus one has to be careful in not concluding that the 'spin up' problem is worse in 1984, as the larger deficit between precipitation and evaporation in the 12Z first guess forecasts, is at least partly, due to a strong diurnal variation in evaporation.

- There is a distinct difference in the nature of the precipitation as a function of forecast length. Prior to the introduction of the diurnal cycle the precipitation showed a very characteristic trend: a sharp rise to a maximum at about 36 hours, a fall to a minima at about day 4, a slight increase to about day 6 and then a slow fall. This trend was clear in both individual forecasts and ensembles, and in summer and winter. The trend in 1984 is quite different, there is now a more steady rise to a maximum at about day 5 then a slow decrease.

- A diurnal cycle in evaporation and precipitation is apparent. It is interesting that this cycle takes several days to establish itself.

3.4 Characteristic regional systematic errors in the thermodynamic structure

Behind the general trend of a cooling and drying of the tropical mid and lower troposphere there exists considerable regional and seasonal variations. As examples, two regions will be discussed in more detail: the equatorial Atlantic and North Africa.

(a) The equatorial Atlantic

Fig. 22 shows the area mean monthly mean forecast changes of a) temperature; b) specific humidity; c) equivalent potential temperature and d) relative humidity as a function of height for the 6, 24, 48 and 120 hour forecasts for JJA 1984. The area is taken to be 3.75°N, 39.375°W, 18.75°S, 9.375°E.

The inability of the forecast model to maintain subsidence inversions of the sub-tropical highs, in a realistic manner, is a very characteristic feature of the tropical forecasts. An example of the structure of the south Pacific trades (19.6°S, 131.3°W) in a single forecast (from 12Z 21/6/79) at day 10 is

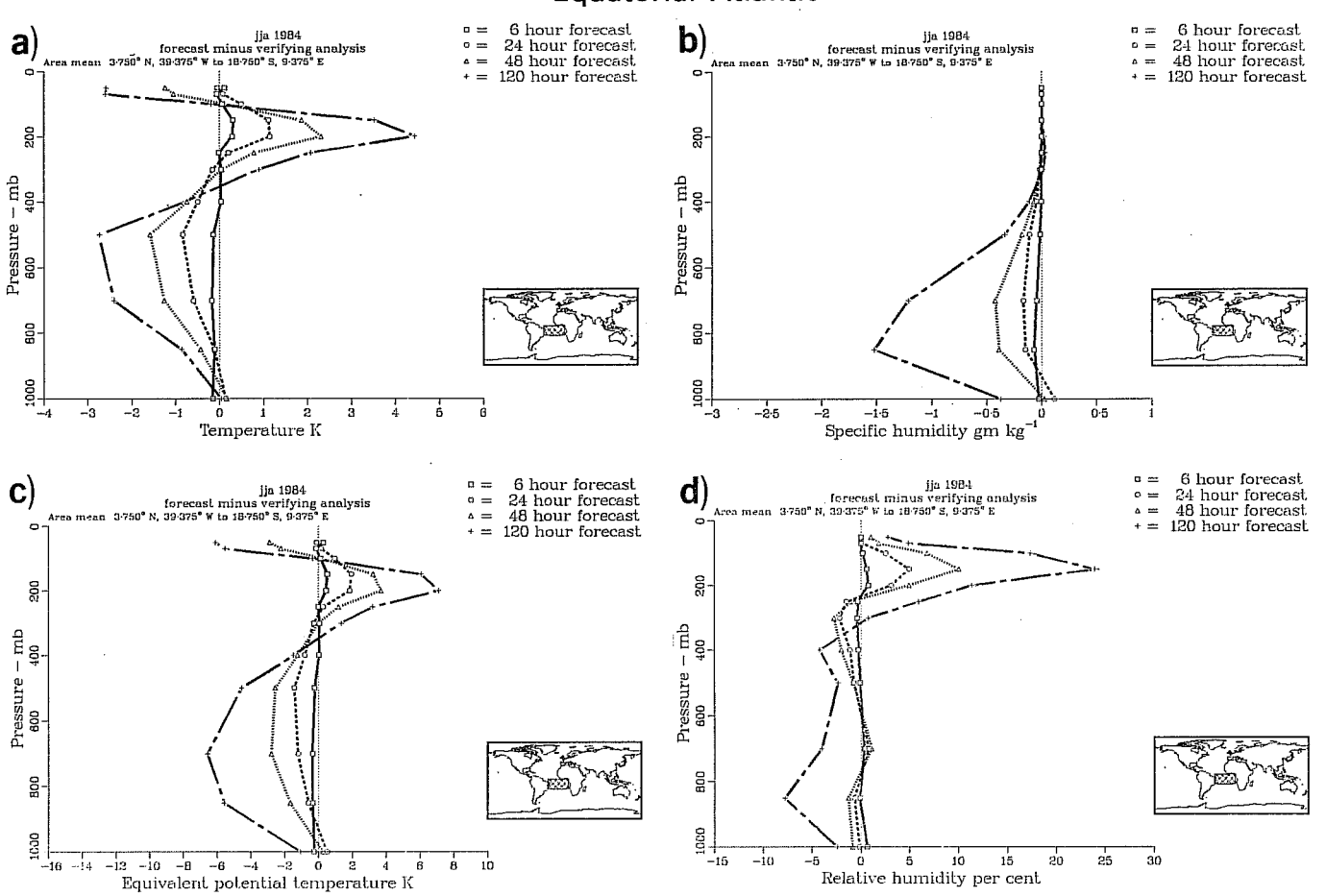

Fig. 22 Area weighted mean vertical profile of the monthly mean forecast changes for JJA 1984, for the equatorial Atlantic (3.75°N, 39.375°W, 18.75°S, 9.375°E). The solid line marked with square symbols, represents the six-hour (first guess) forecast minus the verifying analysis. The dashed line, marked with circular symbols, represents the 24 hour forecast minus the verifying analysis. The dotted line, marked with triangular symbols, represents the 48-hour forecast minus the verifying analysis. The dashed dotted line, marked with + symbols, represents the 120-hour forecast minus the verifying analysis. The hatched area in the inset figures gives a rough indication of the location of the area mean.
a) Temperature Units: °C b) Specific humidity Units: gm kg^{-1}
c) Equivalent potential temperature Units: K d) Relative humidity Units: percent

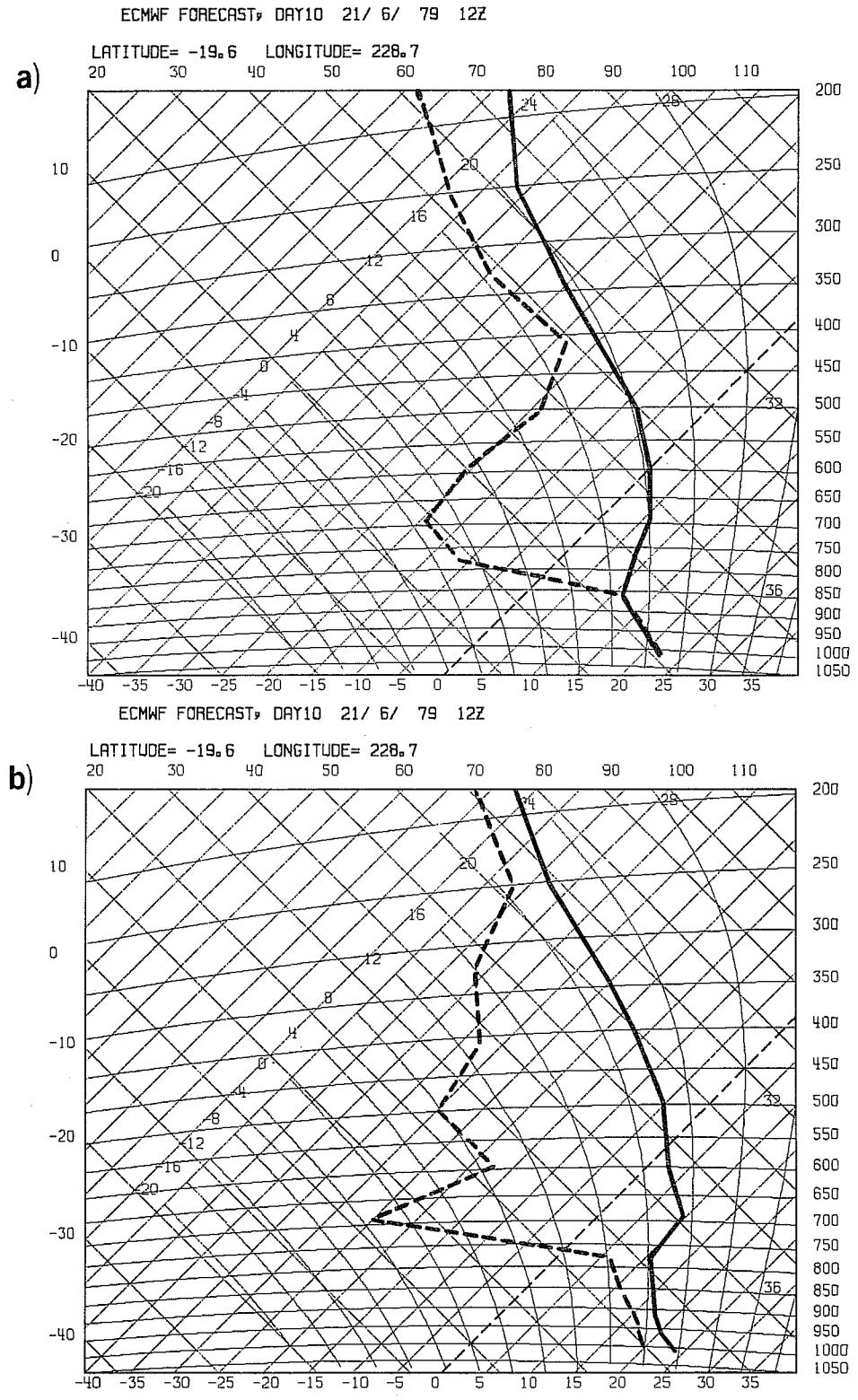

Fig. 23 Thermodynamic soundings at day 10 for the Pacific trades (19.6°S, 131.3°W) for a forecast run from 12Z, 21st June 1979.
a) with no parameterisation of shallow convection
b) including a parameterisation of shallow convection

illustrated in Fig. 23a. As discussed in Tiedtke (1981), the structure of the trade wind boundary layer in the forecasts is, in principle, in agreement with observations, i.e. it is characterised by a well-mixed moist boundary layer below a very dry free atmosphere. The model is, however, unable to produce the characteristic cloud layer that occurs at the top of the mixed layer, and the mixed layer accounts for the whole of the boundary layer. Whilst the model boundary layer, as a whole, is too shallow in these regions, the mixed layer is too deep and saturated throughout, with little evidence of a convectively unstable layer (cumulus cloud layer) above. The moistening of the surface layers can be clearly seen in the monthly mean forecast changes in specific humidity, Fig. 22b.

Tiedtke (1982) points out that the reduced depth of the mixed layer in the forecasts implies that the accumulated water vapour content and the amount of its downstream transport to the tropics must be underestimated. The height of the trade wind boundary layer is determined by a balance of the large scale atmospheric sinking motion with the upward turbulent transports (mainly by cumulus convection), Augstein et al. (1973). The most likely cause of the imbalance in the forecasts is the underestimation of this shallow convection.

Parameterisation schemes to represent the effects of shallow convection have been developed at ECMWF. One of these is based on the assumption that the net effect of convection can be attributed to the turbulent fluxes of heat and moisture (Tiedtke, 1984), where the fluxes are parameterised on the basis of mixing length theory. The scheme seems to perform best when its application is restricted to within the cloud layer.

Fig. 23b shows the same day ten forecast as Fig. 23a, but now with the parameterisation of the effects of shallow convection included in the model. With the revised physics a rather shallow well mixed boundary layer is topped by a cloud layer which extends over several model layers. The depth of the total moist layer (boundary layer plus cloud layer) is also considerably deeper (by about 50-100 mb).

A comparison of summer 1983 (not shown) and summer 1984 forecasts shows very similar errors, indicating that the diurnal cycle had little or no impact on the thermodynamic errors over the equatorial Atlantic. This is probably due to the absence of cloud-radiation interaction with low level clouds in the model.

(b) North Africa

Fig. 24 shows the area mean monthly mean forecast changes for north Africa (0°-30°N, 0°-48.75°E). The format of the maps is the same as for the equatorial Atlantic (Fig. 22). The temperature differences over north Africa show a marked variation between summer and winter (not shown). In both seasons there is a warming in the upper troposphere between about 100 and 300 mb, the warming is slightly stronger in summer, which shows a cooling that is about zero at 400 mb and increases towards the ground.

The specific humidity differences show a distinct tendency towards drying out the atmosphere in both summer and winter. The drying is however larger in winter than in summer. This difference between the seasons is in the opposite sense to the temperature differences, where the cooling in the lower troposphere is larger in summer than in winter. As one might expect these

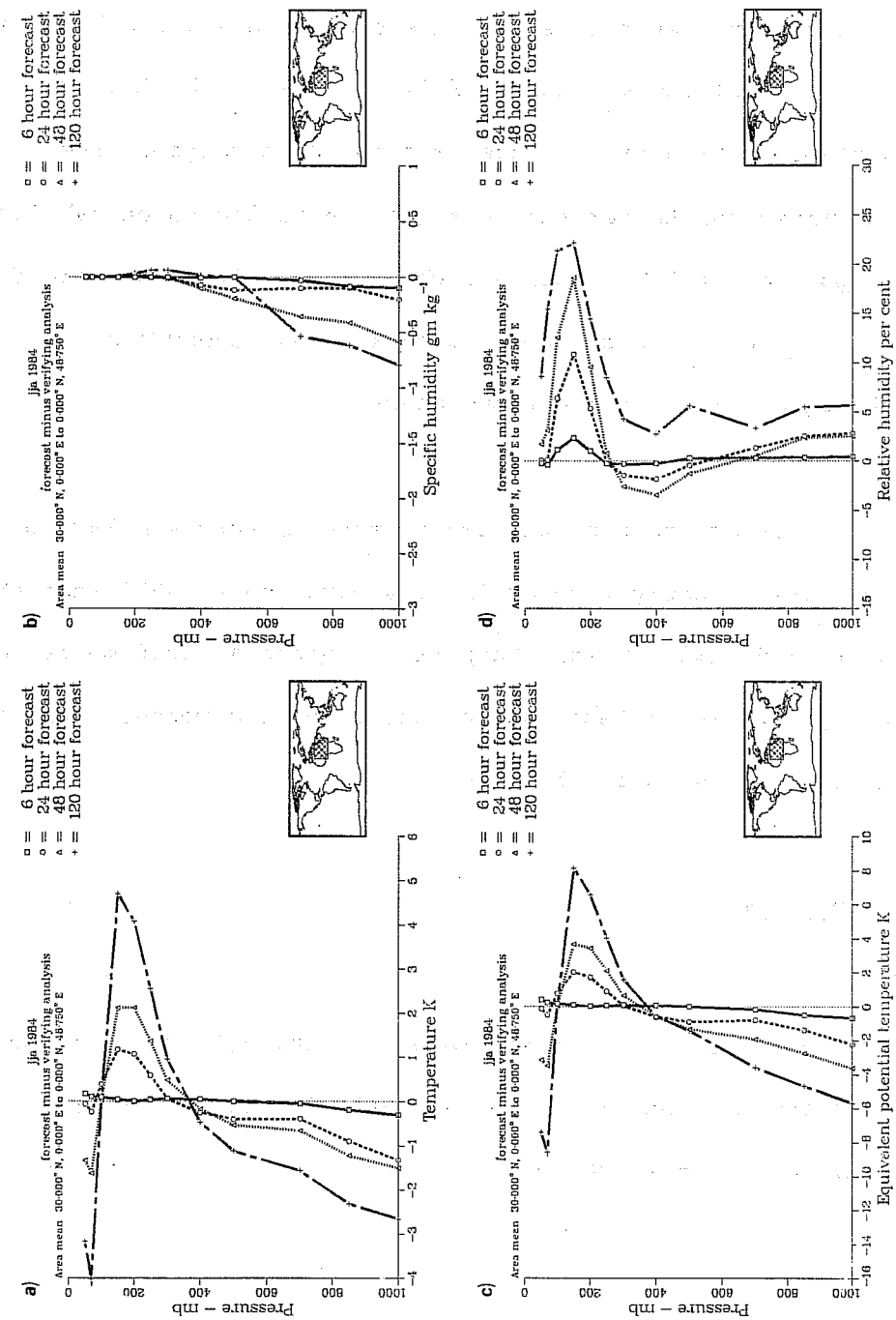

Fig. 24 As Fig. 22 but for North Africa (30°N, 0°E, 0°N, 48.75°E)

opposing trends in temperature and specific humidity result in rather different behaviour for the relative humidity differences between the two seasons. In summer the relative humidity increases in the lower troposphere whereas in winter it decreases. The net effect of these changes is clear from the θ_e curves. In summer when the temperature changes are large but the moisture changes are small the θ_e changes follow those of the temperature: a trend towards a stabilisation of the model atmosphere throughout the troposphere. In winter the temperature changes are acting to destabilise the mid and lower troposphere but the moisture changes largely compensate for this, resulting in θ_e curves which show a general trend towards a stabilisation throughout much of the troposphere.

The character of the errors between the two summers is very similar, but overall the errors are slightly reduced in 1984 compared to 1983 (not shown) in both temperature and humidity (the temperature error at 1000 mb is reduced by about 1°C at day 5). It is tempting to attribute this modest improvement to the implementation of the diurnal cycle.

3.5 The divergent flow

(a) Analysis

Figs. 25-28 show the velocity potential fields at 850, 700, 300 and 150 mb respectively or a) the mean uninitialised analysis for summer 1984; b) the 48 hour forecasts; and c) the 120 hour forecasts.

The analyses for summer 1983 (not shown) and summer 1984 are in general similar.

At 850 mb the analyses show the divergent flow close to the equator to be largely meridional, strong divergent flow extends from Africa, across the Indian Ocean and Indonesia into the western Pacific; a weaker westward flow occurs over the central Pacific. The strongest flow is onto the African continent from the Atlantic into the Gulf of Guinea and from the north and south into the Red Sea. At 700 mb the meridionality is lost, the main features are a divergent flow off the African continent, eastward flow across Asia and southward flow across Brazil.

It is interesting to compare the 700 and 850 mb fields. At both levels the strongest divergent flow occurs over the African continent, but it is in opposite directions, particularly over the west coast of Africa. This flow appears quite unique, having a very strongly sheared divergent flow over a shallow layer. Charney (1975) points out that the high albedo of a desert contributes to a net radiative heat loss relative to its surroundings. The resultant horizontal temperature gradients induce a frictionally controlled circulation which transports heat aloft, and thermal equilibrium is maintained through sinking motion and adiabatic compression. As Charney shows, the circulation required by this balance is a low level inflow, ascending motion, and outflow at about 700 or 800 mb; above this well-mixed layer there is subsidence. In the region of the Congo, the vertical shear in the divergent wind is over 6 m s^{-1} between 700 and 850 mb.

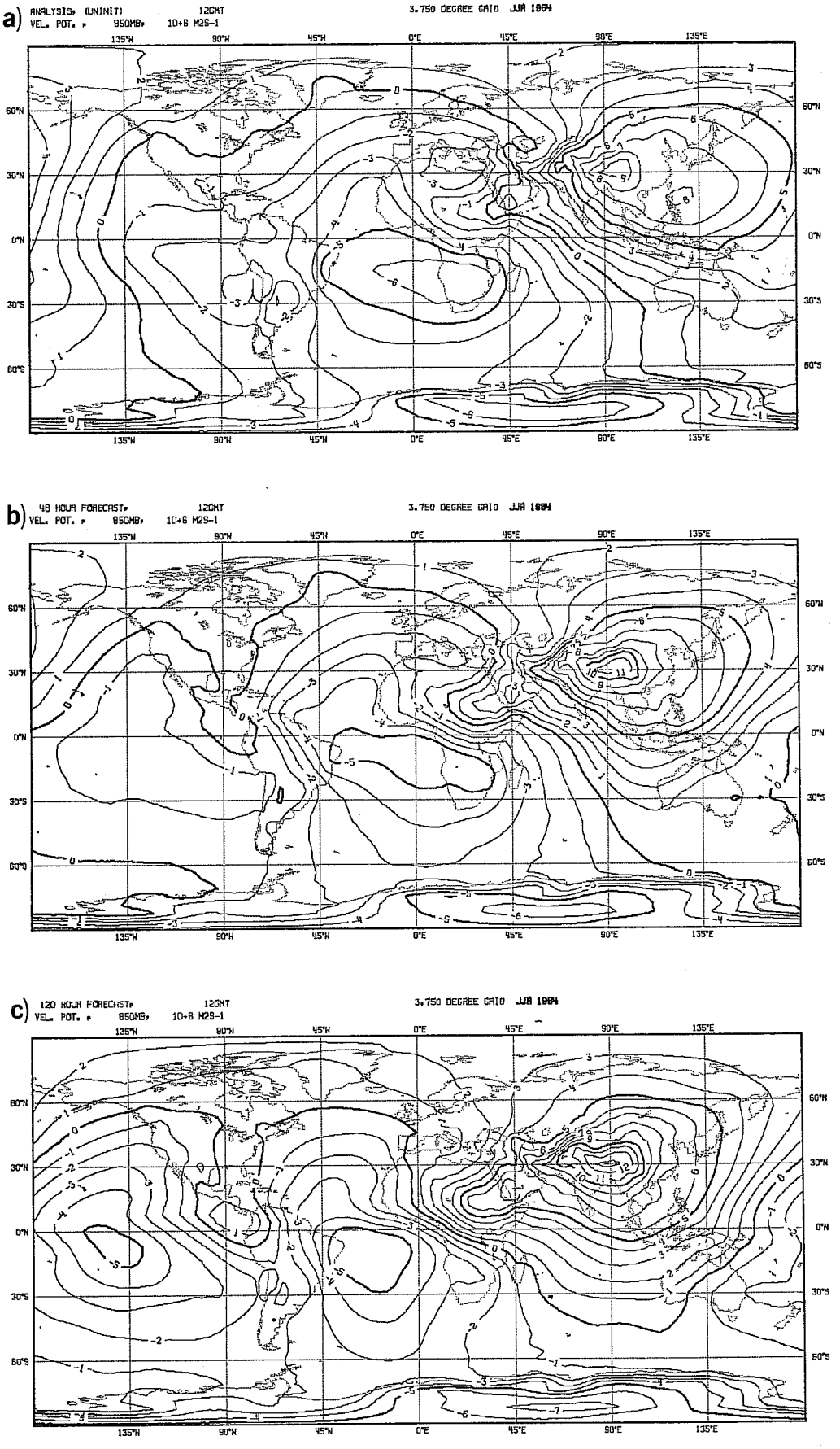

Fig. 25 Velocity potential field for JJA 1984 at 850 mb. Resolution 3.75° lat/long, contour interval 10^6 m^2s^{-1}.
a) Uninitialised analysis b) 48 hour forecast c) 120 hour forecast

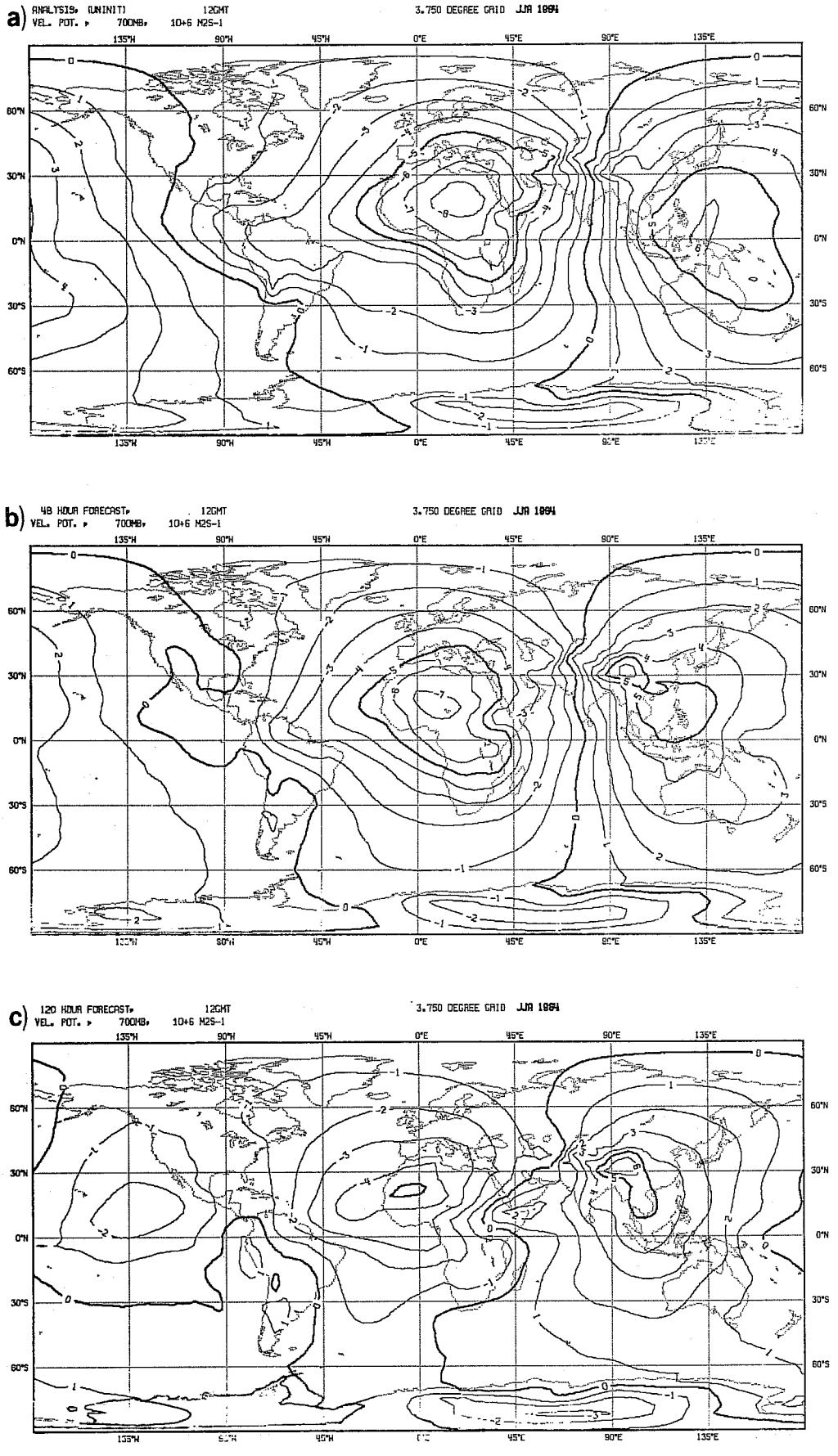

Fig. 26 As Fig. 25 but for 700 mb

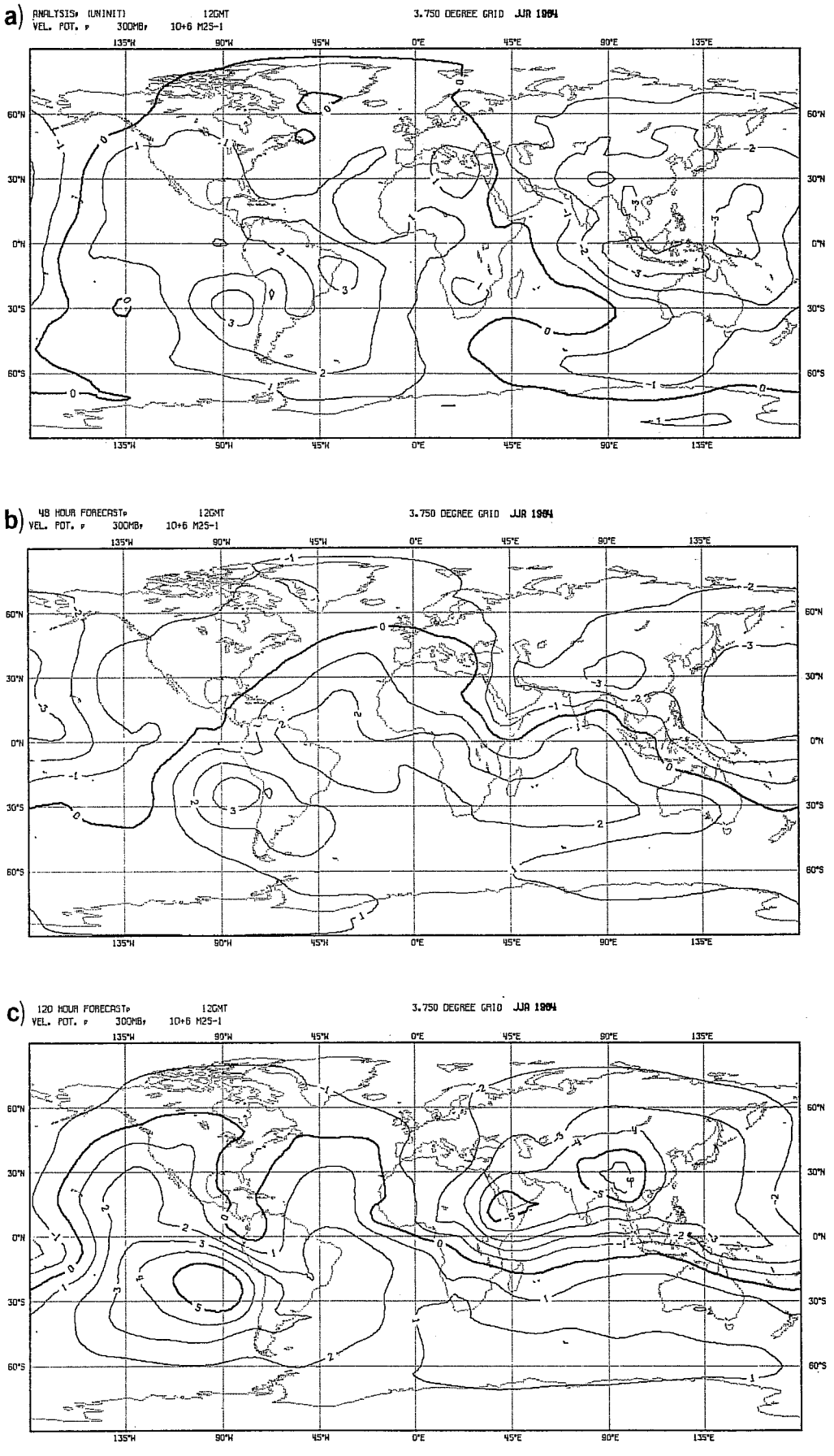

Fig. 27 As Fig. 25 but for 300 mb

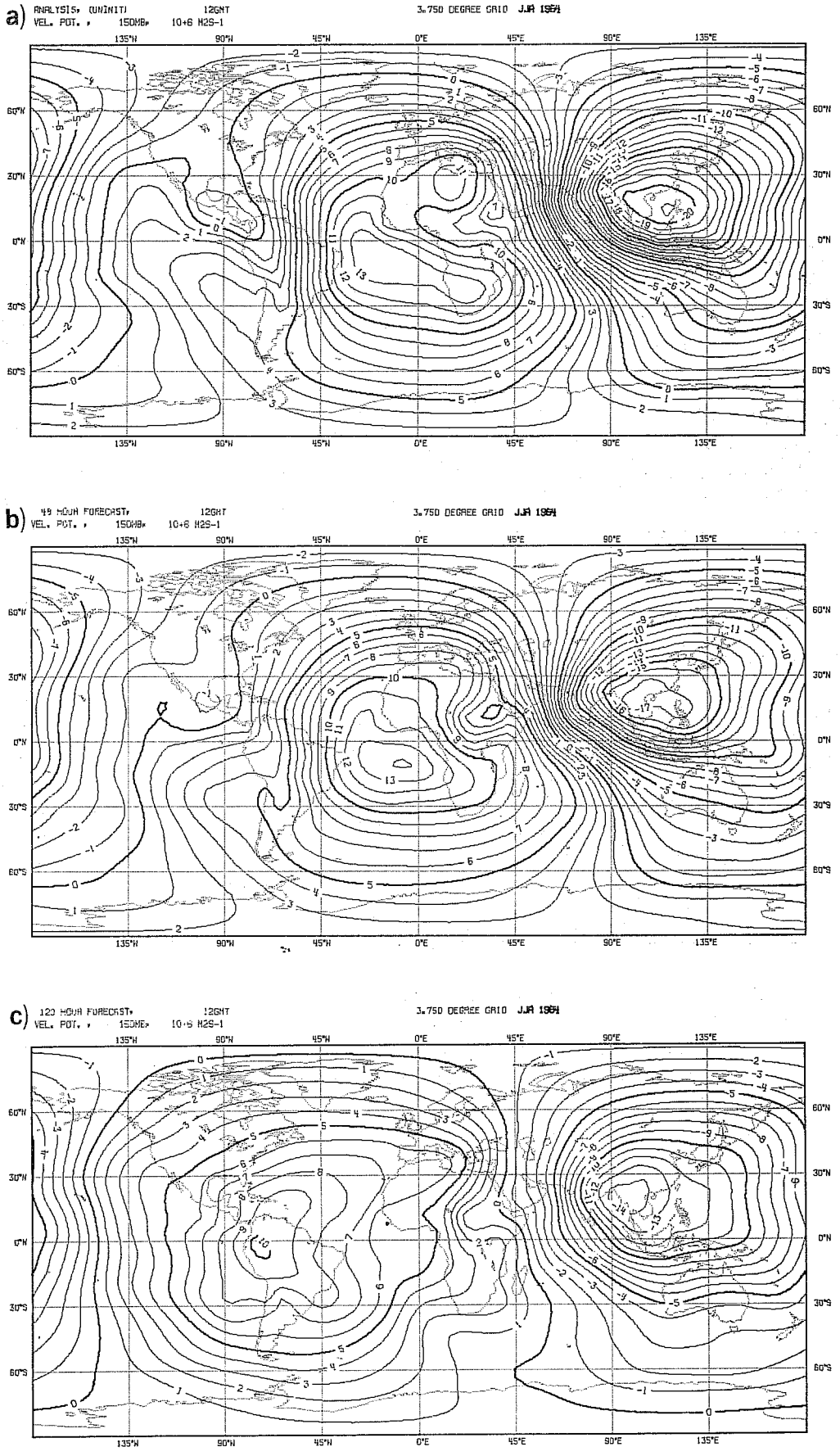

Fig. 28 As Fig. 25 but for 150 mb

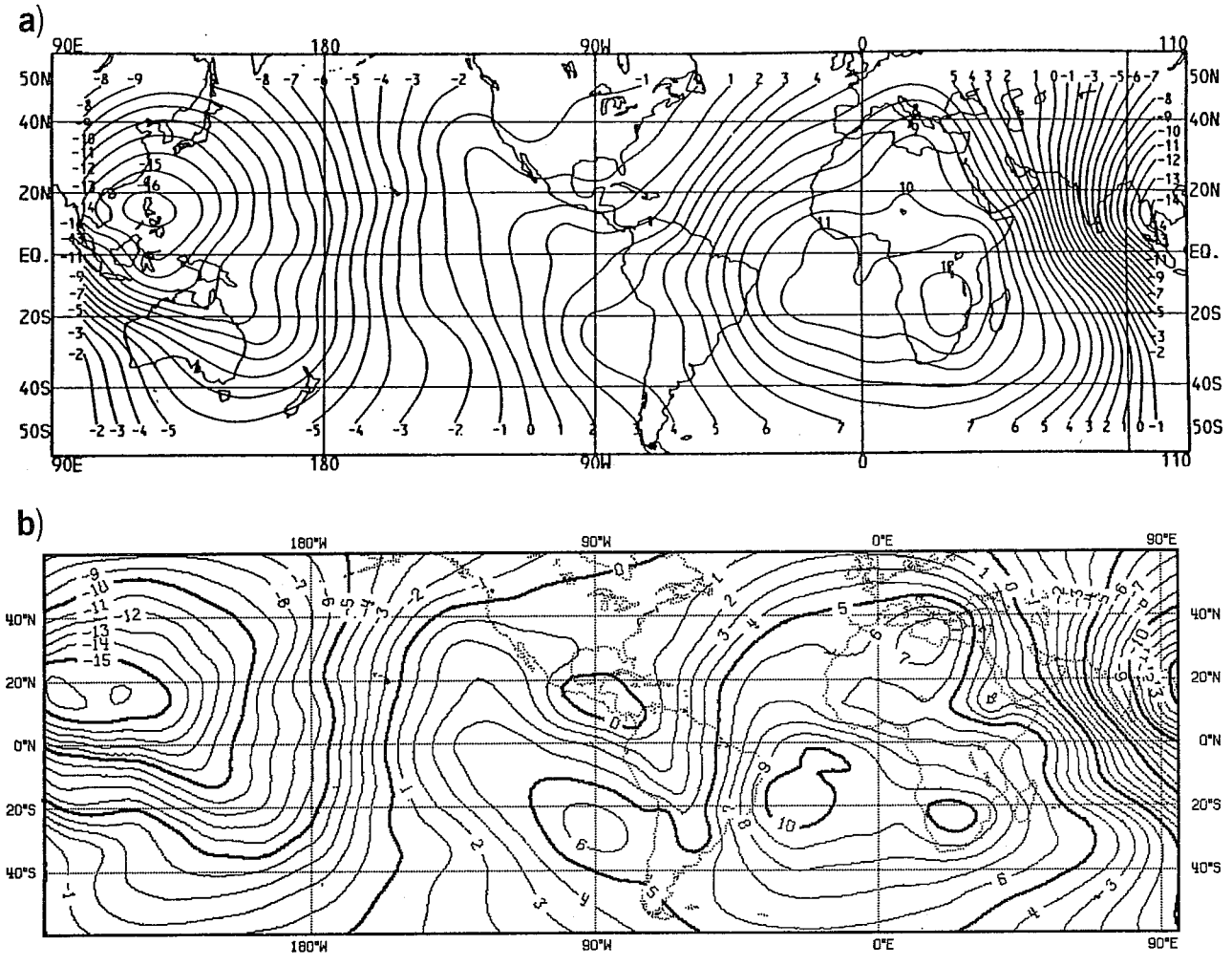

Fig. 29 200 mb velocity potential field. JJA 1984
a) NMC analysis. Velocity potential computed from the mean 200 mb wind. Winds are analysed and velocity potential is computed on a 2.5° global grid and interpolated to a 5° Mercator grid for display. NOAA (1984a).
b) ECMWF uninitialised analysis, on a 2.5° grid.

At 300 mb the divergent flow is much weaker, the flow over the eastern Indian Ocean is in the opposite direction to that at low levels; there is also evidence of convective outflow over Brazil.

At 150 mb the divergent flow is stronger than at the other levels and contains both significant meridional and longitudinal components. Strong southward flow occurs over Indonesia, westward flow over India and eastward flow over the central Pacific. On the broadest scales the flow is opposite to that at 850 mb suggesting a north-south vertical circulation over Indonesia and the eastern Pacific; and an east-west vertical circulation over the Arabian Sea, South America and the central Pacific.

It is interesting to compare the ECMWF analyses with those of the National Meteorological Center (USA). NMC publish monthly climatic bulletins, which contain, amongst other things, their 200 mb analyses of the velocity potential field. This field for JJA 1984 is shown in Fig. 29a, together with the corresponding field for the ECMWF uninitialised analysis, Fig. 29b. Over the western and mid Pacific, and the Indian Ocean the NMC and ECMWF analyses agree quite well, but there are large disagreements in the eastern Pacific, South America and over Africa. The NMC analysis is relatively featureless over these regions. It is not clear how one should interpret these differences in the analyses - they do suggest, however, that tropical analysis is not yet all that it could be.

(b) Forecast

At 1000 (not shown) and 850 mb the divergence field is maintained and even intensified slightly by the forecasts. The divergent flow at 700 mb is dominated by the outflow from the low level desert circulation over North Africa (discussed earlier); this intense low level circulation is spread vertically by the model, reducing its intensity at 700 mb. By day 5 the 700 mb divergent flow is much reduced in the region of the Gulf of Guinea but remains strong in the region of the Red Sea. On the largest scales there is a distinct westward shift of the centre of divergent outflow from northwest Africa in the analysis to the northeast equatorial Atlantic by day 5.

At 300 mb the forecasts build up the meridional gradients in the velocity potential and (in summer at least) weaken the circulations over South America and the south Pacific convergence zone. The meridionality of the velocity potential (or Hadley circulation) is lost at 150 mb but increased at 300 mb. These changes in the ageostrophic flow are such as to imply easterly acceleration at 150 mb and westerly acceleration at 300 mb. Comparing with Fig. 14d which shows the day 5 zonal mean wind error for JJA, 1984 one indeed sees maximum easterlies at 150 mb and a relative minimum at 300 mb and 10°S which is the location of strongest ageostrophic flow in July (Fig. 18).

At this point it is worthwhile returning to the discussion of regional errors, this time in the context of the divergent flow.

Fig. 30 shows the uninitialised analysis of the divergent component of the wind at a) 700 mb and b) 850 mb for 1984, for the African continent. As mentioned earlier the flow over North Africa may be characterised as a desert

circulation having a very strongly sheared divergent flow over a shallow layer near the surface (Charney, 1975). The shear is slightly larger in summer 1983 (not shown) than summer 1984. In summer 1983 a divergent wind of over 4 m s^{-1} flows onto Cameroun at 850 mb and at 700 mb the flow over the Gulf of Guinea is in totally the opposite direction, with a divergent wind of over 3 m s^{-1} flowing off the Ivory Coast and over most of the Gulf of Guinea. The largest vertical shear occurs in the region of the Congo.

At 850 mb the 48 hour forecast (Fig. 31) maintains the divergent flow quite well and even intensifies it slightly. The largest discrepancies occur in the regions of Ethiopia and the mountains of Cameroun, where the analysis shows a distinct convergence towards these from all sides. The forecast, while reproducing this to a certain extent, exhibits in the case of Cameroun more of a tendency to flow over the mountains, leading to excessive convergence downstream; this suggests that the model orography is not providing sufficient drag in this region. At 700 mb the 1983 and 1984 forecasts reproduce the divergent outflow quite well off the Spanish Sahara but the 1983 forecasts considerably underestimate it elsewhere along the west African coast; the 1984 forecasts are much better in this respect but far from perfect. The forecasts considerably overestimate the convergence over Ethiopia and the divergence over the Upper Volta. The excessive convergence over Ethiopia may be indicative of excessive model drag (model mountains too high perhaps?).

(c) Vertical structure of ω

The vertical structure of ω varies between regions. Fig. 32 shows the area mean ω fields for a) the Gulf of Guinea, and b) Indonesia, for February 1984. The profiles are quite different in character between the two regions. For

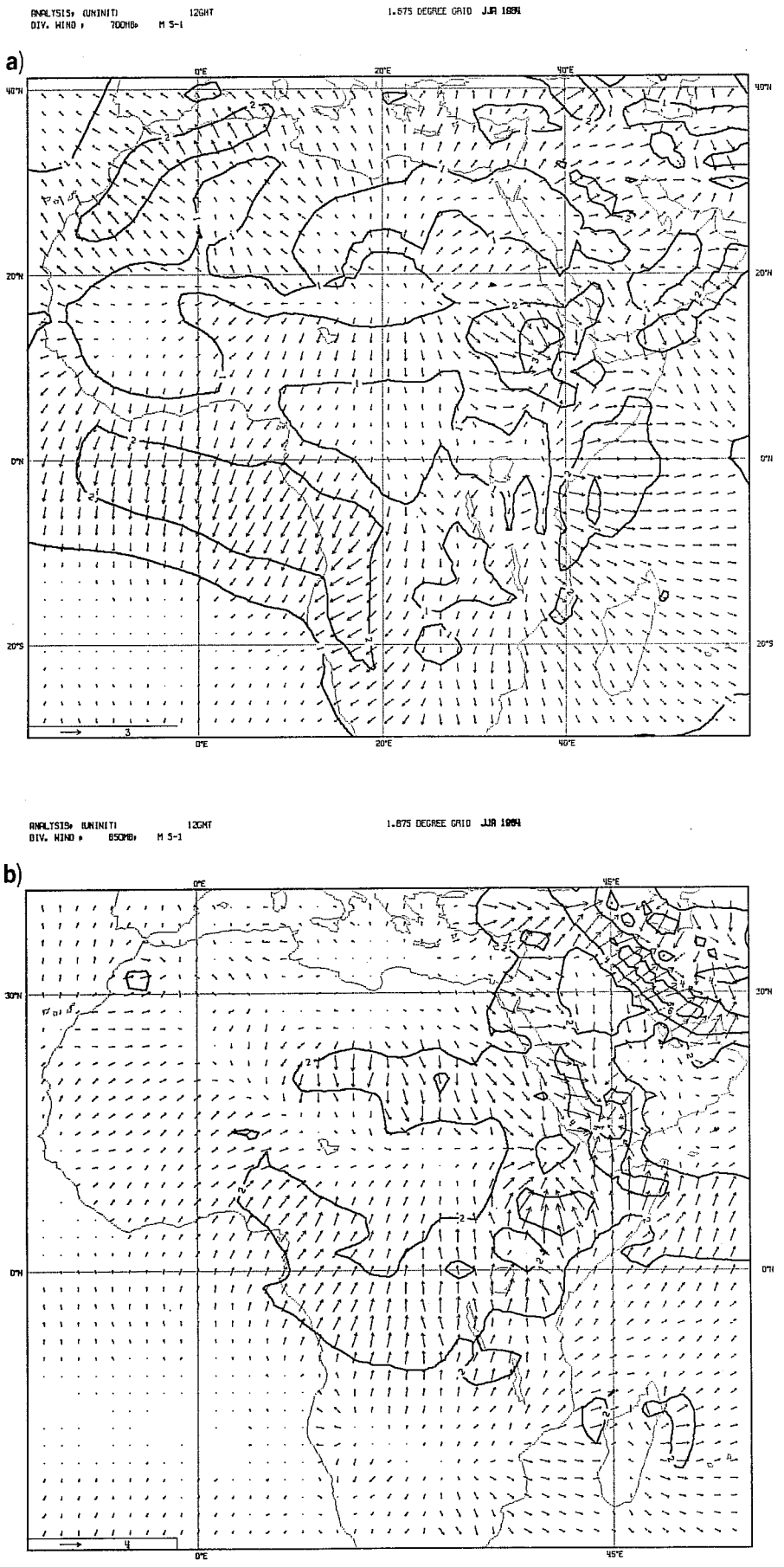

Fig. 30 Divergent component of the analysed wind field for JJA 1984, 1.875° grid. Units m s^{-1} a) 700 mb b) 850 mb

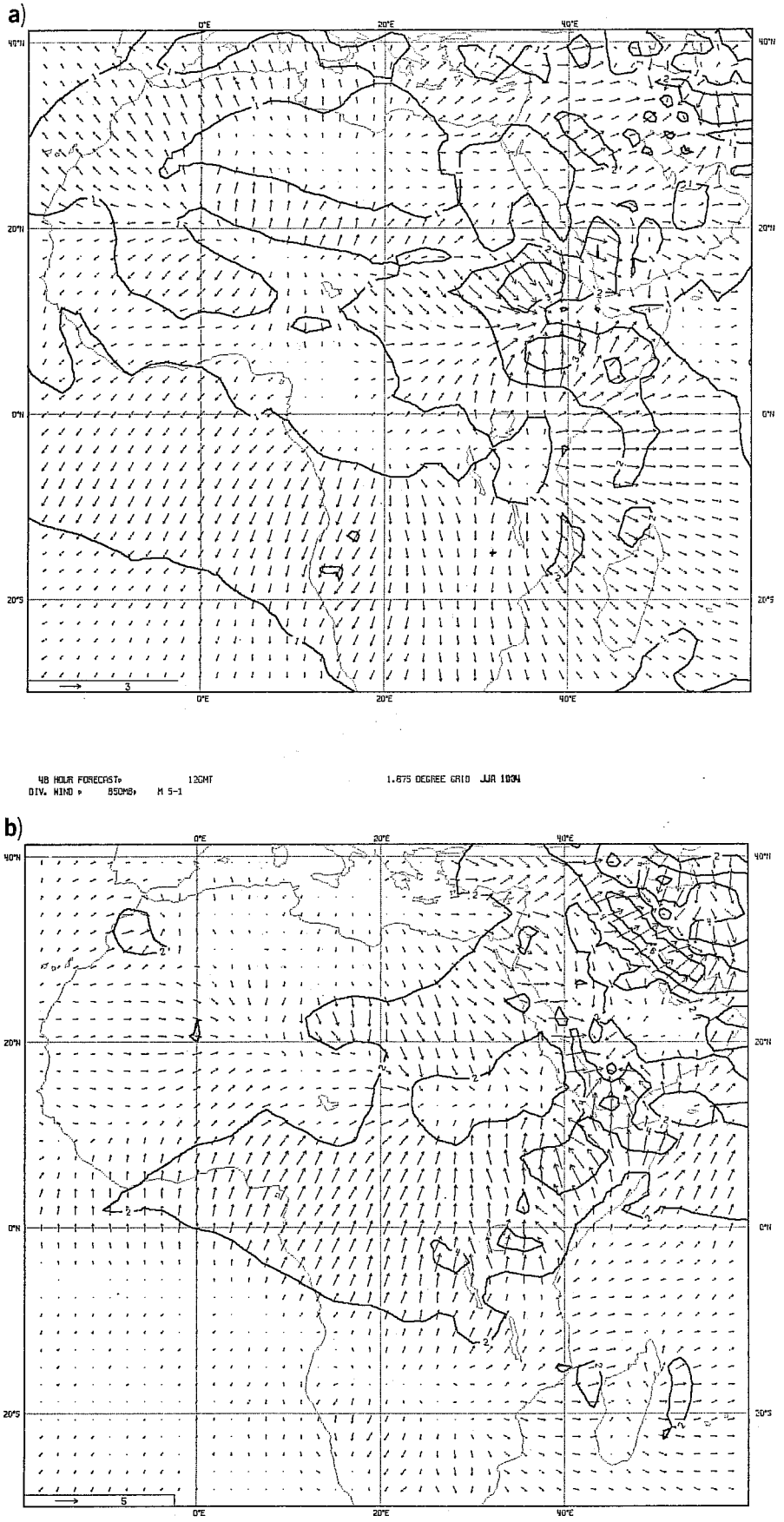

Fig. 31 As Fig. 30 but for the 48-hour forecast

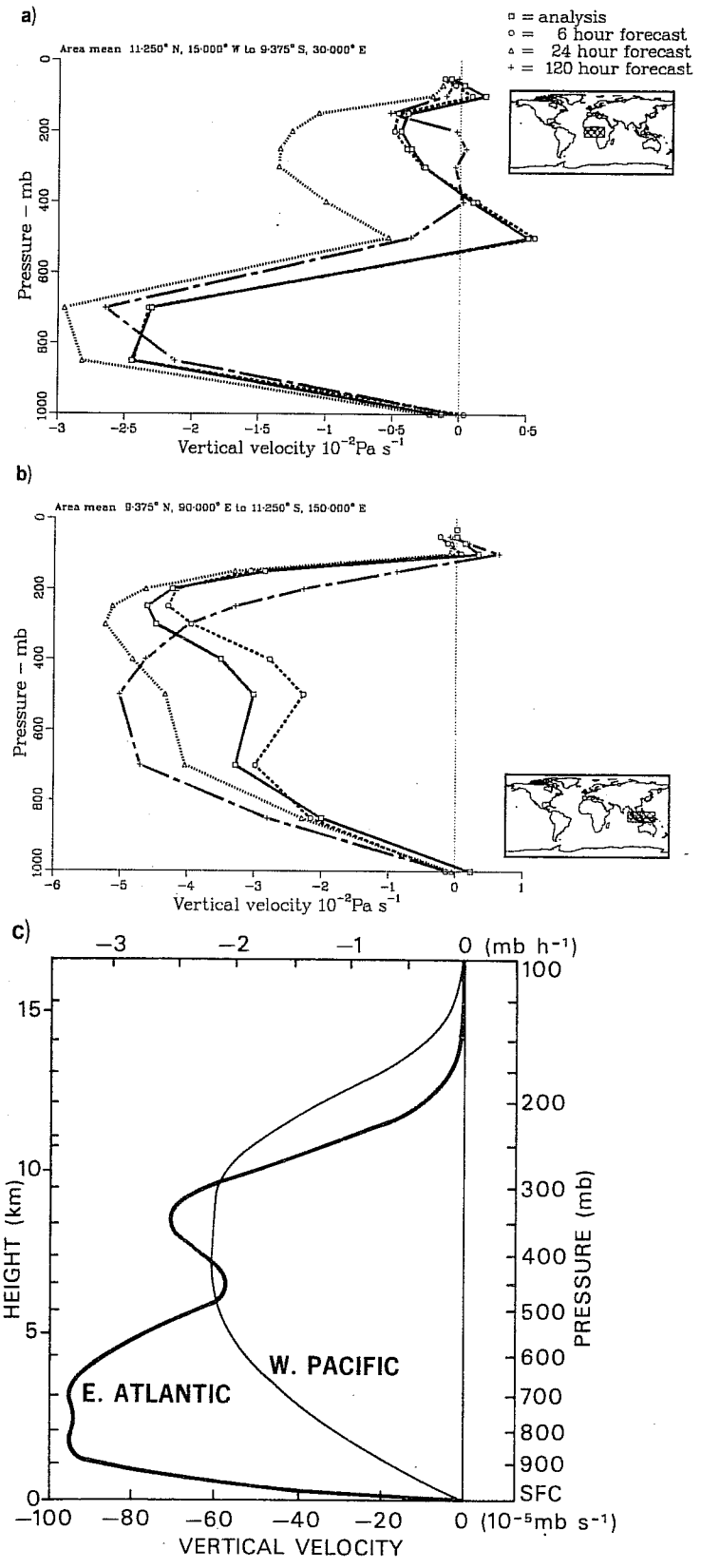

Fig. 32 Vertical profiles of omega

a) As Fig. 22 but for the ω field over the Gulf of Guinea/central Africa (11.25°N, 15°W, 9.375°S, 30°E) in February 1984.

b) As Fig. 22 but for the ω field over Indonesia (9.375°N, 90°E, 11.25°S, 150°E) in February 1984.

c) ω profile deduced from observational soundings (adapted from Thompson et al. (1979)).

the Gulf of Guinea the analysis shows a well-defined maximum in ω over quite a shallow layer between 1000 and 500 mb, slight descent at 500 mb and a weaker ascent between 400 and 100 mb. The analysis for the Indonesian region shows a general ascent, with a slight double structure, the ω field having maxima at 700 and 250 mb.

In order to ascertain what validity these structures may have it is interesting to compare them with some inferred from atmospheric soundings. Fig. 32c shows the ω profile for GATE (adapted from Thompson et al., 1979) marked as "E. Atlantic". The GATE area may well have a different climatology to that of the Gulf of Guinea, but these profiles are assumed characteristic of easterly waves and as such may have some relevance to the Gulf of Guinea region. The ω profile for the GATE area shows a distinct double structure in the vertical with peaks at about 700 mb to 850 mb and at about 350 mb; it shows the same characteristics as the analysed mean fields from the Gulf of Guinea and lies somewhere in between the February and July (not shown) means. Also shown in Fig. 32c is an ω profile for the western Pacific; this profile is assumed characteristic of deep convection and as such should bear comparison with the analysed fields over Indonesia.

The observational profile shows a fairly broad area of maximum ascent between about 500 and 300 mb, while the analysis, Fig. 32b, shows a general ascent with a slight double structure, the ω field having maxima at 700 and 250 mb.

For the Gulf of Guinea region the 6-hour forecasts maintain the analysed structure quite well. The 24-hour forecast shows an intensification, particularly in the upper troposphere. Day 5 also maintains much of the structure, but weakens the ascent in the upper troposphere to almost zero.

Thompson et al. (1979) hypothesise the existence of three main cloud populations with outflows near 800, 500 and 250 mb. The 5-day forecast has too little convergence at 1000 mb and not enough divergence, or too much convergence at 700 mb, suggesting the need for low level clouds in the model.

Forecasts for the Indonesian region, also tend to smooth out the double structure in the ω profile, reducing the ω field between 100 and 350 mb and increasing it at 500 mb. Comparing with the ω field inferred from observational soundings ("W. Pacific" in Fig. 32c) it is clear that this shows more resemblance in structure to the day 5 forecast than to the analysis. It is not certain what one should infer from this.

Direct comparison of magnitudes is difficult as an area mean will almost inevitably incorporate both updraft and downdrafts in varying amounts depending on the size and location of the region with respect to the convection, and upon the type of convection. Perhaps the most one can say is that the area mean omegas from the model agree to within an order of magnitude with those inferred from observational soundings. More exact comparisons can only be made through a detailed examination of model results and observations from specific cases.

If one examines the structures associated with very intense ascent in the tropics point by point, rather than looking at area means, one finds, for the analyses, a distinct bimodal vertical structure with the most vigorous ascent at about 700 mb and somewhat less vigorous ascent at about 200 mb; less commonly the 200 mb ascent will be as vigorous, or more so, than that at 700 mb. The type of structure where there is a single maximum in the mid-troposphere is less common in very intense situations, but can be found.

Many other structures can be found which are a combination of these extremes. In all cases the forecasts reduce the bimodal structure in favour of an increase in mid-troposphere ascent. In view of the strong negative correlation that exists between the total diabatic heating and the ω field in the tropics, the errors in the vertical profile of ω suggest problems with the diabatic heating profile. An explanation of this error would require a much more detailed study of the sources and sinks in the upper troposphere.

The analyses produce vertical structure of ω similar to profiles inferred from observations which are characteristic of easterly waves and of deep convection. In the former case the forecasts are unable to maintain the structure for long, tending to smooth out the vertical structure; this is likely to be partly related to the absence of boundary layer clouds and the associated heat and moisture fluxes. In the case of deep convection, the forecasts increase the vertical velocities in the mid troposphere and decrease them in the upper troposphere, which is consistent with the increasing stability of the upper troposphere.

3.6 The wind field

The errors in the tropical wind field show a remarkably similar pattern throughout the year (allowing for small seasonal shifts and changes in amplitude), an exception to this are the errors associated with the simulation of the monsoon. Figs. 33 and 34 show the vector wind errors for summer 1983 and summer 1984 respectively, for a) 150 mb and b) 850 mb, for the 5-day forecast. The improvement between 1983 and 1984 in the rms vector wind errors, noted in Sect. 1, is less obvious when one examines the errors in detail. There are small areas of notable improvement, e.g. Brazil, and areas of notable worsening, e.g. the eastern Pacific. At 150 mb, as in the rms scores, the signal is quite clear: the summer 1984 forecasts are significantly worse.

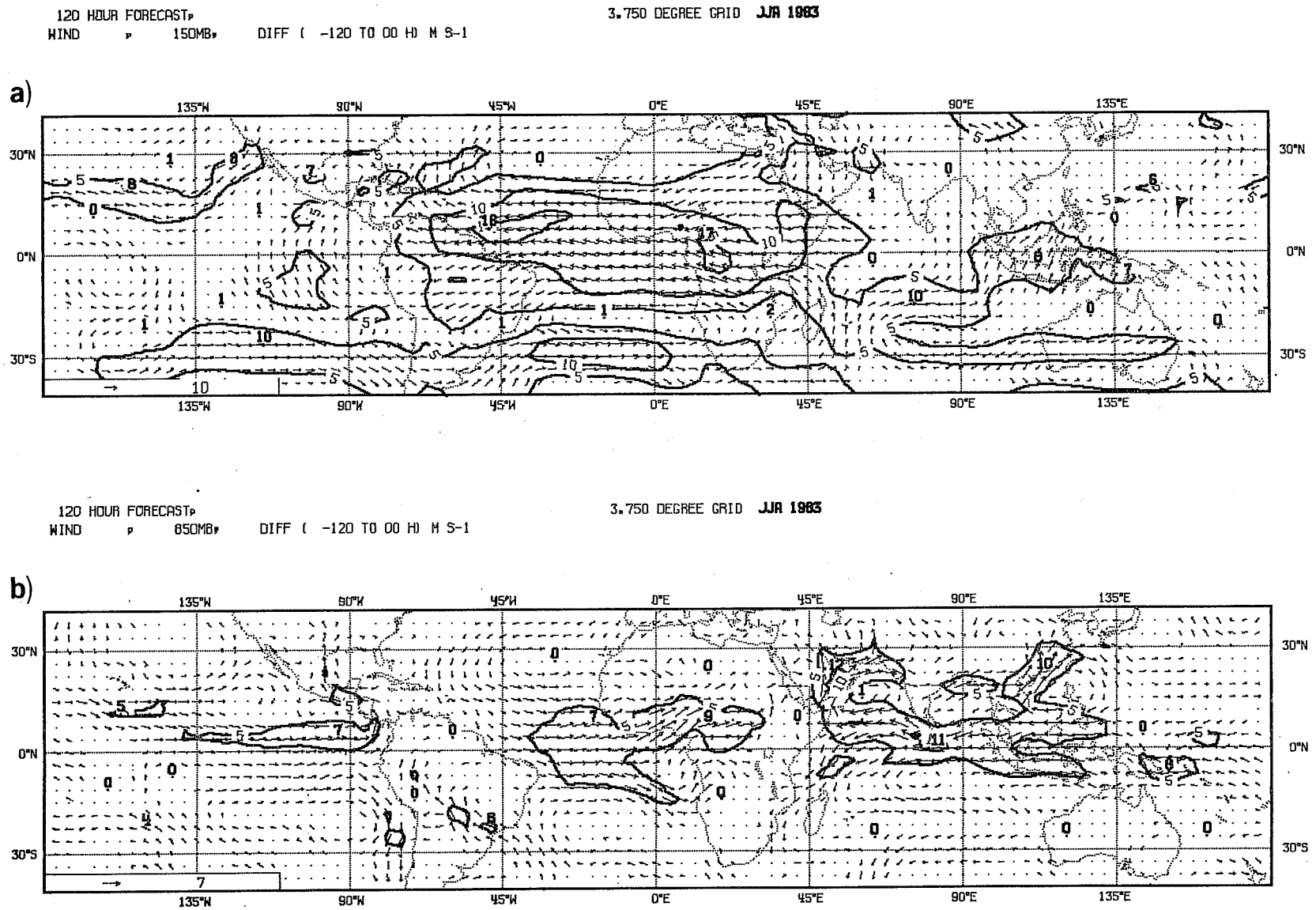

Fig. 33 Model forecast vector wind error at 120 hours for JJA 1983. 3.75° grid. Contour interval 5 m s^{-1} a) 150 mb b) 850 mb

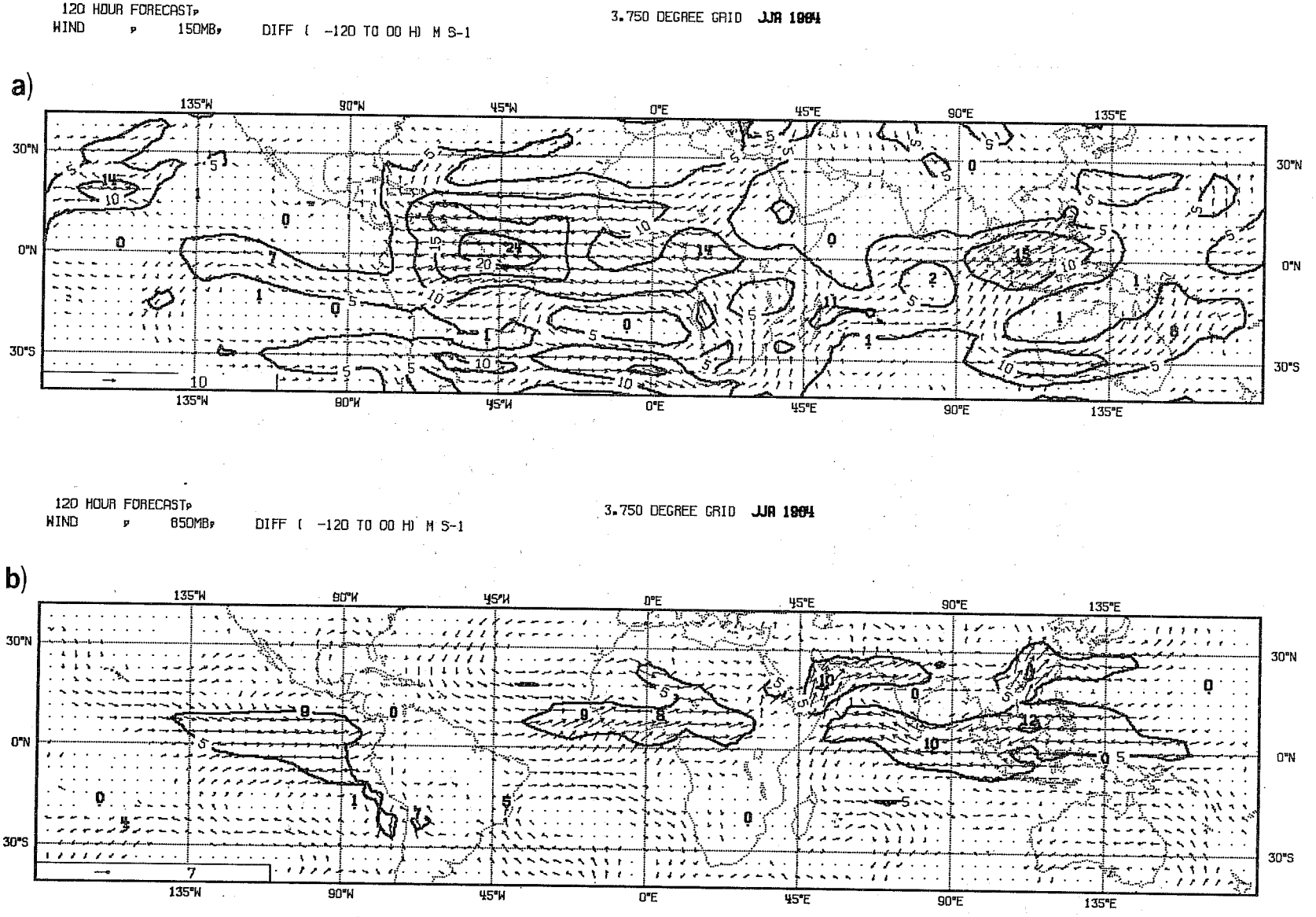

Fig. 34 As Fig. 33 but for JJA 1984

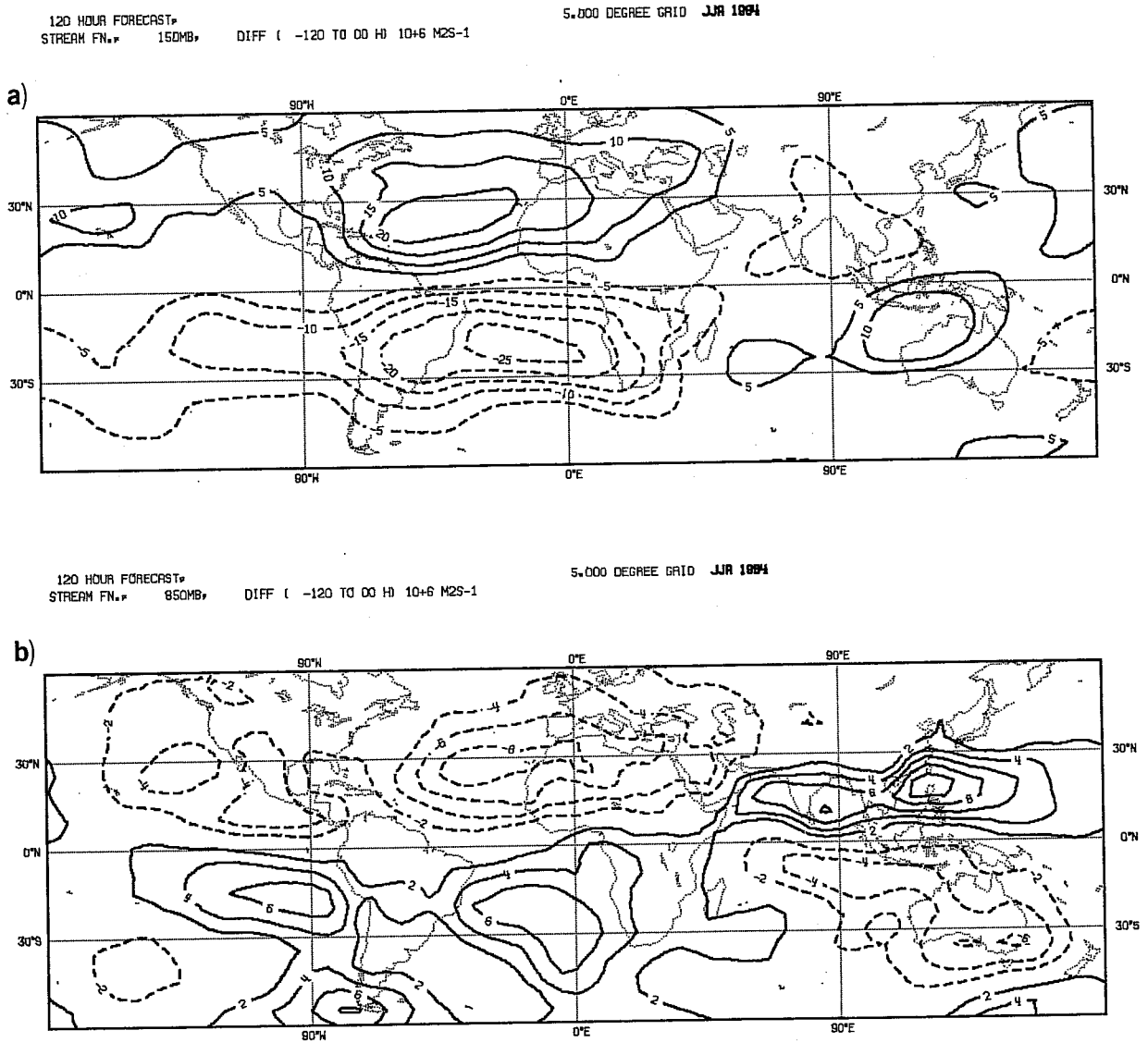

Fig. 35 As Fig. 34 but for the stream function on a 5° grid

There is a very coherent structure to the errors at both levels, this can be most easily seen from the streamfunction fields, which are shown in Fig. 35 for JJA 1984. At 850 mb there is a clear cyclonic circulation over the north and south Atlantic and over the eastern Pacific. At 150 mb the errors are the reverse of this: a strong anticyclonic circulation over the north and south Atlantic and the eastern Pacific. The errors are very baroclinic and extend meridionally as far as 40° to 50° north and south. If these errors are forced from the tropics, and their structure suggests that they might be (Heckley, 1983), then the tropical errors are changing the baroclinicity of the mid-latitudes and hence affecting the mid-latitude forecasts of baroclinic waves etc. These changes in baroclinicity are not small, for July 1983 the error in the vertical wind shear between 200 and 850 mb. Over the north Atlantic the wind shear is over 15 m s^{-1}. Some of the changes in the tropics are even larger. Klinker and Capaldo (1984) have used a wavenumber-frequency analysis of forecasts and analyses to describe the forecast errors. They were able to demonstrate that many errors in the forecast baroclinic waves are consistent with the errors in the baroclinicity of the large-scale forecast flow. There have been other studies which have demonstrated the impact of the tropics on mid-latitude prediction in individual cases, e.g. Haseler (1982). The meridional scale for these wind errors, however, speaks for itself.

3.7 Precipitation

Some mention has already been made of the precipitation in the discussion of the humidity field. Fig. 21 showed the mean precipitation for the tropical belt as a function of forecast length by way of illustrating the 'spin up' problem and its effect on the model humidity field. Fig. 36 shows the geographical distribution of this precipitation for JJA 1983 during a number of forecast intervals: a) 0-6 hours; b) 0-24 hours; c) 96-120 hours,

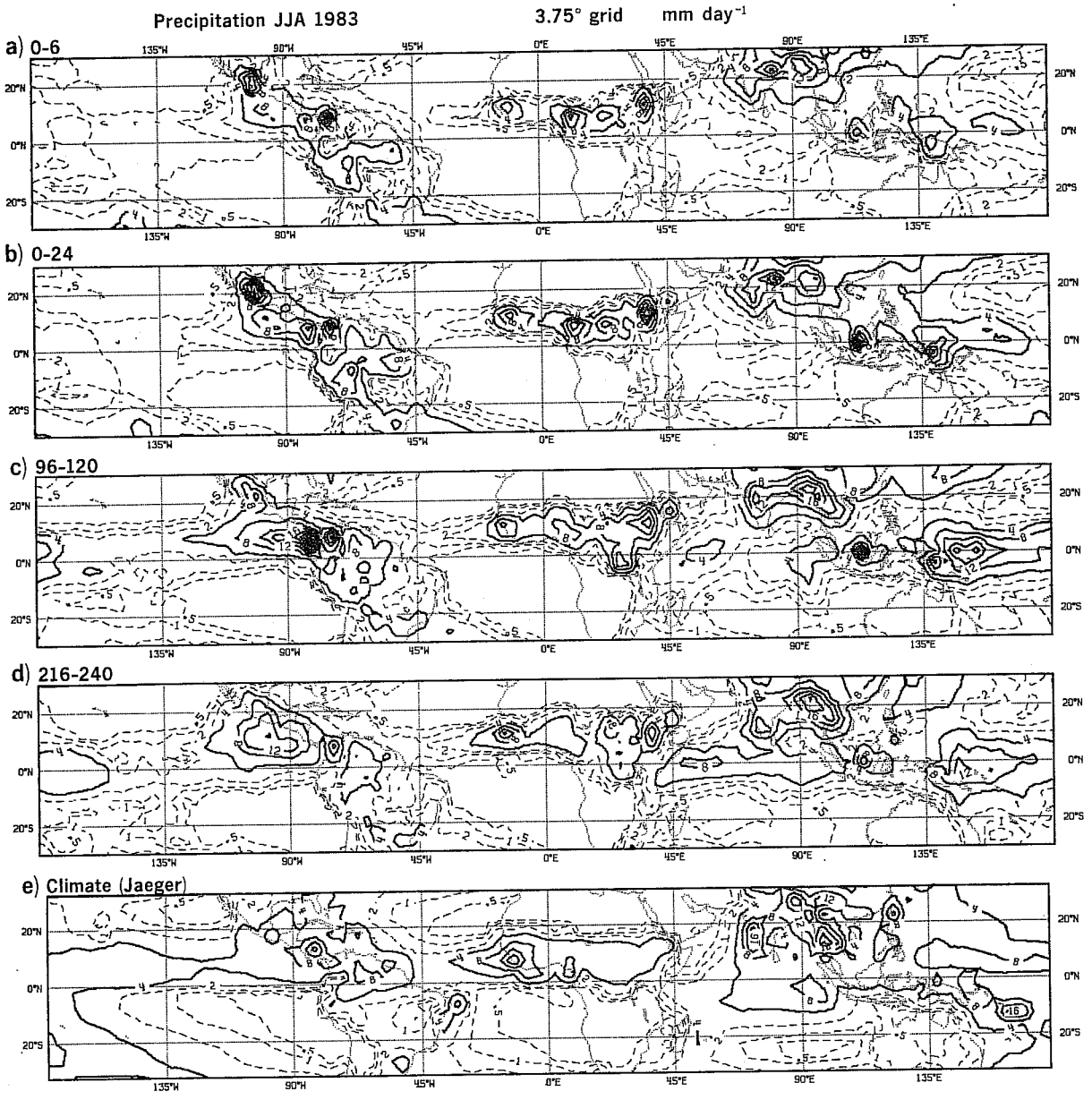

Fig. 36 Precipitation for the tropical belt for JJA 1983, mm day^{-1}

a) 0-6 hour forecasts 3.75° grid
b) 0-24 hour forecasts 3.75° grid
c) 96-120 hour forecsts 3.75° grid
d) 216-240 hour forecasts 3.75° grid
e) Climatology (Jaeger, 1976) 5° grid

Solid contours 4 mm day^{-1} intervals; dashed contours .5 mm day^{-1}, 1 mm day^{-1}, 2 mm day^{-1}.

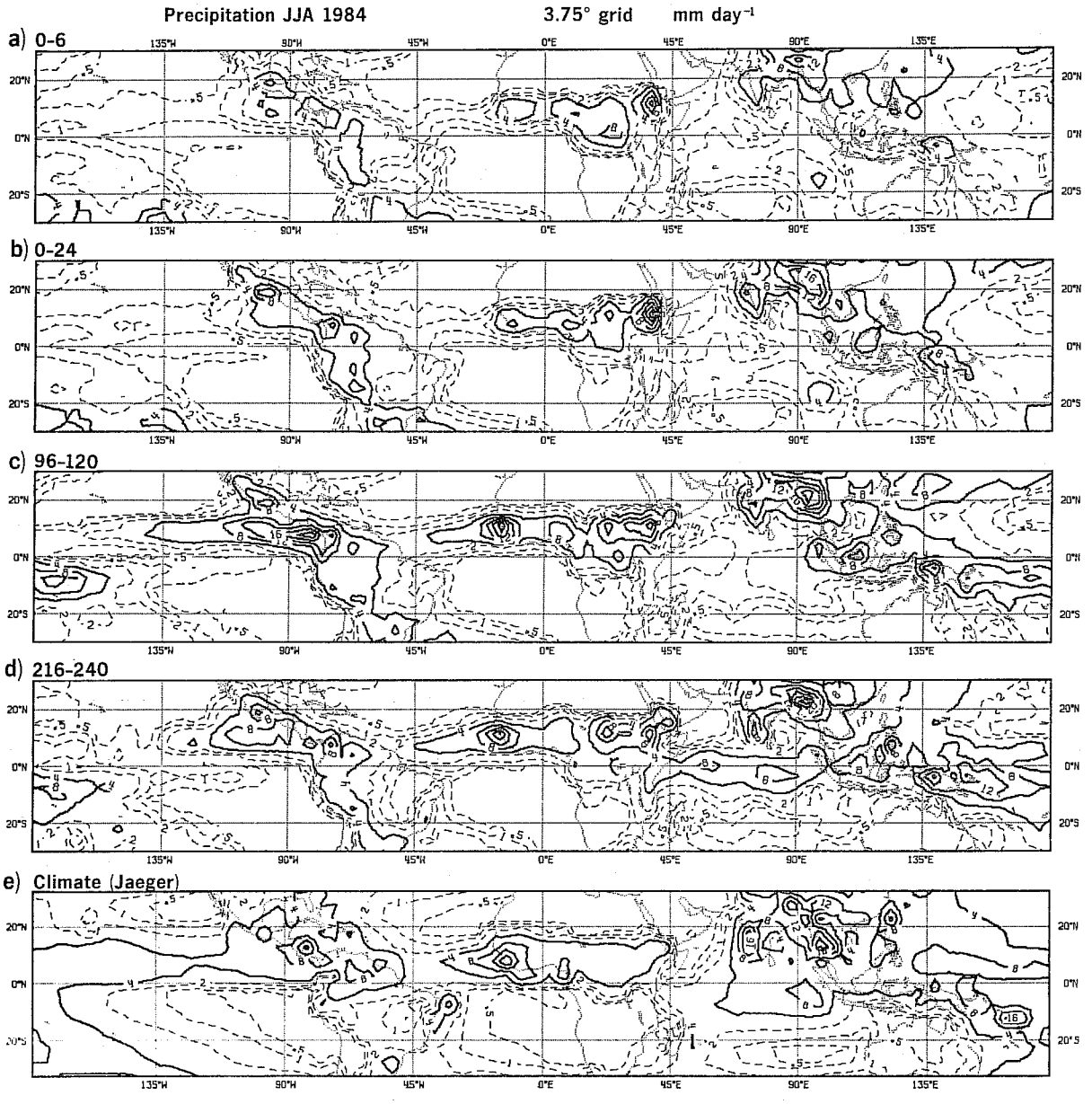

Fig. 37 As Fig. 36 but for JJA 1984

d) 216-240 hours. Fig. 36e shows the corresponding climatology for JJA (Jaeger, 1976). The 'spin up' of the precipitation appears to be more of a problem over the oceanic areas than over the land areas. Precipitation is too weak over the ITCZ's, particularly in the Pacific. Over land the precipitation is in general of the right order of magnitude. A number of 'trouble spots' are clearly apparent however. For example, the Ethiopian highlands, Borneo, Mexico and Colombia all give problems, particularly in the first few days of the forecasts. Dry areas in the north and south Pacific and Atlantic are too extensive, over land however, they are better simulated.

The corresponing plots for JJA 1984 are shown in Fig. 37. Most of the comments on the 1983 forecasts apply equally well to those of 1984. There are however, a number of significant differences. The ITCZ in the Atlantic is now in quite good agreement with Jaeger's (1976) climatology. In the Pacific, the ITCZ extends a little further westwards, but is still too weak in the Central Pacific. Of the trouble spots referred to above, the problem remain, but are reduced in Borneo and Mexico, and almost eliminated in Colombia. However the Ethiopian highlands remain a problem. The operational orography was modified on 1st February 1984, but a comparison of the precipitation fields for January and February 1984 did not reveal a significant change in the character of the precipitation; also increases in horizontal diffusion of divergence introduced in March 1984 produced little obvious change in the precipitation on this scale. Which suggests that the change in character of the precipitation between the two summers is largely a consequence of the implementation of the diurnal cycle.

The increase in precipitation towards day 5, illustrated in Fig. 21, seems to be a general increase over both land and sea as is the decrease towards day 10.

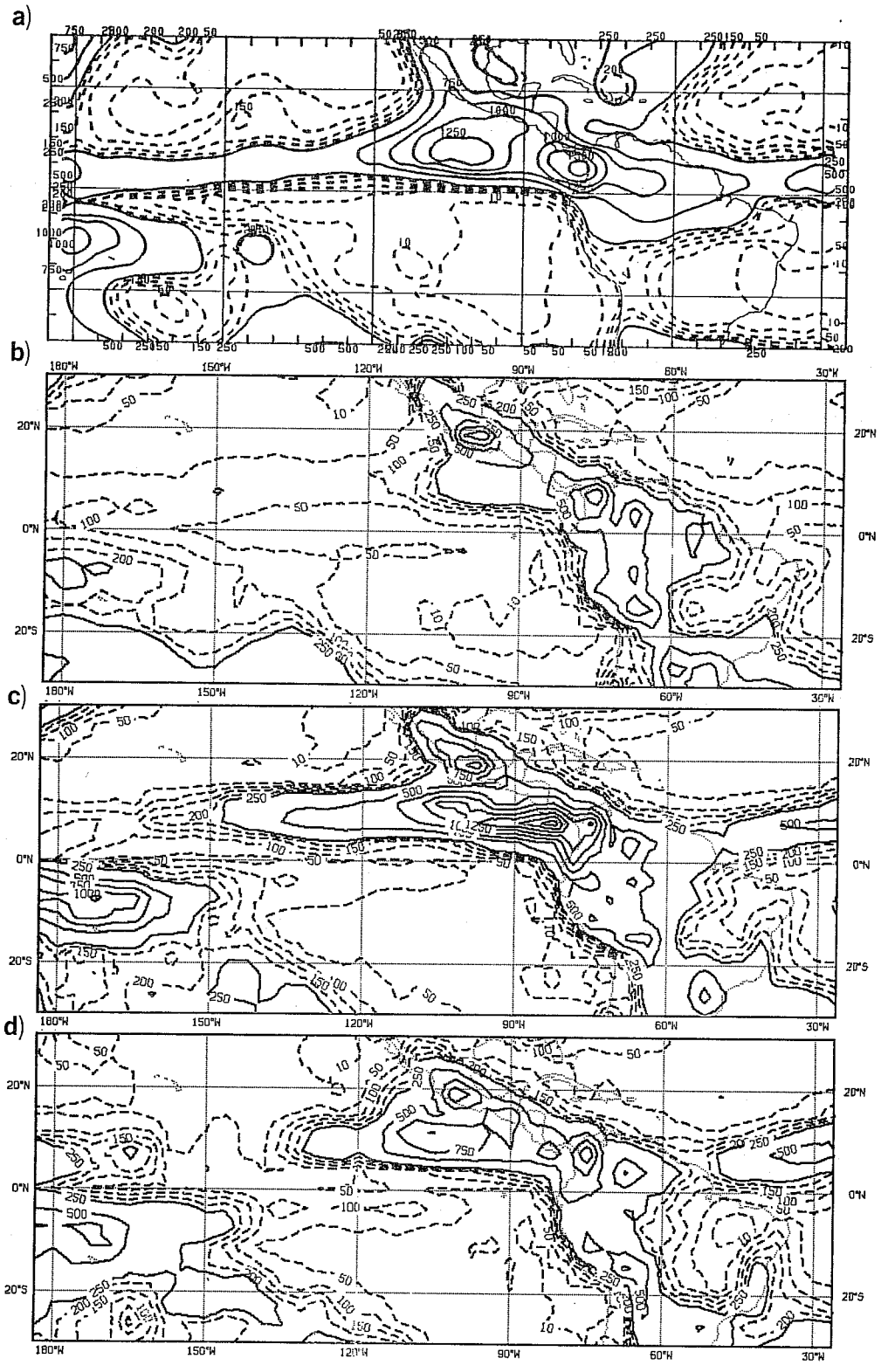

Fig. 38 Accumulated precipitation for JJA 1984. mm
a) GOES precipitation index. Estimated tropical precipitation for 2.5° areas derived from fractional coverage of cloud colder than 235K by method of Arkin (1983). NOAA (1984b)
b) ECMWF forecast precipitation 0-24 hours 3.75° grid
c) ECMWF forecast precipitation 96-120 hours 3.75° grid
d) ECMWF forecast precipitation 216-240 hours 3.75° grid
Solid contours at 250 mm intervals; dashed contours at 10, 50, 100, 150 and 200 mm.

As a more quantitative measure of the forecast skill, the precipitation may be compared with that inferred from cloud cover. Fig. 38 shows a) estimated precipitation from Arkin (1984); and the corresponding forecast amounts for b) 0-24 hours; c) 96-120 hours; and d) 216-240 hours. The 0-24 hour precipitation is generally quite poor, except for north-west South America; the Pacific ITCZ is too weak, as is the Atlantic ITCZ. There is too much rain over Mexico and too much over central South America. The forecasts fail to capture the very dry areas, of less than 10 mm, particularly over the sub tropical oceanic highs.

The 96-120 hour precipitation looks in many ways much better, there is a quite respectable simulation of the SPCZ and the Atlantic ITCZ, but the Pacific ITCZ, although much better simulated, fails to extend far enough westwards. The precipitation in the region of Panama is a little too intense, 200 mm whereas Arkin gives 1500 mm; also the precipitation is too intense over Mexico and central South America. As for the 0-24 hour precipitation the very dry areas are poorly simulated.

The 216-240 hour precipitation shows a very similar geographical distribution to that of 96-120 hours, but the intensity is reduced. Interestingly the Atlantic ITCZ suffers rather less from this reduction than its Pacific counterpart.

4. GLOBAL ENERGY BALANCE

Fig. 39 shows the global surface heat budget for JJA 1984 as a function of forecast length. Hoyt (1976) calculated the radiation and energy budgets of the Earth using three different models of cloud cover. The shaded area represents his range of values for the annual mean, global mean, solar radiation absorbed by the Earth's surface, as determined from his three models.

The full budget is not shown for the forecast model, since dissipation has been neglected, but the magnitude of this term is only of order 2 W m^{-2}, and therefore its omission is justified. Comparing the individual terms with climatological estimates, Oort (1971), the sensible heat flux is about right, at ~20 W m^{-2}. Hoyt's (1971) calculations put the net thermal radiation at the surface at about 65 ± 2 W m^{-2}, with little seasonal variability; and the solar radiation absorbed by the Earth's surface at about 158 ± 10 W m^{-2}, but his July values are lower at about 154 ±9 W m^{-2} (the range given here is the range of his results - not an estimate of the accuracy). Compared to Hoyt's values the forecast surface thermal radiation is a little weak. The forecast solar radiation starts off weak but reaches plausible values within a few days. The big discrepancy is in the latent heat flux, which is probably the main cause of the imbalance of up to 20 W m^{-2} in the surface energy budget. This imbalance is in the sense of a surface heating.

The small values of latent heat flux indicate that there is insufficient evaporation occurring from the surface which, in turn, through the hydrological balance, suggests that there is insufficient precipitation. That is, the simulated hydrological cycle is too slow: evaporation and precipitation are not occurring fast enough to produce the required latent

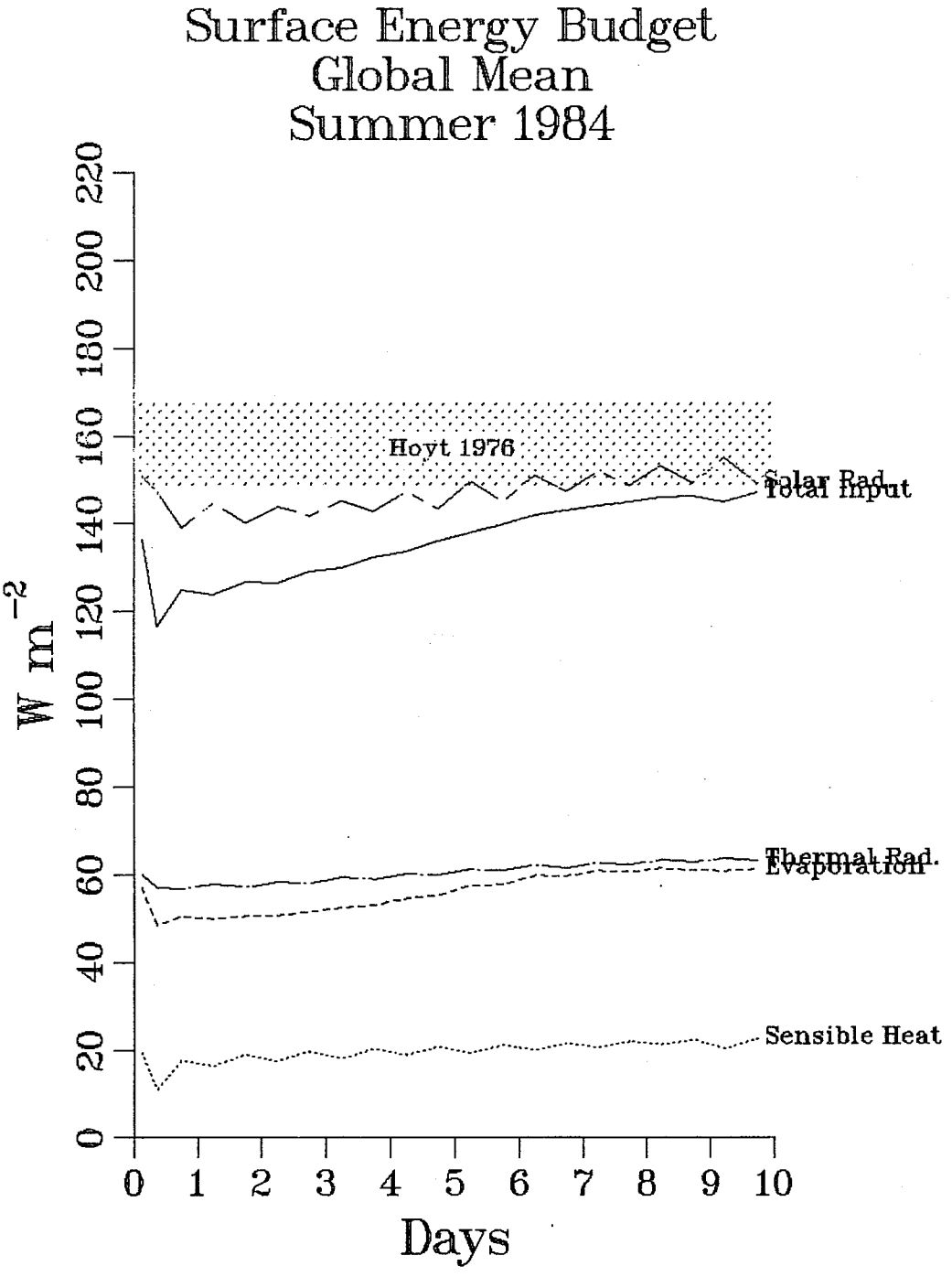

Fig. 39 Global mean surface energy budget for JJA 1984. Dotted line, sensible heat; dashed line, evaporation; dashed-dotted line, thermal radiation from the surface; broken line, solar radiation absorbed by surface; solid line: total input to atmosphere = thermal + evaporation + sensible heat.
Shaded region indicates an estimate of the global mean, annual mean solar radiation absorbed by the surface, calculated by Hoyt (1976)
Units: W m^{-2}

flux. Evidence that this is so may be found in Fig. 40 which shows the global mean hydrological budget of JJA 1984 as a function of forecast length. The estimated climatology shown in the figure represents the mean and standard deviation of a number of separate estimates of the annual mean discussed by Hoyt (1976), these are reproduced in Table 1.

Table 1 Annual totals of evaporation (mm day^{-1}) as determined in various studies. Adapted from Hoyt (1976) (see Hoyt (1976) for references)

E	Source
2.57	Brickner (1905)
2.49	Fritzche (1906)
2.67	Brooks (1930)
2.75	Meinardus (1934)
2.28	Möller (1951)
2.66	Wust (1954)
2.74	Budyko (1963)
2.75	Sellers (1965)
2.26	Nace (1968)
2.79	Lvovitch (1969)
2.67	Baumgartner and Reichel (1973)
2.85	Manabe and Holloway (1975)
2.50	Model A Hoyt (1976)
2.79	Model B Hoyt (1976)
2.71	Model C Hoyt (1976)
Mean 2.6 ±.2	

A more recent study by Elliott and Reed (1984) suggests a global mean of 85 cm (2.33 mm day^{-1}) which is more in line with the forecast values but departs considerably from the earlier estimates. This is an area where there is still considerable uncertainty, even for a global mean, annual mean value.

Despite the large uncertainty in the true climatological value it is quite clear that throughout most of the forecast period, at least, the precipitation rate is well below that which would be required for energy balance. Fig. 40 also shows that after the first few hours of the forecast, precipitation exceeds evaporation. This occurs because, as discussed earlier, the analyses are initially too moist in the lower troposphere. The excessive humidity in the boundary layer acts to inhibit evaporation and a balance, globally, only becomes established towards the end of the 10-day period. In trying to achieve this balance it is the evaporation that steady increases; the precipitation does not begin to decrease until after day 5 (when the moisture supply in the lower troposphere begins to reduce as the atmosphere begins to dry out). The final hydrological cycle that is achieved is still too weak to provide the right kind of energy balance. Whilst the excessively moist boundary layer inhibits achieving the correct hydrological cycle through inhibiting evaporation, it is perhaps more a symptom than a cause of the problem.

A plausible explanation for the model hydrological cycle being so slow lies in the absence of shallow convection. The basic problem is one of increasing the moisture flux from the planetary boundary layer in the sub-tropics which may then act as a source for the penetrative cumulus convection that occurs downstream in the tropics. Indeed the case for shallow convection is rather strong: the model is unable to realistically maintain subsidence inversions,

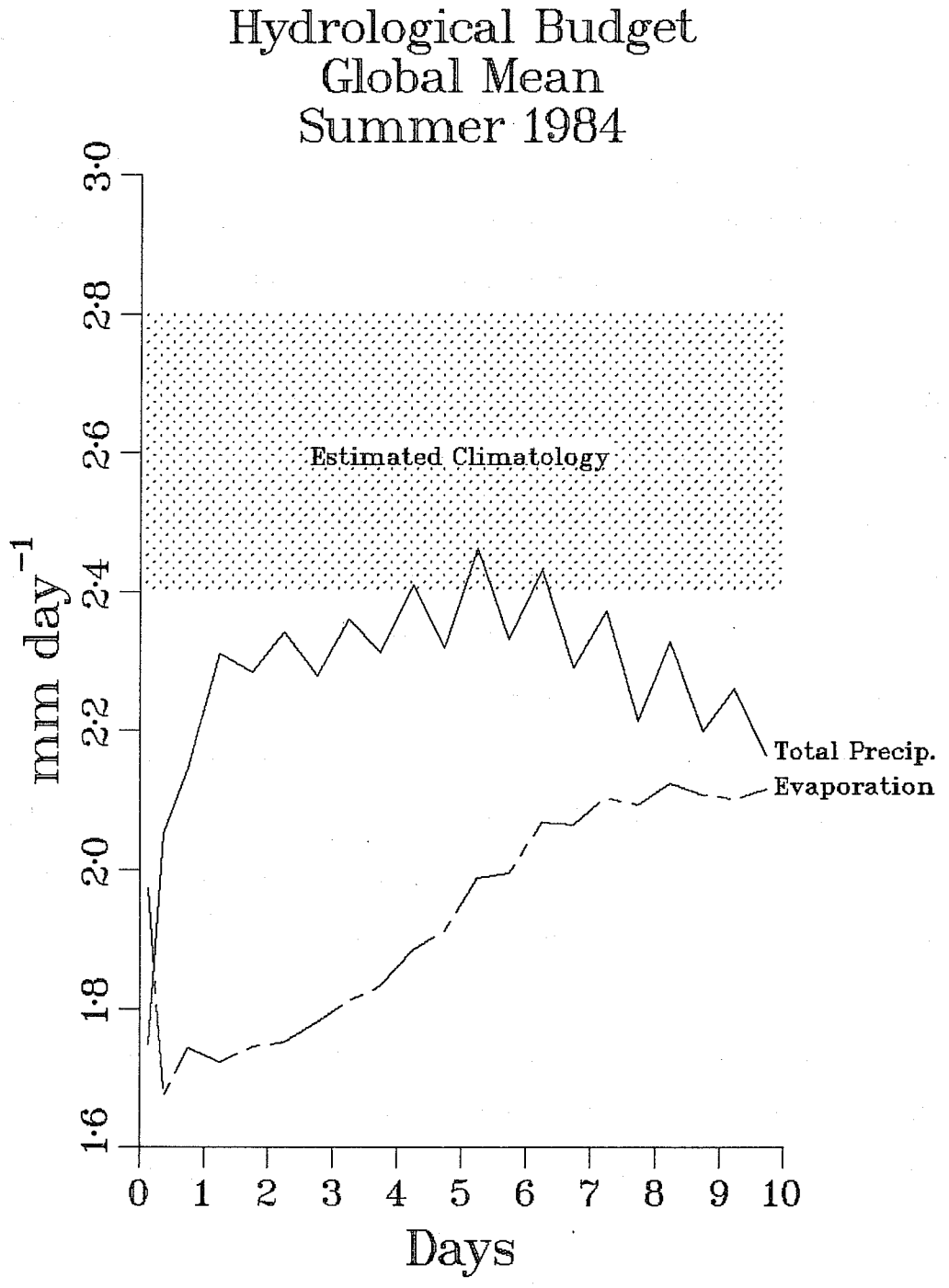

Fig. 40 Global mean hydrological budget. JJA 1984. Units mm day^{-1} Shaded region indicates an estimate of the mean and standard deviation of the annual mean global precipitation calculated from a number of estimates discussed by Hoyt (1976).

it fails to main the correct low level vertical structure in the forecasts, and it fails to transport moisture out of the boundary layer at the required rate. Parameterisation of shallow cumulus convection does have a significant impact on the model; experiments carried out at the ECMWF show substantially increased latent heat flux, removal of the cooling of the tropical troposphere and reduction in the wind errors at low levels (Tiedtke, 1984).

Fig. 41 shows the amospheric energy budget for JJA 1984. The spin-up of the precipitation during the first few hours of the forecasts is, not surprisingly, also apparent in the atmospheric energy balance during the period. The deficit in the atmospheric energy balance corresponds to a global cooling which, as seen earlier from the temperature errors, is what occurs. The shaded area is an estimate of the net radiative heat loss of the atmosphere for the global mean annual mean, from Hoyt (1976) it shows the range of results obtained by his three models mentioned earlier. His July calculations are about 5 W m^{-2} higher than the annual mean, suggesting that the forecast net radiation may be a little low.

For completeness it is worth looking at the radiation balance at the top of the model atmosphere (Fig. 42); this figure also shows an annual mean climatological value from Hoyt (1976) for the upward flux of thermal radiation at the top of the atmosphere. Hoyt's value for July for the thermal radiation is about 246 $\pm$1 W m^{-2} and about 230 $\pm$6 W m^{-2} for the solar radiation. These figures suggest that the forecast values of both thermal and solar radiation at the top of the model atmosphere may be a little high.

Analysed fields of thermal radiation at the top of the atmosphere, Fig. 43a (NOAA, 1948a) show considerable horizontal structure in the tropics and sub tropics, with low values along the ITCZ's associated with the very cold high clouds in the regions, and high values over the deserts. Although the 0-24 hour forecasts, Fig. 43b, simulate the high desert values reasonably well, they are otherwise almost featureless. The 96-120 hour forecast, Fig. 43c, which has the best representation of the ITCZ's in terms of precipitation (Figs. 37,38), makes some attempt at the cloud bands in the eastern Pacific and the eastern Atlantic, but they fail to penetrate very far westwards. Absence of these high clouds in the ECMWF model is partly attributable to the following:

- the analysed humidity is too dry above about 300 mb (See Sect.3.3).

- a weak moisture transport out of the trade wind boundary layer leads to a reduced downstream transport into the deep tropics and therefore a reduced source for the deep penetrative cumulus convection along the ITCZ.

The result is that cloud top does not rise much above about 500 mb in the forecast model.

The solar radiation has a rather unusual behaviour during the first few days: dropping suddenly during the first few hours, followed by a steady increase.

In Figs. 39-42, 44 the influence of the diurnal cycle can be seen. It is interesting that it takes several days to establish itself, a regular signal only becoming apparent at about day 5. Some cycle is apparent in all the

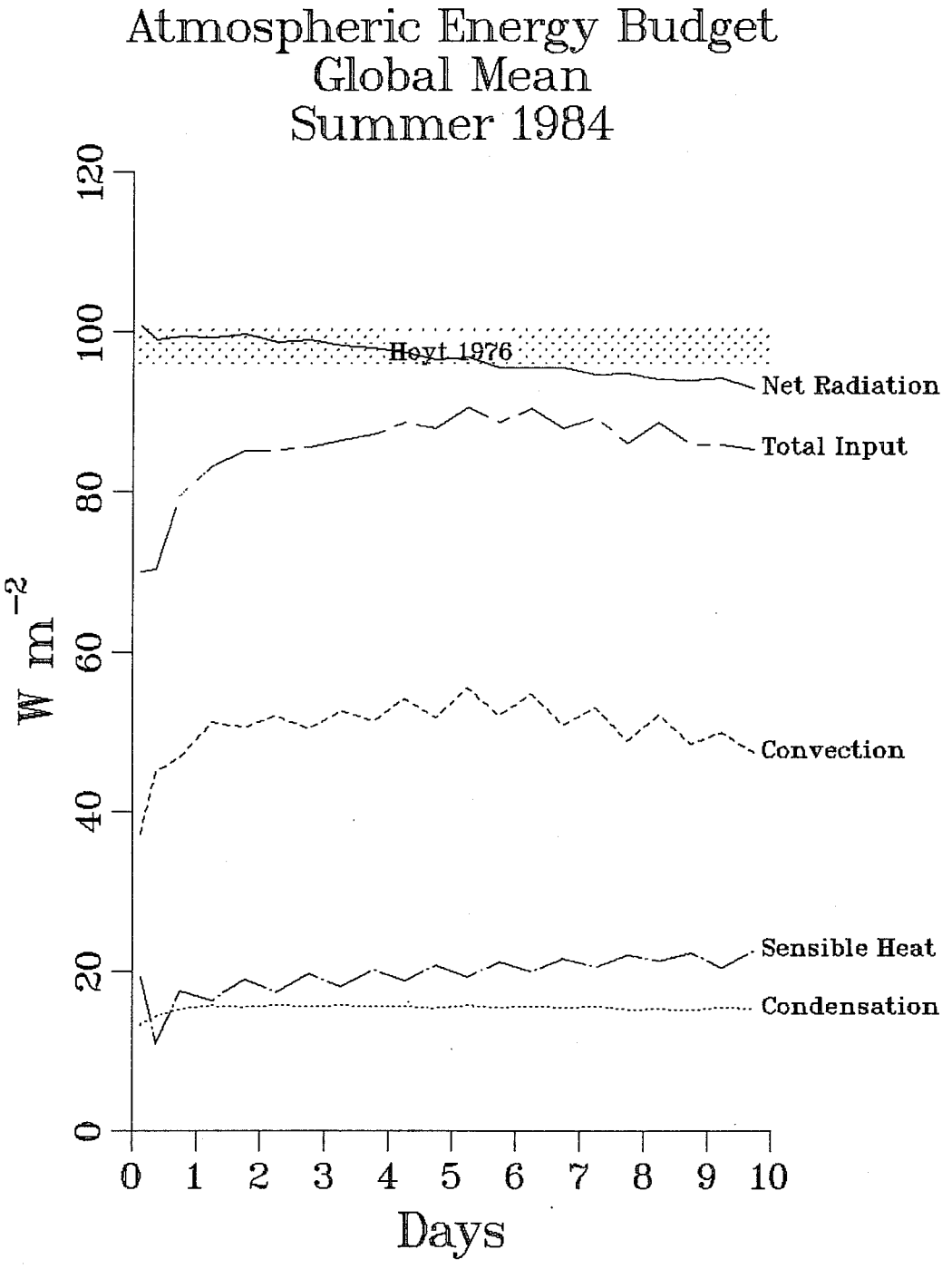

Fig. 41 Global mean atmospheric energy budget for JJA 1984. Dotted line, large-scale precipitation; dashed line, convective precipitation; dashed-dotted line, sensible heat; total input = condensation + convection + sensible heat; net radiation = - (solar radiation at the top of the atmosphere - solar radiation at the ground + thermal radiation at the ground - thermal radiation at the top of the atmosphere). Shaded region indicates an estimate of the net radiative heat loss for the global mean annual mean, calculated by Hoyt (1976).

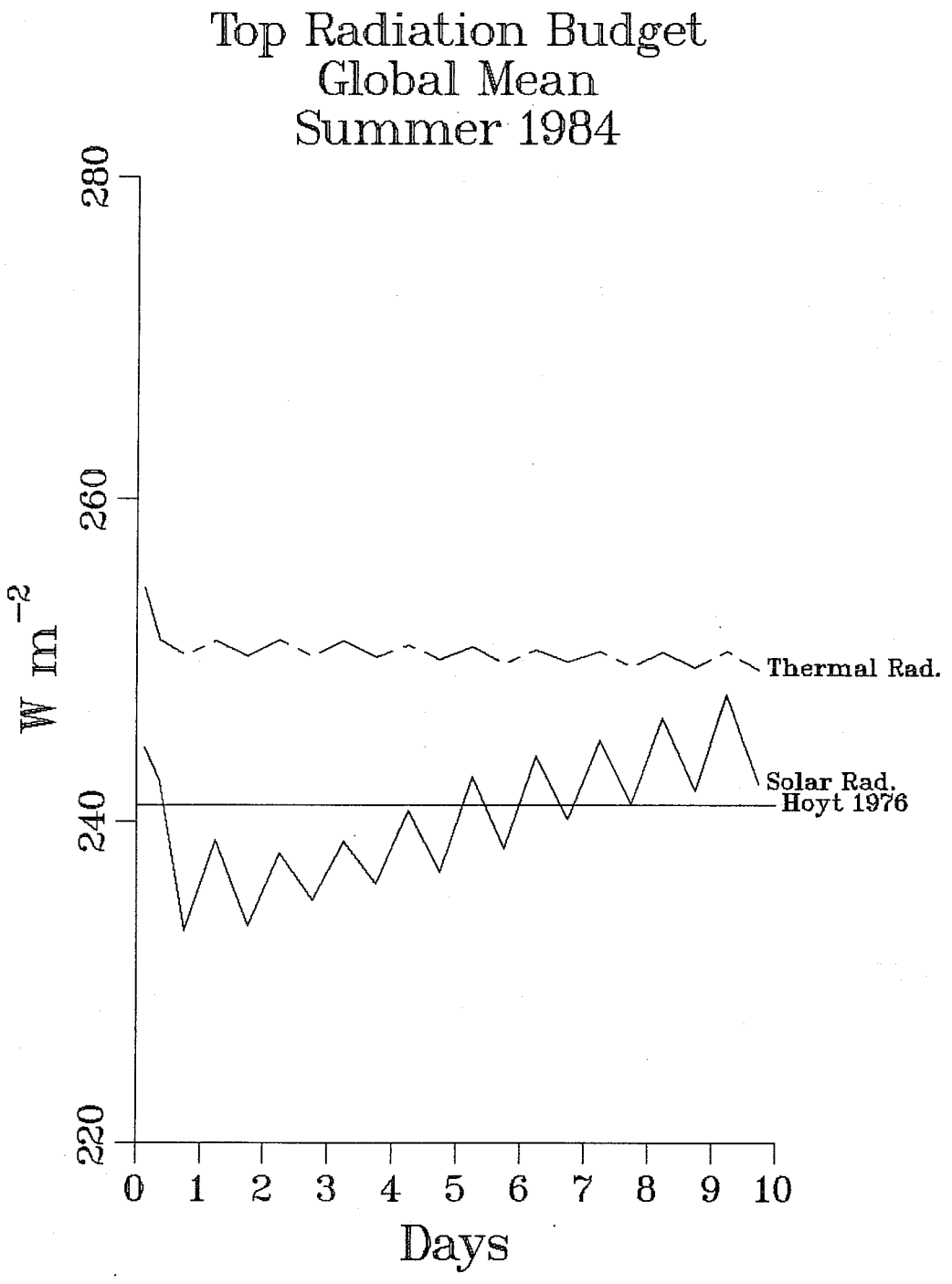

Fig. 42 Global mean radiation budget at the top of the atmosphere JJA 1984. Solid line, solar radiation; dashed lined, thermal radiation. Line marked 'Hoyt (1976)' is an estimate of the annual mean from Hoyt (1976).

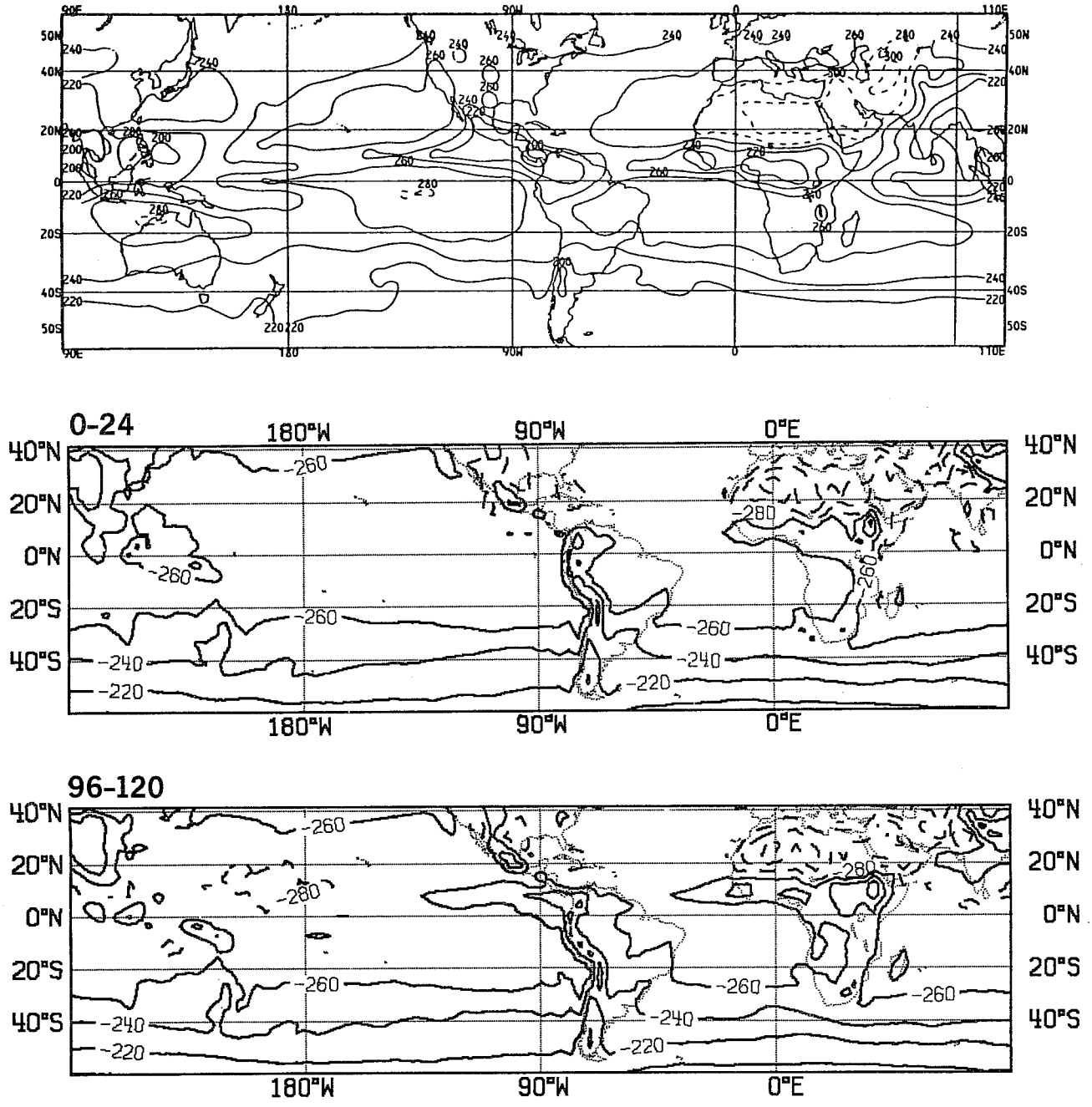

Fig. 43 Outgoing longwave radiation at the top of the atmosphere for JJA 1984.
a) NOAA 7 AVHRR IR window channel measurements by NESDIS/ESL. Data are accumulated and averaged over 2.5° areas and interpolated to a 5° Mercator grid for display
b) ECMWF forecast 0-24 hours (3.75° grid)
c) ECMWF forecast 96-120 hours (3.75° grid)
Contour interval 20 W m^{-2}. Contours of 280 W m^{-2} and above are dashed.

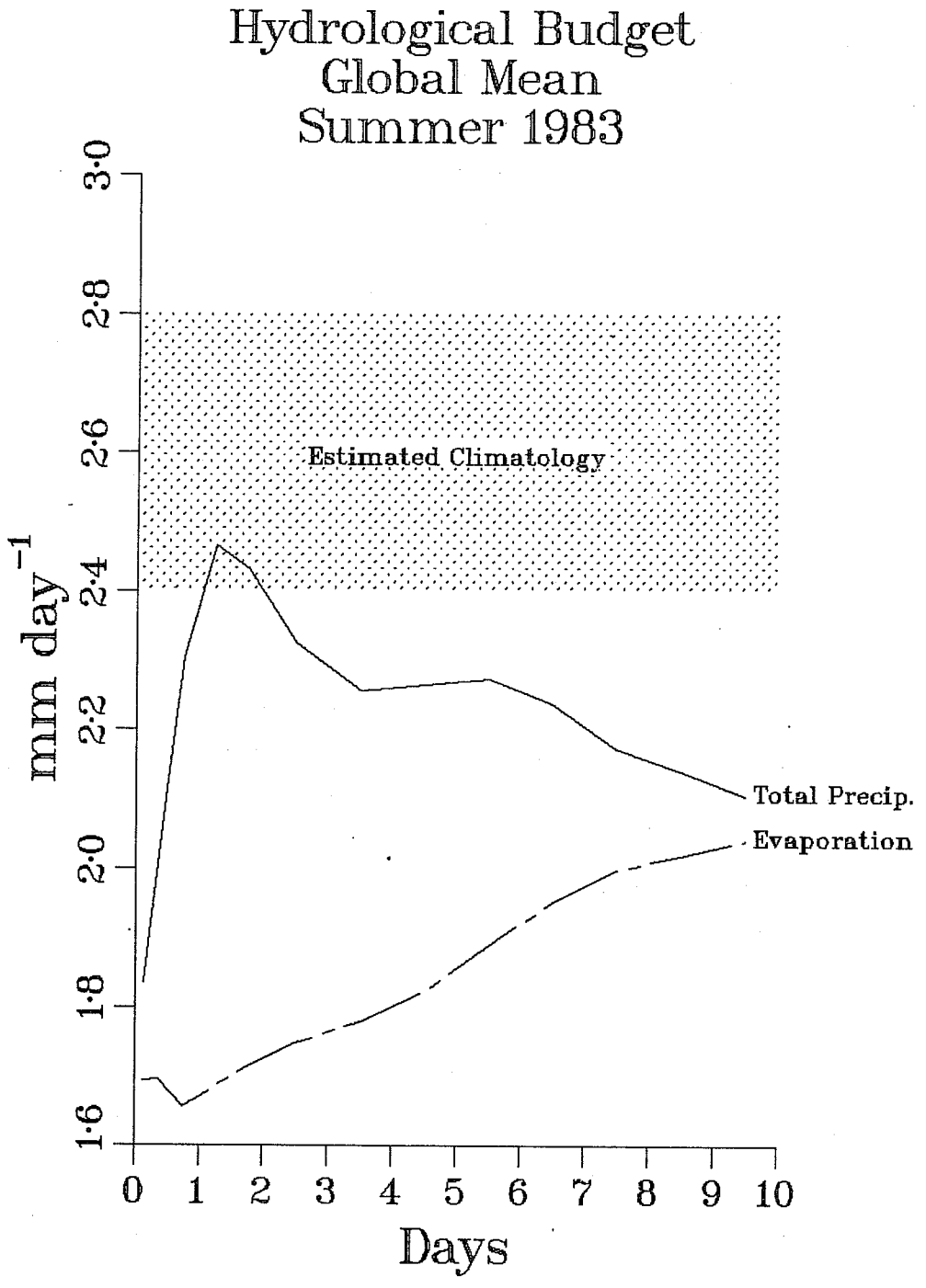

Fig. 44 As Fig. 40 but for JJA 1983

fields, it is strongest in the solar radiation and to a lesser extent in the convective precipitation. The signal is weakest in the large scale precipitation. These figures concern themselves with global mean values; in terms of local diurnal changes one might expect rather different behaviour. It would be inappropriate here to go into a detailed evaluation of the diurnal cycle in the model; that should be done as a separate study. However, in terms of these global mean quantities there is one aspect that stands out in the hydrological budget. Fig. 44 shows the global mean hydrological budget for JJA 1983 as a function of forecast length. The precipitation shows a very rapid rise to a maximum between day 1 and day 2, then decreases to fairly steady values by about three days. The 'overshoot' of the precipitation occurs largely in the tropics and it closely follows similar behaviour in the divergence field. This aspect of the 'spin-up' is sensitive to the horizontal diffusion of divergence. In March 1984 the diffusion coefficient for divergence was increased from 2×10^{15} to 2×10^{16} m^4 s^{-1}. This had the effect of removing the 'overshoot' in the spin-up of the divergence and also of the convective precipitation. This sensitivity to diffusion is a cause for some concern. The increased diffusion in effect masks the real problem of establishing the correct balance initially. The introduction of the diurnal cycle in May, increased the overall values of the precipitation and introduced a diurnal modulation. As can be seen in comparing Figs. 42 and 44 these effects continue to give a more modest increase after the first few hours of the forecasts, reaching a maximum at about day 5, followed by a slight decline.

5. GENERAL DISCUSSION

The objective scores of wind and, to a lesser extent, of temperature indicate definite temporal cycles in tropical predictability, and strong regional variations. Indonesia, for example, exhibits a semi-annual cycle in the forecast errors, whilst India shows an annual cycle apparently related to the seasonal excursions of the northern hemisphere sub-tropical jet. Underlying these annual and semi-annual cycles is a steady improvement in forecast predictability over the last few years with (at least for the wind scores) few sharp jumps in the trend. Relative to persistence, the wind scores show the 200 mb flow to be rather more predictable than that of 850 mb, and at both levels the forecasts lead persistence to at least three days (nearer eight days at 200 mb).

Within a few days the systematic errors are large compared to the variability of the fields themselves and show a remarkable temporal consistency from month to month. The forecasts show a cooling in the equatorial stratosphere, a warming on and immediately below the equatorial tropopause and a cooling in the equatorial mid and lower troposphere. These temperature changes indicate a more stable mid and upper troposphere and a less stable lower troposphere. Increased stability in the upper troposphere is associated with a weakened ageostrophic circulation at these levels: the ageostrophic flow in the upper troposphere becomes weaker and spread over a deeper layer. Changes in the ageostrophic flow are consistent with the production of equatorial easterlies at about 150 mb and westerlies at about 300 mb. The warming at and immediately below the equatorial tropopause is horizontally fairly uniform in the deep tropics but has large horizontal gradients in the sub-tropics. The thermal wind associated with these gradients in effect moves the sub-tropical jets upward and poleward.

The moisture analysis is too wet in the lower troposphere and this is at least partly due to the slow spin-up of the model precipitation in the first guess forecasts. Prior to the introduction of the diurnal cycle the forecast precipitation reached its maximum after about two days then decreased to fairly steady values by about three days; since the introduction of the diurnal cycle the precipitation increases more slowly in the first few days, reaching a maximum at about day 5, then decreasing slightly towards day 10. After the first few hours, precipitation exceeds evaporation out to about ten days, by which time the model reaches its own hydrological balance. The hydrological cycle in the model is too slow: there is insufficient precipitation and evaporation. The radiation balance is initially about right, the weak latent heat flux due to insufficient precipitation fails to balance the radiative cooling and the model cools in the mid and lower troposphere until its radiative cooling is in balance with the weak latent heating. The evidence suggests that the weak latent heat flux is due to the absence of shallow convection. This is supported by the errors in the thermodynamic structures which show the model's inability to maintain subsidence inversions, the tendency to smooth out low level vertical structures and the model's inability to transport moisture out of the boundary layer efficiently.

The problems with the moisture field, the spin up of the model's physics and the feedback on the dynamics indicate a requirement for a more refined moisture analysis and, perhaps more importantly, a requirement for better 'initialisation'. It is becoming increasingly clear that it is necessary to have the energy balance correct at the start of the forecast. The moisture and divergence fields can be initialised, within the bounds of observational constraints, to be consistent with the convective and radiative

parameterisations such that the observed rainfall is reproduced by the model at the outset. This approach has been pioneered by Krishnamurti et al. (1983) and has been demonstrated by them to considerably improve the tropical forecasts.

Allowing for small seasonal shifts and changes in amplitude, and with the exception of errors associated with the monsoon circulation, the wind errors show a remarkably similar pattern throughout the year. They have a very coherent structure in both the upper and lower troposphere and are highly baroclinic. At 850 mb there is a clear cyclonic circulation in the error field over the north and south Atlantic and over the Pacific. At 150 mb the errors are the reverse of this: a strong anticyclonic circulation over the north and south Atlantic and the eastern Pacific. The errors extend meridionally as far as 40° to 50° north and south. If these errors are forced from the tropics, and the indications are that they are, then the tropical errors are substantially changing the baroclinicity of the extra-tropical flow and hence influencing the mid-latitude forecasts of baroclinic waves.

Comparison of summer 1984 and summer 1983 forecasts reveals a modest but clear improvement in low level thermodynamic structure and wind field, particularly over the tropical continents. The rainfall distribution is also improved and the character of the model 'spin-up' is changed. The implementation of the diurnal cycle is an obvious candidate for these changes, as is the changed horizontal diffusion which affects the spin-up of divergence. At upper levels the picture is less clear, whilst the temperature errors in the stratosphere are reduced, wind errors at some levels, e.g. 200 mb are increased. A detailed study of the role of the diurnal cycle in the model and its interaction with the other parameterised processes may be needed to explain some of these negative aspects.

Acknowledgements

The scores shown in Sect. 2 were produced with assistance from Rauno Nieminen. The author is grateful to many members of the ECMWF Research Department for helpful discussions during the course of this work and for constructive criticism of the text.

REFERENCES

Arpe, K., 1985: Comparison of FGGE III-b analyses by ECMWF and by GFDL for the period 27 February to 7 March 1979 taking recent improvements of the ECMWF analysis scheme into account. Seminar on Progress in Diagnostic Studies of the Global Atmospheric Circulation as a Result of the Global Weather Experiment. Helsinki 28-31 August, 1984, GARP Special Report No.42, III38-III42.

Augstein, E., H. Riehl, F. Ostapoff and V. Wagner, 1973: Mass and energy transports in an undisturbed Atlantic tradewind flow. Mon.Wea.Rev., 101, 101-111.

Arkin, P.A., 1983: A diagnostic precipitation index from satellite imagery. Tropical Ocean-Atmosphere Newsletter, March 1983. University of Washington, Joint Institute for the Study of the Atmosphere and Ocean, USA.

Bengtsson, L., M. Kanamitsu, P. Kållberg and S. Uppala, 1982: FGGE 4-dimensional data assimilation at ECMWF. Bull.Amer.Met.Soc., 63, 29-43.

Bengtsson, L. and A.J. Simmons, 1983: Medium range weather prediction - Operational experience at ECMWF. Large-Scale Dynamical Processes in the Atmosphere. Edited by B.J. Hoskins and R.P. Pearce. Academic Press, 337-364.

Charney, J.G., 1975: Dynamics of deserts and drought in the Sahel. Quart.J.Roy.Meteor.Soc., 101, 193-202.

Daley, R., 1983: Spectral characteristics of the ECMWF objective analysis system. ECMWF Tech.Rep.No.40, 119pp.

Elliott, W.P. and R.K. Reed, 1984: A climatological estimate of precipitation for the world ocean. Climate and Appl.Meteor. 23, 434-439.

Geleyn, J.-F. and A. Hollingsworth, 1979: An economical analytical method for the computation of the interaction between scattering and line absorption of radiation. Contr.Atmos.Phys., 52, 1-16.

Gilchrist, A., 1977: The simulation of the Asian summer monsoon by general circulation models. Pure Appl.Geophys., 115, 1431-1448.

Gilchrist, A., P.R. Rowntree and D.B. Shaw, 1982: Large scale numerical modelling. The GARP Atlantic Tropical Experiment (GATE) Monograph, WMO, GARP Publication Series No.25, 183-218.

Haseler, J., 1982: An investigation of the impact at middle and high latitudes of tropical forecast errors. ECMWF Tech.Rep.No.31, 42pp.

Heckley, W.A., 1983: Adjustment in numerical weather prediction models in the tropics. ECMWF Workshop on Current Problems in Data Assimilation. 8-10 November 1982. Reading, UK, 299-342.

Hollingsworth, A., K. Arpe, M. Tiedtke, M. Capaldo, and H. Savijärvi, 1980: The performance of a medium-range forecast model in winter-impact of physical parameterization. Mon.Wea.Rev., 108, 1736-1773.

Hoyt, D.V., 1976: The radiation and energy budgets of the Earth using both ground-based and satellite-derived values of total cloud cover. NOAA Tech.Report ERL 362-ARL 4. U.S. Dept. of Commerce. 124pp.

ICSU/WMO, 1978: Numerical modelling of the tropical atmosphere. GARP Publ.Series No.20. WMO, Geneva.

Jaeger, L., 1976: Monatskarten des Niederschlags für die Ganze Erde. Berichte Deutschen Wetterd. Offenbach/Main, Vol.18 Nr.139, 38pp.

Klinker, E., and M. Capaldo, 1984: Systematic errors in the baroclinic waves of the ECMWF model. ECMWF Tech.Rep.No.41, 86pp.

Krishnamurti, T.N., K. Ingles, S. Cocke, T. Kitade and R. Pasch, 1983: Details of low latitude medium range weather prediction using a global spectral model II. Effects of orography and physical initialisation. FSU Report No. 83-11 available from the Florida State University, USA.

Miller, M.J., and M.W. Moncrieff, 1984: The use and implementation of dynamical cloud models in a parameterisation scheme for deep convection. ECMWF Workshop on Convection in Large Scale Numerical Models. 28 November-1 December 1983. Reading, UK, 33-67.

Nieminen, R., 1983: Operational verification of ECMWF forecast fields and results for 1980-1981. ECMWF Tech.Rep.No.36, 40pp.

NOAA, 1984a: Climate Diagnostic Bulletin, August 1984. NOAA/National Weather Service, National Meteorological Center, Climate Analysis Center, Washington, USA.

NOAA, 1984b: Climate Diagnostic Bulletin, September 1984. Available from NOAA/National Weather Service, National Meteorological Center, Climate Analysis Center, Washington, USA.

Oort, A.H., 1971: The atmospheric circulation: the weather machine of the earth. Sci.Teacher, 38(9), 12-16.

Oort, A.H., 1983: Global atmospheric circulation statistics 1958-1973. NOAA Professional Paper 14. Available from the US Government Printing Office, Washington DC, USA.

Ritter, B., 1985: The impact of alternative treatment of infra-red radiation on the performance of the ECMWF model. Proceedings of the IAMAP International Radiation Symposium. 1984. Perugia, Italy. 277-280. Published by DEEPAK, USA.

Rowntree, P.R., 1978: Numerical prediction and simulation of the tropical atmosphere. Meteorology over the tropical oceans. Ed. by D.B. Shaw. Roy.Met.Soc., Bracknell, 219-249.

Sellers, W.D., 1966: Physical Climatology. Chicago, Univ. of Chicago Press, 272pp.

Shaw, D., Lönnberg, P. and A. Hollingsworth, 1984: The 1984 revision of the ECMWF analysis system. ECMWF Research Dept. Tech.Memo No.92, 69pp.

Simmons, A.J., 1983: Adiabatic formulation of the ECMWF forecasting system. ECMWF Seminar/Workshop on the Interpretation of Numerical Weather Prediction Products, 13-24 September 1982, Reading, UK, 59-81.

Slingo, J., 1986: Parameterization of cloud cover. Proceedings of the 1985 ECMWF Seminar on Physical Parameterization for numerical models., 9-13 September 1985, Reading, UK. To be published by ECMWF.

Thompson, R.M., S.W. Payne, E.E. Recker and R.J. Reed, 1979: Structure and properties of synoptic-scale wave disturbances in the intertropical convergence zone of the eastern Atlantic. J.Atmos.Sci., 36, 53-72.

Tiedtke, M., 1982: Assessment of the PBL-flow in the EC-model. Workshop on Planetary Boundary Layer Parameterisation, 25-27 Nov 1981, Reading, UK, 155-191.

Tiedtke, M., 1984: The sensitivity of the time-mean large-scale flow to cumulus convection in the ECMWF model. ECMWF Workshop on Convection in Large-Scale Numerical Models, 28 Nov.-1 Dec. 1983, Reading, UK, 169-175.

Tiedtke, M., 1986: Effect of physical parameterization on the large scale flow in the ECMWF model. Proceedings of the 1985 Seminar on Physical Parameterization for Numerical Models, 9-13 September 1985, Reading, UK. To be published by ECMWF.

Tiedtke, M., J-F. Geleyn, A. Hollingsworth and J-F. Louis, 1979: ECMWF Model parameterisation of sub-grid scale processes. ECMWF Tech.Rep.No.10, 46pp.

Wergen, W., 1985: Diabatic non-linear normal mode initialisation in a hybrid coordinate spectral model. ECMWF Tech.Rep. (to be published).

Wicombe, W.J. and J.W. Evans, 1977: Exponential sum fitting of radiative transmission functions. J.Comput.Phys., 24, 416-444.

ECMWF PUBLISHED TECHNICAL REPORTS

No.1 A Case Study of a Ten Day Prediction

No.2 The Effect of Arithmetic Precisions on some Meteorological Integrations

No.3 Mixed-Radix Fast Fourier Transforms without Reordering

No.4 A Model for Medium-Range Weather Forecasting - Adiabatic Formulation

No.5 A Study of some Parameterizations of Sub-Grid Processes in a Baroclinic Wave in a Two-Dimensional Model

No.6 The ECMWF Analysis and Data Assimilation Scheme - Analysis of Mass and Wind Fields

No.7 A Ten Day High Resolution Non-Adiabatic Spectral Integration: A Comparative Study

No.8 On the Asymptotic Behaviour of Simple Stochastic-Dynamic Systems

No.9 On Balance Requirements as Initial Conditions

No.10 ECMWF Model - Parameterization of Sub-Grid Processes

No.11 Normal Mode Initialization for a Multi-Level Gridpoint Model

No.12 Data Assimilation Experiments

No.13 Comparisons of Medium Range Forecasts made with two Parameterization Schemes

No.14 On Initial Conditions for Non-Hydrostatic Models

No.15 Adiabatic Formulation and Organization of ECMWF's Spectral Model

No.16 Model Studies of a Developing Boundary Layer over the Ocean

No.17 The Response of a Global Barotropic Model to Forcing by Large-Scale Orography

No.18 Confidence Limits for Verification and Energetic Studies

No.19 A Low Order Barotropic Model on the Sphere with the Orographic and Newtonian Forcing

No.20 A Review of the Normal Mode Initialization Method

No.21 The Adjoint Equation Technique Applied to Meteorological Problems

No.22 The Use of Empirical Methods for Mesoscale Pressure Forecasts

No.23 Comparison of Medium Range Forecasts made with Models using Spectral or Finite Difference Techniques in the Horizontal

No.24 On the Average Errors of an Ensemble of Forecasts

ECMWF PUBLISHED TECHNICAL REPORTS

No.25 On the Atmospheric Factors Affecting the Levantine Sea

No.26 Tropical Influences on Stationary Wave Motion in Middle and High Latitudes

No.27 The Energy Budgets in North America, North Atlantic and Europe Based on ECMWF Analyses and Forecasts

No.28 An Energy and Angular-Momentum Conserving Vertical Finite-Difference Scheme, Hybrid Coordinates, and Medium-Range Weather Prediction

No.29 Orographic Influences on Mediterranean Lee Cyclogenesis and European Blocking in a Global Numerical Model

No.30 Review and Re-assessment of ECNET - a Private Network with Open Architecture

No.31 An Investigation of the Impact at Middle and High Latitudes of Tropical Forecast Errors

No.32 Short and Medium Range Forecast Differences between a Spectral and Grid Point Model. An Extensive Quasi-Operational Comparison

No.33 Numerical Simulations of a Case of Blocking: the Effects of Orography and Land-Sea Contrast

No.34 The Impact of Cloud Track Wind Data on Global Analyses and Medium Range Forecasts

No.35 Energy Budget Calculations at ECMWF: Part I: Analyses

No.36 Operational Verification of ECMWF Forecast Fields and Results for 1980-1981

No.37 High Resolution Experiments with the ECMWF Model: a Case Study

No.38 The Response of the ECMWF Global Model to the El-Nino Anomaly in Extended Range Prediction Experiments

No.39 On the Parameterization of Vertical Diffusion in Large-Scale Atmospheric Models

No.40 Spectral characteristics of the ECMWF Objective Analysis System

No.41 Systematic Errors in the Baroclinic Waves of the ECMWF Model

No.42 On Long Stationary and Transient Atmospheric Waves

No.43 A New Convective Adjustment Scheme

No.44 Numerical Experiments on the Simulation of the 1979 Asian Summer Monsoon

No.45 The Effect of Mechanical Forcing on the Formation of a Mesoscale Vortex

ECMWF PUBLISHED TECHNICAL REPORTS

No.46 Cloud Prediction in the ECMWF Model

No.47 Impact of Aircraft Wind Data on ECMWF Analyses and Forecasts during the FGGE Period, 8-19 November 1979 (not on WP, text provided by Baede)

No.48 A Numerical Case Study of East Asian Coastal Cyclogenesis

No.49 A Study of the Predictability of the ECMWF Operational Forecast Model in the Tropics

No.50 On the Development of Orographic Cyclones

No.51 Climatology and Systematic Error of Rainfall Forecasts at ECMWF

No.52 Impact of Modified Physical Processes on the Tropical Simulation in the ECMWF Model

No.53 On the Performance and Systematic Errors of the ECMWF Tropical Forecasts (1982-1984)